SJSU SAN JOSÉ STATE UNIVERSITY

MTI MINETA TRANSPORTATION INSTITUTE

Developing an Integrated Risk Assessment Framework to Quantify the Resilience of Critical Railway Infrastructure: Characterization of Risks and Hazards to the U.S. Rail Network Through Empirical Data and Past Events

Haizhong Wang Brian M. Staes Benyamin Ghoreishi

MINETA TRANSPORTATION INSTITUTE

Founded in 1991, the Mineta Transportation Institute (MTI), an organized research and training unit in partnership with the Lucas College and Graduate School of Business at San José State University (SJSU), increases mobility for all by improving the safety, efficiency, accessibility, and convenience of our nation's transportation system. Through research, education, workforce development, and technology transfer, we help create a connected world. MTI leads the California State University Transportation Consortium (CSUTC) funded by the State of California through Senate Bill 1 and the Climate Change and Extreme Events Training and Research (CCEETR) Program funded by the Federal Railroad Administration. MTI focuses on three primary responsibilities:

Research

MTI conducts multi-disciplinary research focused on surface transportation that contributes to effective decision making. Research areas include: active transportation; planning and policy; security and counterterrorism; sustainable transportation and land use; transit and passenger rail; transportation engineering; transportation finance; transportation technology; and workforce and labor. MTI research publications undergo expert peer review to ensure the quality of the research.

Education and Workforce Development

To ensure the efficient movement of people and goods, we must prepare the next generation of skilled transportation professionals who can lead a thriving, forward-thinking transportation industry for a more connected world. To help achieve this, MTI sponsors a suite of workforce development and education opportunities. The Institute supports educational programs offered by the Lucas Graduate School of Business: a Master of Science in Transportation Management, plus graduate certificates that include High-Speed and Intercity Rail Management and Transportation Security Management. These flexible programs offer live online classes so that working transportation professionals can pursue an advanced degree regardless of their location.

Information and Technology Transfer

MTI utilizes a diverse array of dissemination methods and media to ensure research results reach those responsible for managing change. These methods include publication, seminars, workshops, websites, social media, webinars, and other technology transfer mechanisms. Additionally, MTI promotes the availability of completed research to professional organizations and works to integrate the research findings into the graduate education program. MTI's extensive collection of transportation-related publications is integrated into San José State University's world-class Martin Luther King, Jr. Library.

Report 25-20

Developing an Integrated Risk Assessment Framework to Quantify the Resilience of Critical Railway Infrastructure: Characterization of Risks and Hazards to the U.S. Rail Network Through Empirical Data and Past Events

Haizhong Wang

Brian M. Staes

Benyamin Ghoreishi

August 2025

A publication of the
Mineta Transportation Institute
Created by Congress in 1991

College of Business
San José State University
San José, CA 95192-0219

TECHNICAL REPORT DOCUMENTATION PAGE

1. Report No. 25-20	**2. Government Accession No.**	**3. Recipient's Catalog No.**	
4. Title and Subtitle Developing an Integrated Risk Assessment Framework to Quantify the Resilience of Critical Railway Infrastructure: Characterization of Risks and Hazards to the U.S. Rail Network Through Empirical Data and Past Events		**5. Report Date** August 2025 **6. Performing Organization Code**	
7. Authors Haizhong Wang, 0000-0002-0028-3755 Benyamin Ghoreishi, 0000-0001-6773-5325 Brian M. Staes, 0000-0002-3219-4386		**8. Performing Organization Report** CA-MTI-2413	
9. Performing Organization Name and Address Mineta Transportation Institute College of Business San José State University San José, CA 95192-0219		**10. Work Unit No.** **11. Contract or Grant No.** 69A36523420190CRSCA	
12. Sponsoring Agency Name and Address U.S. Department of Transportation Federal Railroad Administration 1200 New Jersey Avenue, SE Washington, DC 20590		**13. Type of Report and Period Covered** **14. Sponsoring Agency Code**	
15. Supplemental Notes 10.31979/mti.2025.2413			
16. Abstract To improve understanding of the impact of natural hazards on the U.S. railway system, this project developed a comprehensive, geospatially precise dataset that maps historical hazard events to specific rail segments. The project provides insight into when, where, and how much damage natural hazards have inflicted on rail infrastructure across the country. While a rail-specific hazard database did not previously exist, this research combines data from the Geological Survey (USGS) Flood Events Database, Hydrologic Unit Codes (HUC), the National Centers for Environmental Information (NCEI) from the National Oceanic and Atmospheric Administration (NOAA), and the National Weather Service (NWS) forecast zones. Using accident cause codes (e.g., T002 for flood- related track damage and T109 for sun kinks) and the external hazard data, the researchers were able to estimate both the location and economic cost of damage. Findings revealed that from 2000 to 2023, certain hazard-linked derailments caused millions in track damage—$43 million from floods (M103) and up to $85 million from extreme heat events (T109). This work lays the foundation for a national rail-hazard damage database, one that can be enhanced with industry-provided operational data. By linking hazard intensity with economic impact, the study offers critical data to inform further research as well as policymakers, planners, and industry leaders looking to improve the resilience of the U.S. rail network in the face of a changing climate and growing hazard exposure.			
17. Key Words Railway infrastructure, railroad engineering, disaster resilience, hazard evaluation, databases.	**18. Distribution Statement** No restrictions. This document is available to the public through The National Technical Information Service, Springfield, VA 22161.		
19. Security Classif. (of this report) Unclassified	**20. Security Classif. (of this page)** Unclassified	**21. No. of Pages** 127	**22. Price**

Form DOT F 1700.7 (8-72)

DOI: 10.31979/mti.2025.2413

Mineta Transportation Institute
College of Business
San José State University
San José, CA 95192-0219

Tel: (408) 924-7560
Fax: (408) 924-7565
Email: mineta-institute@sjsu.edu

transweb.sjsu.edu/research/2413

Contents

List of Figures

LIST OF TABLES

1. Introduction

Climate change is a evolving and prevalent feature of the Earth's natural environmental processes. The expedited extremes produced through climate change as a result of human activity indeed portray an ever-present risk to the U.S. rail infrastructure system, now and increasingly into the future. With the prominence of global climate model (GCM) ensemble data, compiled by national and international labs whose results follow the International Panel on Climate Change, future predictions on the type of prevailing environmental conditions that will be present across the various regions of the U.S. into the coming decades are able to be utilized (Taylor et al., 2012; Eyring et al., 2016). The scale of the GCM datasets allows for region-specific natural hazard variables that are expected to occur, such as rainfall intensity and heat waves. The risk and severity of specific natural hazards can now be assigned with some certainty directly to existing rail infrastructure in the US, based on future climate scenarios. This has implications for expectations for rail transportation disturbances, understanding of the increased risk of derailment scenarios caused by natural hazards, and limitations of rail operations for all rail tracks in the U.S. for the coming decade (Rossetti, 2003).

The outline for this chapter is as follows:

- Section 6.1 identifies available datasets in relation to both natural hazards and the U.S. Rail Inventory. The output of this section is a series of shapefiles representing rail segments impacted by natural hazards, each containing attribute fields that describe the characteristics of the associated events.

- Section 6.1.1 depicts the approach for assigning flood-driven events, including riverine and flash flood events as well as descriptions of coastal flooding.

- Section 6.1.2 investigates heat-based events and extreme heat events that have been captured historically through various databases with an assignment protocol that considers National Weather Service geographic grids in relation to the U.S. Rail Inventory.

- Lastly, Section 6.1.3 explores an approach towards mapping historical events and suspected landslide-based hazards that have occurred near the U.S. Rail Inventory. This includes probabilistic scenarios that were derived from the United States Geological Survey (USGS), leading to individual natural hazard shapefiles for the U.S. rail system.

While such methodologies are developed within this research report, an initial investigation was conducted into the historic natural hazards that have impacted the U.S. rail network. This required an initial scan of specific natural hazards and those datasets which come from an array of different agencies, both federal and local. Specific methodologies were also developed to incorporate the

geospatial characteristics of these natural hazards and assign them to the rail track, capturing key event variables relevant to comparative analysis, including measures of magnitude.

1.1 Characterization of Risks and Hazards to the U.S. Rail Network Through Past Events

The U.S. freight rail network extends 140,000 route miles, contributing $80 billion to the U.S. economy. The prominence of disruptions to this network creates distinct challenges, imposing community and economic constraints when these systems have failures (FRA, 2020). Such challenges involve the various climate regions that this network operates in throughout the U.S. and the various natural hazards that are induced to the rail infrastructure. While the Federal Emergency Management Agency (FEMA), through its national risk index, identifies 18 natural hazards (FEMA, 2023), only a few of these have a direct impact on rail damage that will increase in severity and frequency as the result of climate change (Palin et al., 2021). These include:

- Extreme Heat & Cold
- Coastal Flooding & Hurricanes
- Riverine Flooding
- Landslides

While a range of natural hazards can impact rail infrastructure, this study focuses on flooding, extreme heat, and landslides due to their well-documented relevance to rail system vulnerability and the availability of comprehensive historical datasets. Flooding receives particular emphasis because it has been shown to cause widespread and repeated disruptions to U.S. rail networks and is supported by robust, high-resolution data from agencies such as USGS and National Centers for Environmental Information (NCEI). These factors allow for a more detailed and reliable hazard-to-rail assignment process. Other hazard types may be considered in future research as additional standardized datasets become available.

While there exists a database that tracks all derailments and incidents exceeding the Federal Railroad Administration's (FRA) monetary reporting threshold of $11,500 (FRA, 2024), there is not currently a centralized database that captures historical natural hazard damages to U.S. rail infrastructure assets. To address this gap, this study proposes the development of a first-of-its-kind national database of historic natural disasters potentially affecting railroad infrastructure, including events that did not result in derailments or meet the reporting threshold but may have caused operational disruptions or long-term asset degradation. Since such impacts are often unrecorded, this study infers likely exposure by identifying rail segments within the spatial footprint of hazard events using geospatial analysis. This approach allows for the identification of at-risk segments that are not reflected in incident reports but may still experience degradation or

operational stress over time. The database is structured as a set of hazard-specific shapefiles designed for use by academia, industry, and federal agencies.

Although the methodology to accurately assign each of the different natural hazards to the rail infrastructure from various historic databases will occur in a later section of this report, a first step towards that progression is to establish those national-level databases that will provide the specific natural hazard data. With this understanding, the following sections explore the various types of natural hazards that have impacted the U.S. rail infrastructure network, leveraging the limited yet known instances where these hazards have caused derailments, in an attempt to identify other sections of rail track that were damaged by historical natural hazard events but did not result in derailment, and for which data therefore does not exist.

2. Flooding

Floods typically happen when water spills or soaks land that is normally dry. They can be due to a range of reasons such as heavy rains, the melting of snow at a high rate, dam breaks or breaches, and ocean waves coming onshore. Floods can emerge over a few hours or days, giving inhabitants time to prepare for them, while flash floods may come suddenly and without warning (*NGC*; *NOAA n.d.a*).

Because the terminology surrounding flood events is diverse and often technical, it is important to define key terms used throughout this study. Table 1 presents a categorized glossary of flood-related terms based on definitions provided by the National Oceanic and Atmospheric Administration (*NOAA n.d.b*).

Table 1. Categorization and Definitions of Flood-Related Terms (*NOAA n.d.b*)

Category	Term	Definition
Flood Types	100-year Flood	A statistic indicating the magnitude of a flood expected to occur on average once every 100 years at a given point or reach on a river, based on historical flood data.
	Annual Flood	The maximum discharge peak during a given water year (October 1–September 30).
	Backwater Flooding	Upstream flooding caused by downstream conditions such as channel restriction and high flow in a downstream confluence stream.
	Base Flood	The national standard for floodplain management in hydrologic terms. It has a 1% chance of occurring in any given year, also called a 100-year flood.
	Closed Basin Lake Flooding	Flooding in lakes with either no outlet or a relatively small one. Seasonal increases in rainfall cause the lake level to rise faster than it can drain.
	Coastal Flooding	Flooding that occurs when water is driven onto land from an adjacent body of water, typically during significant storms.
	Coastal/Lakeshore Flooding	Flooding due to sea waters or large lakes rising above normal tidal action, affecting areas such as ocean fronts, bays, sounds, and inland waterways.
	Daily Flood Peak	The maximum mean daily discharge occurring in a stream during a given flood event.
	Dry Floodproofing	Sealing a building against floodwaters using waterproofing compounds or plastic sheeting, making areas below the flood protection level impermeable.
	Flash Flood	A rapid and extreme flow of high water into a normally dry area or rapid water level rise in a stream or creek above a predetermined level, usually within six hours of the causative event.

Category	Term	Definition
	Flood	Any high flow, overflow, or inundation by water causing or threatening damage.
	Flood Wave	A rise in streamflow to a crest and subsequent recession, often caused by precipitation, snowmelt, dam failure, or reservoir releases.
	Flooded Ice	Ice flooded by meltwater or river water and heavily loaded with water and wet snow.
	Floodway	The part of the flood plain reserved for emergency diversion of water during floods, kept clear of encumbrances.
	Lakeshore Flooding	Flooding of land areas adjacent to lakes due to water exceeding normal levels.
	Lowland Flooding	Inundation of low areas near rivers, often rural, but may also occur in urban areas.
	Major Flooding	A term for extensive inundation and property damage, often leading to evacuation.
	Minor Flooding	A term indicating minimal or no property damage but potential inconvenience.
	Moderate Flooding	Inundation of secondary roads and properties, often requiring evacuation.
	Small Stream Flooding	Flooding of small creeks, streams, or runs.
	Snowmelt Flooding	Flooding caused primarily by melting snow.
	Urban and Small Stream Flooding	Flooding of small streams, streets, and low-lying areas, typically an inconvenience.
	Urban Flooding	Flooding of streets, underpasses, and low-lying areas, generally an inconvenience.
	Wet Floodproofing	Allowing a building to flood while taking measures to minimize damage, such as moving valuables to higher places or anchoring structures.
Flood Warnings and Advisories	Coastal/Lakeshore Flood Advisory	Indicates minor flooding above normal high tide levels. Advisories are issued using the Coastal/Lakeshore Hazard Message (CFW) product.
	Coastal/Lakeshore Flood Warning	Indicates serious flooding that will pose a threat to life and property. Warnings are issued using the Coastal/Lakeshore Hazard Message (CFW) product.
	Coastal/Lakeshore Flood Watch	Indicates possible significant impacts due to coastal or lakeshore flooding. Watches are issued using the Coastal/Lakeshore Hazard Message (CFW) product.
	Flash Flood Warning	Issued to the public, emergency management, and other agencies when flash flooding is imminent or highly likely.
	Flash Flood Watch	Issued to indicate current or developing hydrologic conditions favorable for flash flooding but where the occurrence is neither certain nor imminent.

Category	Term	Definition
	Flood Warning (FLW)	A warning issued by the National Weather Service (NWS)to inform the public of flooding along larger streams when there is a serious threat to life or property.
	Flood Watch	Issued to inform the public and cooperating agencies of hydrometeorological conditions that are favorable for flooding but where the occurrence is not certain or imminent.
	Lakeshore Flood Watch	Indicates conditions favorable for lakeshore flooding, although occurrence is not certain or imminent.
	Urban and Small Stream Flood Advisory	Alerts the public to generally non-life-threatening flooding of streets and low-lying areas.
Flood Control and Prevention	Exclusive Flood Control Storage Capacity	The space in a reservoir reserved solely for regulating flood inflows to reduce flood damage.
	Flood Control Storage	Storage of water in reservoirs to abate flood damage.
	Flood Loss Reduction Measures	Strategies to reduce flood losses, including prevention, property protection, emergency services, and structural projects.
	Flood Prevention	Measures to keep flood problems from getting worse, including land acquisition, river channel maintenance, and floodplain regulations.
	Floodproofing	The process of protecting a building from flood damage, including dry and wet floodproofing techniques.
Flood Measurements and Data	100-year Flood Plain	The area that would be inundated in the event of a 100-year flood.
	E-3, Flood Stage Report	A form completed by a Service Hydrologist to document dates when forecast points are above flood stage, including crest dates and stages.
	E-5, Monthly Report of Flood Conditions	A report covering flood occurrences in the past month, including flood stages, crest dates, and climatic summaries.
	E-7, Flood Damage Report	A report documenting damage or loss of life due to flooding. It includes information on flood damage, measures taken, and areas affected.
	Flood Crest	The maximum height of a flood wave as it passes a certain location.
	Flood Frequency Curve	A graph showing the number of times per year, on average, that floods of a certain magnitude occur.
	Flood Hazard Outlook (FHO)	A high-level graphical depiction and key messages highlighting the potential threat of inland flood hazards for the next seven days.

Category	Term	Definition
	Flood of Record	The highest observed river stage or discharge at a given location during the period of record-keeping.
	Flood Plain	The portion of a river valley inundated by river water during historic floods.
	Flood Potential Outlook	An NWS outlook to alert the public of potentially heavy rainfall that could cause rivers and streams to flood.
	Flood Profile	A graph of the water surface elevation of a river in flood, plotted against distance, showing elevation at a given time, crests during a flood, or stages of concordant flows.
	Flood Routing	The process of determining the timing, shape, and amplitude of a flood wave as it moves downstream.
	Flood Stage	An established stage height where a rise in water surface level begins to create a hazard to lives, property, or commerce.
	Flood Statement (FLS)	A statement issued by the NWS to inform the public of flooding along major streams when there is no immediate threat to life or property.
	Flood Wave	A rise in streamflow to a crest and subsequent recession, often caused by precipitation, snowmelt, dam failure, or reservoir releases.
Urban and Regional Flooding	Urban and Small Stream Flooding	Flooding of small streams, streets, and low-lying areas, typically an inconvenience.
	Urban Flash Flood Guidance	A specific type of flash flood guidance estimating the amount of rain needed to cause flooding in urban areas over a specified period.
	Urban Flooding	Flooding of streets, underpasses, and low-lying areas, generally an inconvenience.
Miscellaneous	Direct Flood Damage	Damage to property, structures, goods, etc., by a flood, measured by the cost of replacement and repairs.
	Intangible Flood Damage	Damages due to business disruption, danger to health, shock, and loss of life, often requiring significant judgment for estimating.
	Lakeshore Flood Advisory	Alerts the public of potential minor flooding near lakes.
	Lowland Flooding	Inundation of low areas near rivers, often rural, but may also occur in urban areas.
	National Flood Summary	An NWS product providing nationwide information on current flood conditions.
	Partial-Duration Flood Series	A list of all flood peaks exceeding a chosen base stage or discharge, regardless of the number of peaks per year.
	Rapid Onset Flooding (ROF)	Rapid flooding in stream reaches forecast to double their flow within an hour, occurring within six hours of the causative event.

Category	Term	Definition
	River Flood Statement	Issued by the local NWS to update and expand information on the River Flood Warning. This statement may update or terminate a River Flood Warning.
	River Flood Warning	Issued by the local NWS when forecast points along rivers where flooding is forecasted, imminent, or in progress.
	River Flooding	The rise of a river to an elevation such that it overflows its natural banks.
	Snowmelt Flooding	Flooding caused primarily by melting snow.
	Urban and Small Stream Flood Advisory	Alerts the public to generally non-life-threatening flooding of streets and low-lying areas.
	Wet Floodproofing	Allowing a building to flood while taking measures to minimize damage, such as moving valuables to higher places or anchoring structures.

Note: Although the terms "Base Flood" and "100-year Flood" refer to the same statistical event (a flood with a 1% annual chance of occurrence), they are defined separately because they are used in distinct professional contexts. "Base Flood" is a regulatory term commonly used in floodplain management and insurance (e.g., FEMA regulations), while "100-year Flood" is more commonly used in hydrologic and engineering analyses.

Based on the available data and the relevance of various flood types to rail infrastructure, this report discusses specific types of flooding—particularly floods, flash floods, and coastal floods—in greater detail within the flooding analysis section. In the section on flooding events, the causes of train accidents due to flooding are analyzed first. Subsequently, all available data for flooding events, based on the USGS and NCEI datasets, are thoroughly examined.

Figure 1 has been developed for the flooding dataset. The process begins with various data sources, including the Rail Equipment Accident/Incident Data (READ), Hydrologic Unit Code (HUC), NCEI (NOAA), High-Water Marks (HWM) from USGS, and the U.S. Rail Network Shapefile (USRN). First, the financial impact and frequency of rail accidents caused by flooding are highlighted. Then, historical flood events are assigned to 12-digit HUC sub-watersheds. Following this, flood events are mapped to specific rail segments utilizing the 12-digit HUC.

Figure 1. Process Flowchart for Assigning Flood Events to Rail Infrastructure

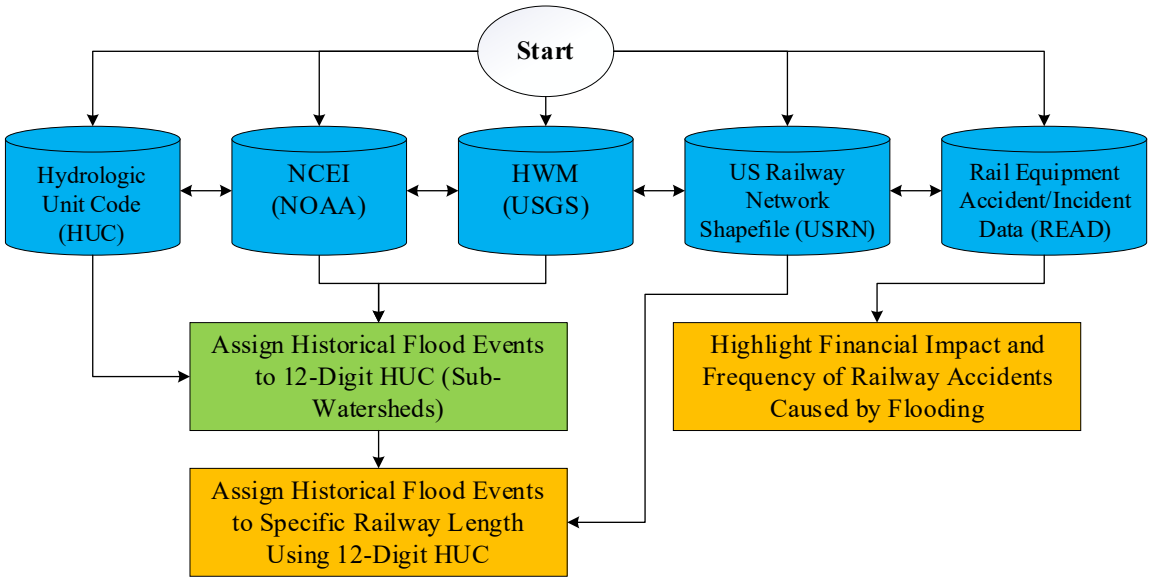

This process flowchart will be updated in upcoming reports or tasks to reflect any new methodologies, data sources, or analysis techniques as they are developed.

2.1 Train Accident Cause Codes

In this section of the report, the accident data related to track damage due to extreme environmental conditions has been analyzed, specifically focusing on incidents categorized under T002 (Washout/rain/slide/flood/snow/ice damage to track) and M103 (Extreme environmental condition – FLOOD). The data selected spans from the year 2000 to 2023, providing insights into the frequency and types of accidents that have occurred during this period.

T002 incidents amounted to 151 cases, with 134 of them (89%) resulting in derailments and the remaining 17 incidents (11%) attributed to obstructions and other specific accident types, as described in narrative reports of the data. While the majority of T002 incidents led to derailments, fewer were due to obstructions and other detailed accident types, indicating that T002 predominantly captures flood-driven events.

For M103 (Extreme environmental condition – FLOOD), there are 172 recorded accident cases. Of these, 99 incidents (57%) resulted in derailments, and the remaining 73 cases (43%) were related to side collisions, obstructions, other impacts, and other types of accidents as described in narrative reports. Figures 2 to 4 and Tables 2 to 4 have been included to show both the count and distribution of these accident types across the states.

Figure 2. The Frequency of T002 Accidents Across States from 2000 to 2023

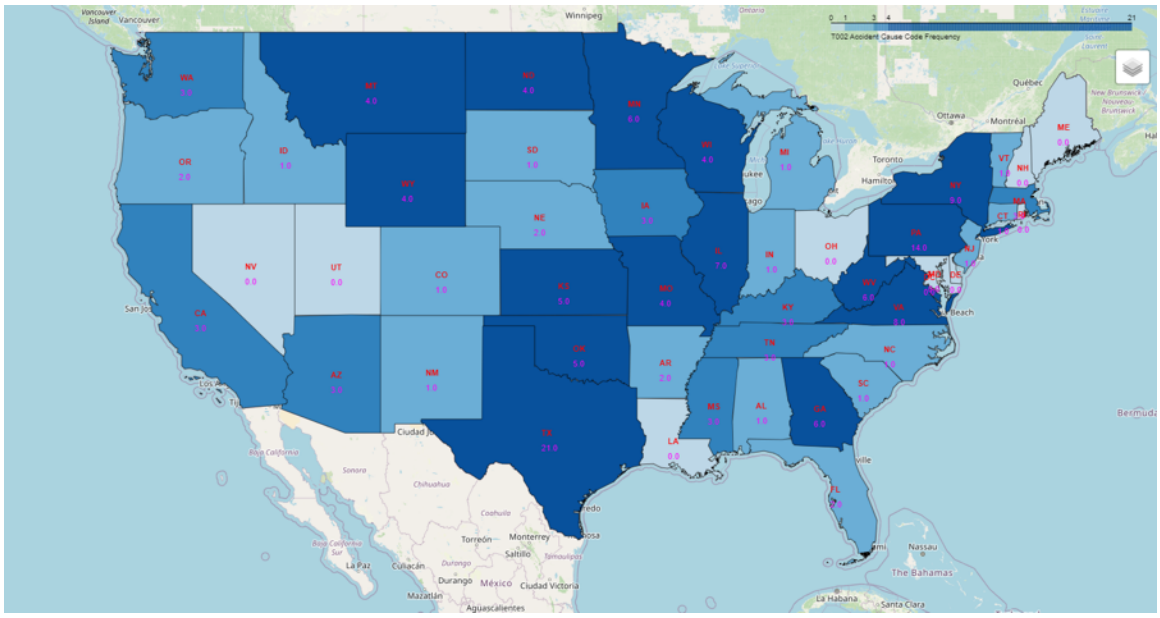

Figure 3. The Frequency of M103 Accidents Across States from 2000 to 2023

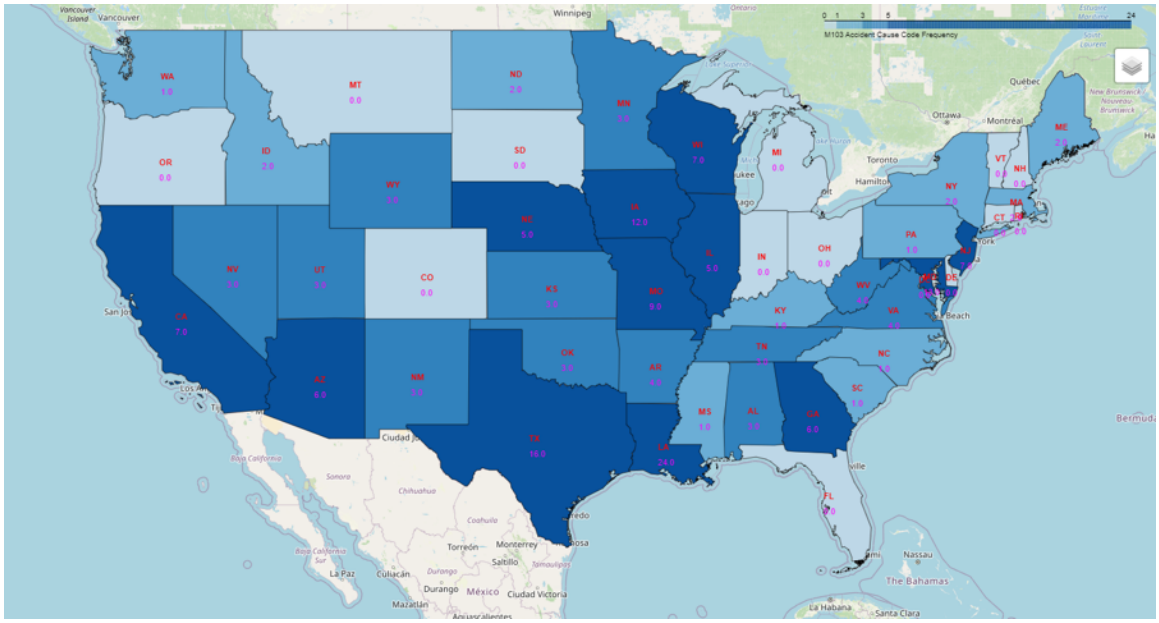

Figure 4. Accumulated Frequency of T002 and M103 Accidents Across States from 2000 to 2023

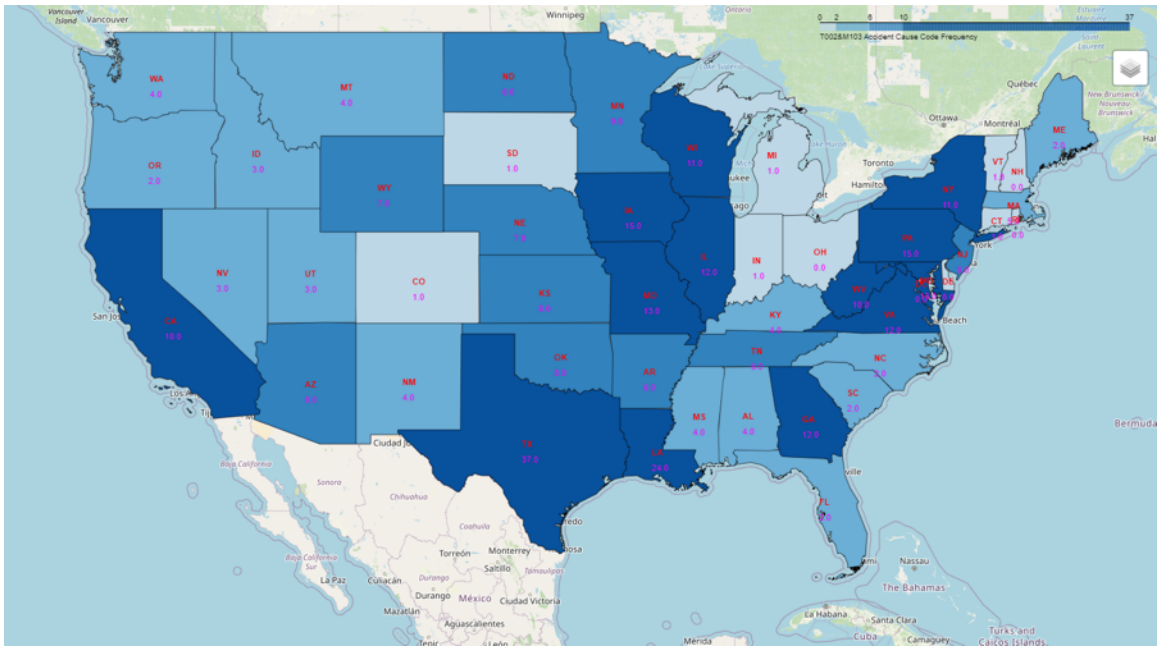

Table 2. The Frequency of T002 Accidents Across States from 2000 to 2023

State Name	T002	State Name	T002	State Name	T002
TEXAS	21	WISCONSIN	4	OREGON	2
PENNSYLVANIA	14	WYOMING	4	ALABAMA	1
NEW YORK	9	ARIZONA	3	COLORADO	1
VIRGINIA	8	CALIFORNIA	3	CONNECTICUT	1
ILLINOIS	7	IOWA	3	IDAHO	1
GEORGIA	6	KENTUCKY	3	INDIANA	1
MINNESOTA	6	MASSACHUSETTS	3	MICHIGAN	1
WEST VIRGINIA	6	MISSISSIPPI	3	NEW JERSEY	1
KANSAS	5	TENNESSEE	3	NEW MEXICO	1
OKLAHOMA	5	WASHINGTON	3	NORTH CAROLINA	1
MISSOURI	4	ARKANSAS	2	SOUTH CAROLINA	1
MONTANA	4	FLORIDA	2	SOUTH DAKOTA	1
NORTH DAKOTA	4	NEBRASKA	2	VERMONT	1

Table 3. The Frequency of M103 Accidents Across States from 2000 to 2023

State Name	M103	State Name	M103	State Name	M103
LOUISIANA	24	ARKANSAS	4	IDAHO	2
TEXAS	16	VIRGINIA	4	MAINE	2
MARYLAND	13	WEST VIRGINIA	4	MASSACHUSETTS	2
IOWA	12	ALABAMA	3	NEW YORK	2
MISSOURI	9	KANSAS	3	NORTH DAKOTA	2
CALIFORNIA	7	MINNESOTA	3	KENTUCKY	1
NEW JERSEY	7	NEVADA	3	MISSISSIPPI	1
WISCONSIN	7	NEW MEXICO	3	NORTH CAROLINA	1
ARIZONA	6	OKLAHOMA	3	PENNSYLVANIA	1
GEORGIA	6	TENNESSEE	3	SOUTH CAROLINA	1
ILLINOIS	5	UTAH	3	WASHINGTON	1
NEBRASKA	5	WYOMING	3		

Table 4. Accumulated Frequency of T002 and M103 Accidents Across States from 2000 to 2023

State Name	Total	State Name	Total	State Name	Total
TEXAS	37	KANSAS	8	IDAHO	3
LOUISIANA	24	NEW JERSEY	8	NEVADA	3
IOWA	15	OKLAHOMA	8	UTAH	3
PENNSYLVANIA	15	NEBRASKA	7	FLORIDA	2
MARYLAND	13	WYOMING	7	MAINE	2
MISSOURI	13	ARKANSAS	6	NORTH CAROLINA	2
GEORGIA	12	NORTH DAKOTA	6	OREGON	2
ILLINOIS	12	TENNESSEE	6	SOUTH CAROLINA	2
VIRGINIA	12	MASSACHUSETTS	5	COLORADO	1
NEW YORK	11	ALABAMA	4	CONNECTICUT	1
WISCONSIN	11	KENTUCKY	4	INDIANA	1
CALIFORNIA	10	MISSISSIPPI	4	MICHIGAN	1
WEST VIRGINIA	10	MONTANA	4	SOUTH DAKOTA	1
ARIZONA	9	NEW MEXICO	4	VERMONT	1
MINNESOTA	9	WASHINGTON	4		

It should be noted that Texas has the highest number of total accidents combining both T002 and M103 categories, with a total of 37 accidents, which is significantly more than any other state. In Louisiana, M103 stands out with the highest number of accidents at 24 but it does not appear in the top five for T002 accidents. Additionally, Iowa and Pennsylvania feature as being among the top five states according to both individual and accumulated accident frequencies.

The frequency of several other states—including Alabama, Colorado, Connecticut, Idaho, Indiana, Michigan, New Jersey, New Mexico, North Carolina, South Carolina, South Dakota, and Vermont—is also very low, with each reporting only one accident either in T002 or M103, indicating better safety records or lower incident reporting/occurrence. This moderate accident frequency is evidenced by Georgia, Illinois, and Virginia appearing consistently on both T002 and M103 lists. Three states—New York, Wisconsin, and California—took up a significant place in this list, each having a high number of cases that placed them in either T002 or M103 categories, though not at the very top. Lastly, the states with the lowest combined accidents, including those with only one case reported in either category, are Connecticut, Indiana, Michigan, South Dakota, and Vermont, highlighting potentially better safety measures or lower traffic volumes in these states.

Figure 5 illustrates the frequency of accidents with cause codes M103 and T002 from 2000 to 2023, showing distinct trends and fluctuations. M103 accidents exhibit pronounced peaks in 2005, 2014, and 2015, with the highest frequency of 20 in 2015, demonstrating precarious flood years that would be identified from the flood databases identified through this research's methodology. T002 accidents display a more consistent pattern, peaking at around 15 in 2002. In the 2020s, both accident types show fluctuating trends, with M103 maintaining higher peaks and T002 showing more stable changes. This data indicates a cyclical pattern in accident occurrences without a clear long-term trend.

Figure 5. Frequency of Accident Cause Code (M103 and T002)
from 2000 to 2023

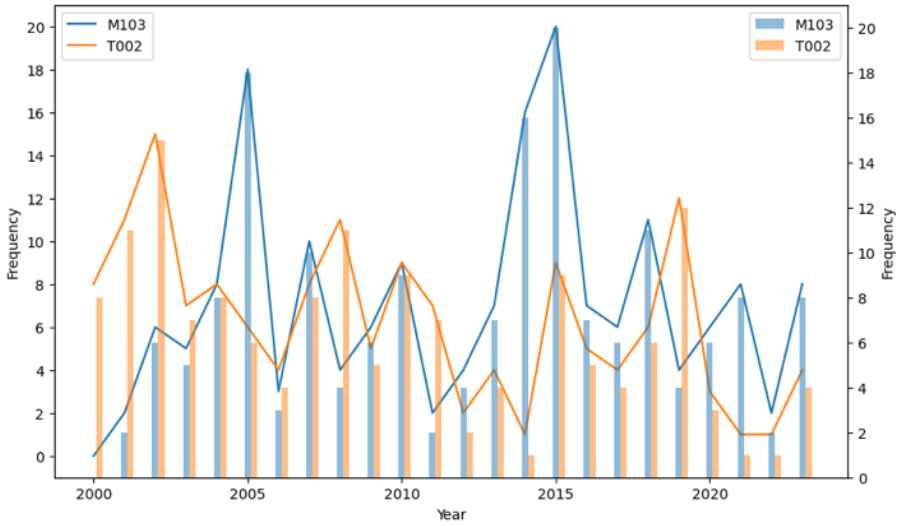

Figure 6 shows the accumulated frequency of accidents with cause codes M103 and T002 from 2000 to 2023, revealing a cyclical pattern with peaks around 2015, with the highest frequency of nearly 30 in 2015. The early 2020s indicate a lower frequency, which may reflect actual improvements in safety measures or changes in reporting practices, such as stricter classification protocols or revisions in how accident causes are documented. Overall, the data highlights fluctuating accident occurrences over the 23-year period.

Figure 6. Accumulated Frequency of Accident Cause Code (M103 and T002)
from 2000 to 2023

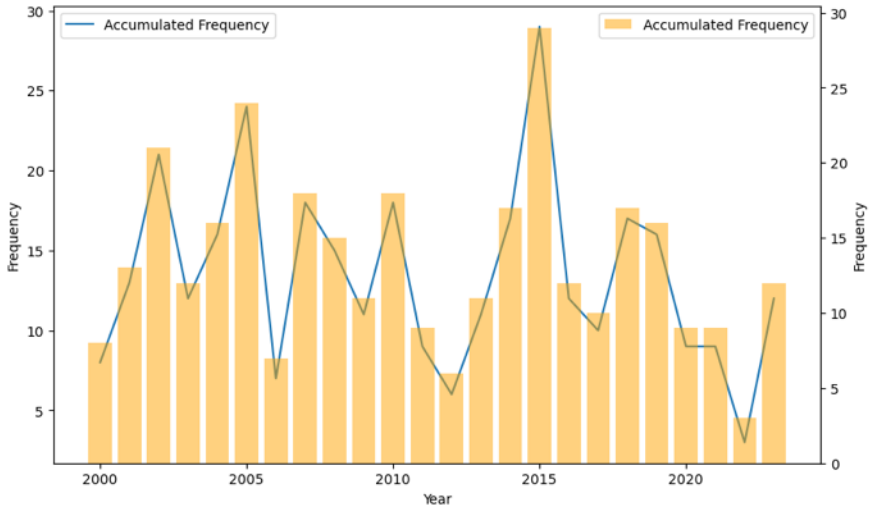

In the accident dataset, there are two types of damage cost for each accident: equipment damage and track damage. There are some accident rows in the dataset where the Total Damage Cost

(based on the dataset) exceeds the sum of the two types of accidents (sum of equipment and track). It is not explained in the dataset what the source of this difference is, and here it has been considered as other costs.

For both M103 and T002, statistics are provided, followed by an accumulated frequency analysis for both categories combined (Tables 5 to 7 and Figures 7 to 9).

Table 5. Breakdown of T002 Accident Damage Costs (2000-2023)

Accident Type	Equipment Damage Cost	Track Damage Cost	Other Costs	Total Damage Cost
Derailment	$39,998,074	$26,523,766	$2,133,462	$68,655,302
Non-Derailment (Other Accidents)	$821,714	$5,993,710	$5,250,000	$12,065,424
Total	$40,819,788	$32,517,476	$7,383,462	$80,720,726

Figure 7. (a) Proportion of Damage Costs for Derailments in T002 Accidents, (b) Proportion of Damage Costs for Non-Derailments in T002 Accidents, (c) Proportion of Total Damage Costs for All T002 Accidents

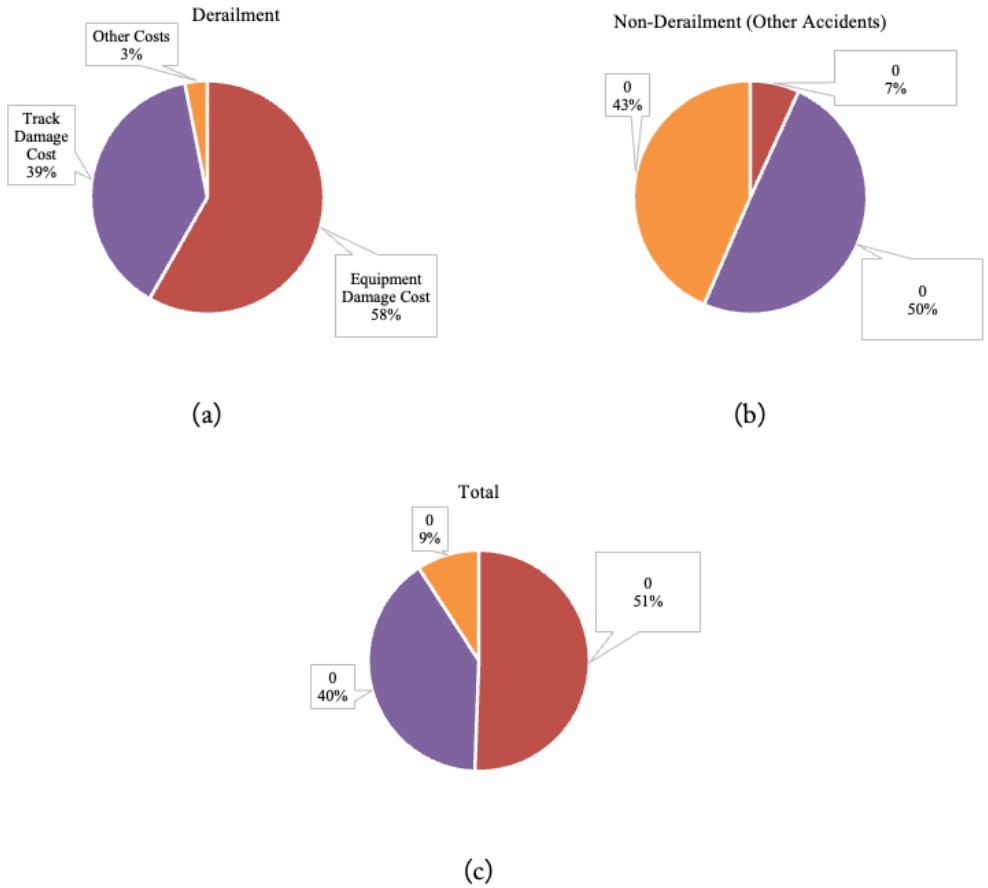

The T002 Accident Cause Code Frequency data shows that derailments account for most of the total damage cost, amounting to $68,655,302, compared to non-derailment accidents which cost $12,065,424. Derailments primarily incur equipment damage (58%), followed by track damage (39%) and other costs (3%). Non-derailment accidents have a significant portion of their costs attributed to track damage (50%) and other costs (43%), with equipment damage being much lower at 7%. Overall, the total damage costs for T002 accidents amount to $80,720,726, with 51% of these costs related to equipment damage, 40% to track damage, and 9% to other costs.

Table 6. Breakdown of M103 Accident Damage Costs (2000-2023)

Accident Type	Equipment Damage Cost	Track Damage Cost	Other Costs	Total Damage Cost
Derailment	$74,867,084	$35,086,804	$6,777,414	$116,731,302
Non-Derailment (Other Accidents)	$11,366,703	$7,763,953	$34,042,146	$53,172,802
Total	$86,233,787	$42,850,757	$40,819,560	$169,904,104

Figure 8. (a) Proportion of Damage Costs for Derailments in M103 Accidents, (b) Proportion of Damage Costs for Non-Derailments in M103 Accidents, (c) Proportion of Total Damage Costs for All M103 Accidents

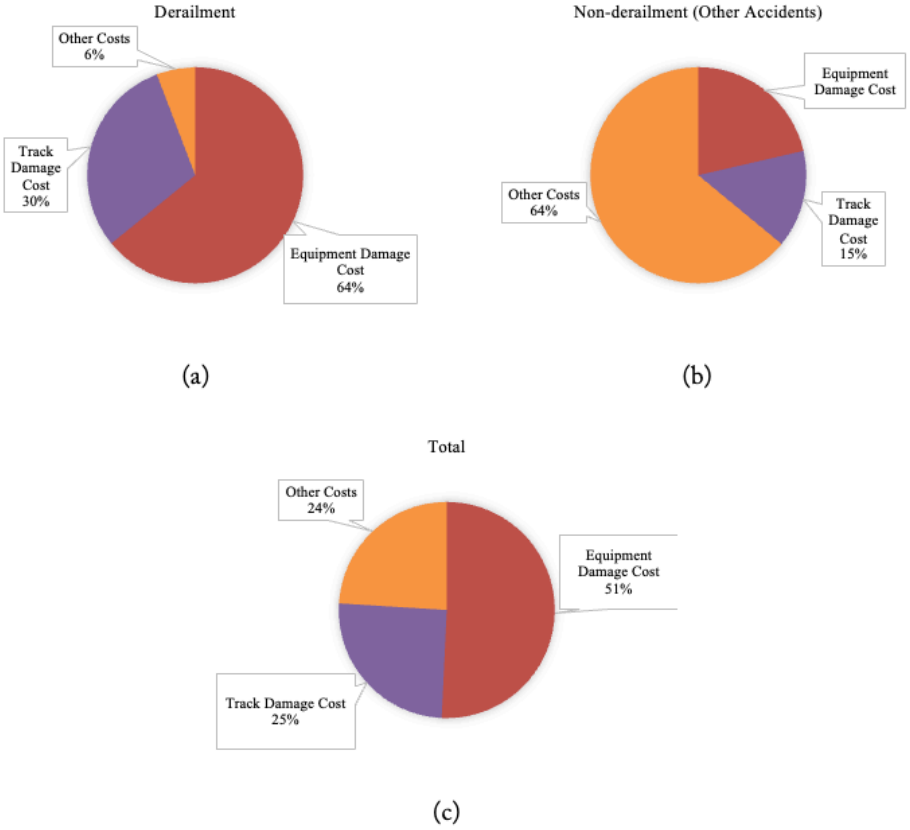

The M103 Accident Cause Code Frequency data reveals that derailments contribute significantly to the total damage cost, amounting to $116,731,302, with equipment damage at 64%, track damage at 30%, and other costs at 6%. In contrast, non-derailment accidents total $53,172,802, with other costs at 64%, track damage at 15%, and equipment damage at 21%. Overall, the total damage costs for M103 accidents reach $169,904,104, with 51% from equipment damage, 25% from track damage, and 24% from other costs.

Table 7. Combined Breakdown of T002 and M103 Accident Damage Costs (2000-2023)

Accident Type	Equipment Damage Cost	Track Damage Cost	Other Costs	Total Damage Cost
Derailment	$114,865,158	$61,610,570	$8,910,876	$185,386,604
Non-Derailment (Other Accidents)	$12,188,417	$13,757,663	$39,292,146	$65,238,226
Total	$127,053,575	$75,368,233	$48,203,022	$250,624,830

Figure 9. (a) Proportion of Damage Costs for Derailments in Combined T002 and M103 Accidents, (b) Proportion of Damage Costs for Non-Derailments in Combined T002 and M103 Accidents, (c) Proportion of Total Damage Costs for All Combined T002 and M103 Accidents

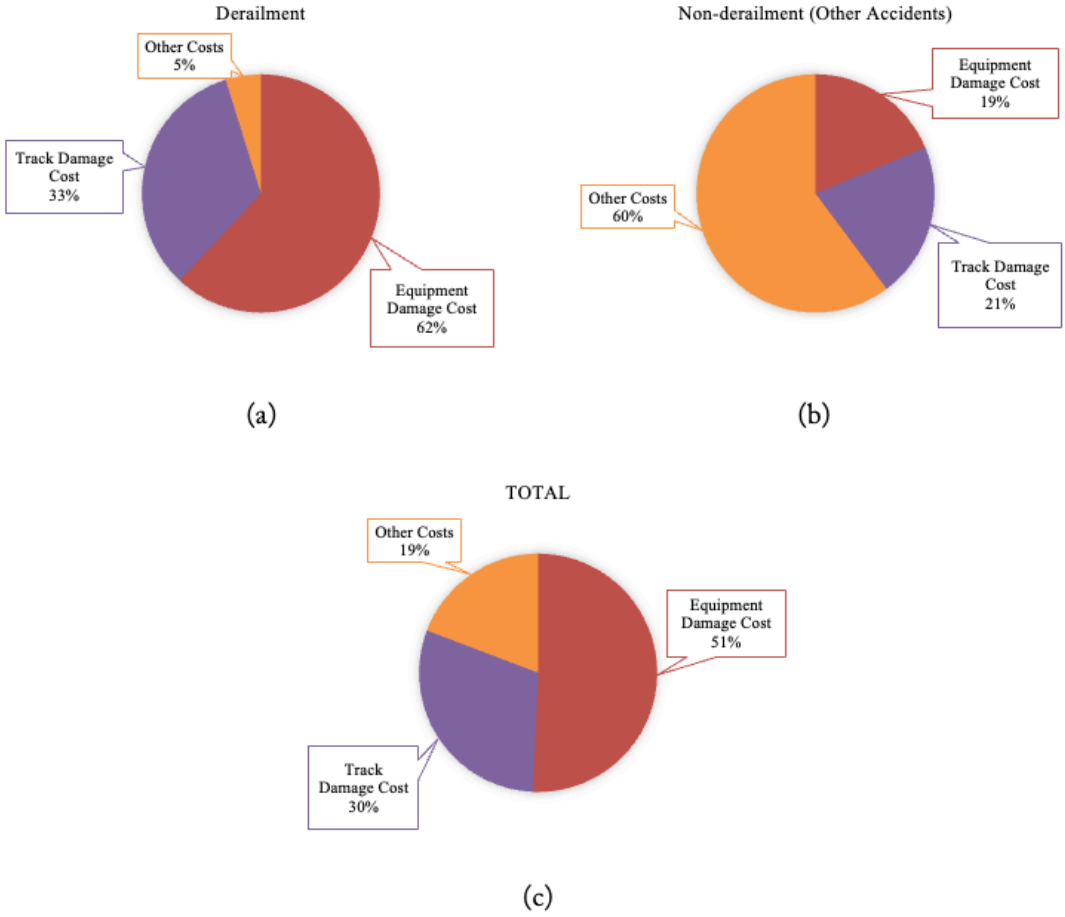

The combined data for T002 and M103 Accident Cause Code Frequency highlights a total damage cost of $250,624,830, with derailments alone costing $185,386,604 and non-derailments costing $65,238,226. Derailments incur significant equipment damage (62%) and track damage (33%), with other costs being minimal (5%). In contrast, non-derailments have a higher proportion of other costs (60%), with equipment damage at 19% and track damage at 21%. The total damage costs are distributed with equipment damage accounting for 51%, track damage accounting for 30%, and other costs accounting for 19%, reflecting the substantial financial impact of these accidents.

The analysis of T002 and M103 accident cause codes from 2000 to 2023 reveals significant insights into the financial impact and frequency of derailments and other accident types. The combined total damage cost of these accidents exceeds $250 million, with equipment damage being the most substantial cost component. This analysis is crucial for understanding the financial burden of

extreme environmental conditions on rail infrastructure, highlighting the need for improved safety measures and targeted interventions to mitigate these high-cost incidents.

The United States Geological Survey (USGS) Flood Event Viewer (FEV) and the National Centers for Environmental Information (NCEI) provide comprehensive datasets on historical flooding events across the United States. These datasets offer valuable insights into the patterns, frequencies, and impacts of floods over the years. Understanding this data is crucial for the U.S. rail network, as flooding poses significant risks to rail infrastructure, causing disruptions, damage, and delays. By analyzing data from these sources, we can better understand the historical context of flooding events. Below, we will investigate flooding events from the mentioned sources in greater detail.

2.1 Hydrologic Unit Code

The Hydrologic Unit Code (HUC) dataset is a ready-made national-level set of geographical polygons derived from land surface areas divided into drainage divisions at various levels or scales (U.S. Geological Survey and U.S. Department of Agriculture–Natural Resources Conservation Service, 2013). HUC is a numerical code assigned to a particular hydrologic unit or drainage area, which consists of a two-digit sequence for each level in the hierarchical delineation system (U.S. Geological Survey and U.S. Department of Agriculture–Natural Resources Conservation Service, 2013). The eight different levels of hydrologic units and their characteristics are shown below (Table 8).

Table 8. Hydrologic Unit Code (HUC) Levels and Characteristics (U.S. Geological Survey and U.S. Department of Agriculture-Natural Resources Conservation Service, 2013)

Hydrologic Unit Name	Historical Name	Average Size (Square Miles)	Approximate Number of Hydrologic Units
2 digit	Region	177,560	21 (Actual)
4 digit	Subregion	16,800	222
6 digit	Basin	10,596	370
8 digit	Subbasin	700	2,270
10 digit	Watershed	227 (40,000–250,000 Acres)	20,000
12 digit	Sub-watershed	40 (10,000–40,000 Acres)	100,000
14 digit	(None)	Open	Open
16 digit	(None)	Open	Open

In this report, the 12-digit Hydrologic Unit Codes (HUCs) were utilized as the primary geographical framework.

Figure 10. Water Resource Region - Wikipedia

Figure 11. Hydrologic Unit Codes (HUCs) - 12-Digit

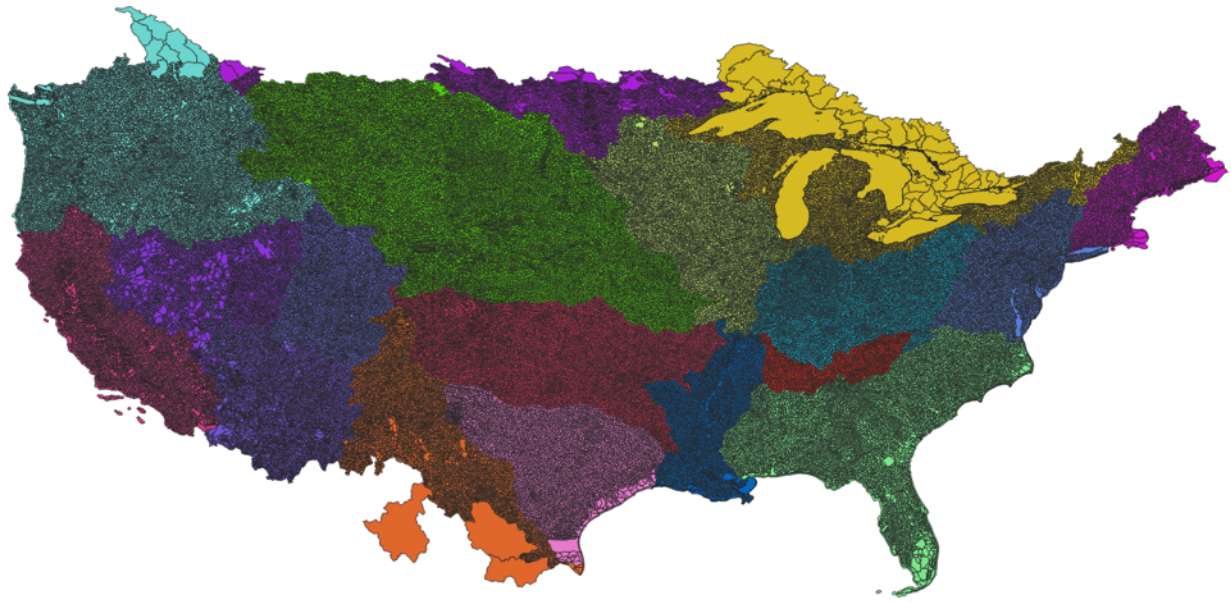

The United States is divided into 21 main geographic areas or regions, according to the first level of taxonomy. These geographical areas comprise either the combined drainage areas of several rivers, such as the Texas-Gulf region, which comprises several rivers emptying into the Gulf of

Mexico, or the drainage area of a major river, such as the Missouri region. Eighteen of the regions occupy the land area of the conterminous United States. Region 19 is constituted by Alaska, Region 20 by the Hawaii Islands, and Region 21 by Puerto Rico and other adjacent Caribbean islands ("Hydrologic Unit Maps - USGS," 2024). The method for utilizing the 12-digit hydrologic unit code to analyze and assign historical flooding events to the U.S. rail network is explained in Section 2.3.

2.3 HWMs Data from USGS STN Flood Event Database

The Short-Term Network (STN), a wide-ranging database meant for recording and evaluating floods, is being run under the United States Geological Survey (USGS). It can be accessed through an easy-to-use internet interface or queried using RESTful API (https://stn.wim.usgs.gov/STNDataPortal/). In the STN, there are several kinds of data which include sensors data, peak summary data, and HWMs. Of all types of flooding events, HWMs provide important information about their extent and impacts. In this section, the dataset on HWMs will be analyzed to assess the severity and patterns of flooding incidences.

The USGS STN Flood Event Data Download interface allows users to customize and download flood event data. This tool provides flexible options for accessing detailed flood event data.

Event Options:

- Event Type: Select the type of event (e.g., Riverine Flood, Hurricane, Tsunami).
- Event Name: Choose from specific events.
- Event Status: Filter by active or completed events.

Location Options:

- State: Select the state for data retrieval.
- County: Narrow down to specific counties.

Data Type Options:

- Data Type: Choose between Sensor Data, HWMs Data, and Peak Summary Data.
- Additional Filters: Customize by sensor type, status, collection condition, and deployment type.

Get Data:

- Download: Data can be downloaded in CSV format.
- REST URLs: Access data via RESTful API for advanced use.

Figure 12 and 13 represent the USGS Flood Event Viewer interface and Data Download screen.

Figure 12. Flood Event Viewer (*USGS n.d.*)

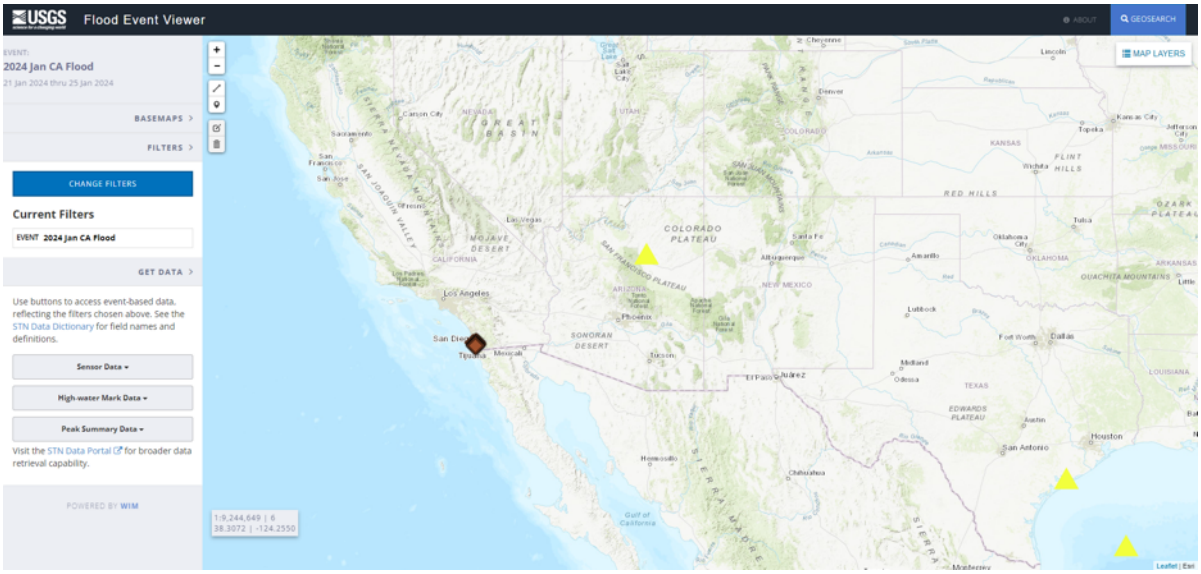

Figure 13. STN Flood Event Data Download (*USGS n.d.*)

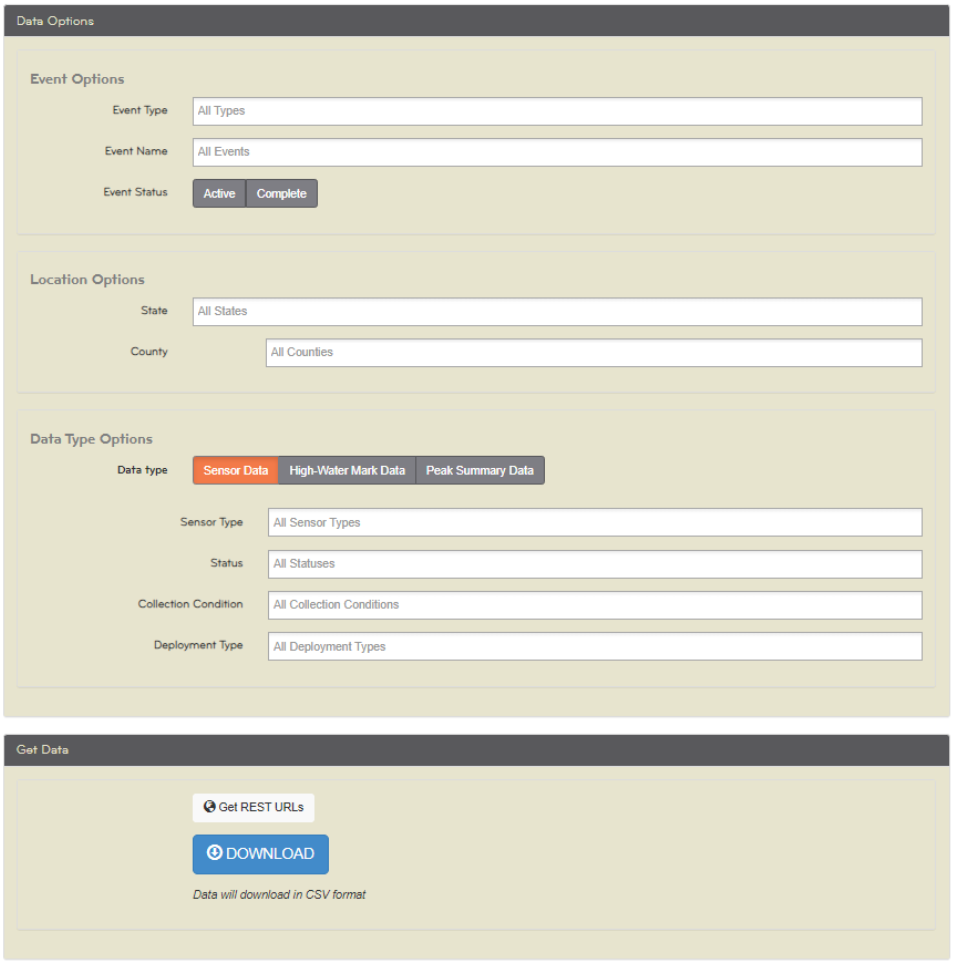

Figures 14 to 16 show a map of the United States with marked locations representing HWM points collected between 1903 and 2024. The key insights from this map are:

- **Total HWM Points:** There are 23,721 HWM points recorded, indicating extensive data collection on flood events over the years.
- **Bridge-Related HWM Points:** Out of 23,721 HWM points, 8,341 HWM points have descriptions mentioning a bridge, highlighting locations where flood events impacted bridge infrastructure.
- **Geographic Distribution:** The map highlights significant clusters of HWM points, especially in the eastern United States, the Ohio River Valley, the middle northern states, and along the Mississippi River. California also shows notable clusters in the Los Angeles and San Diego areas, indicating higher flood activity in these regions.

Figure 14. USGS Flood Event Points (HWM) Spanning 1903 to 2024

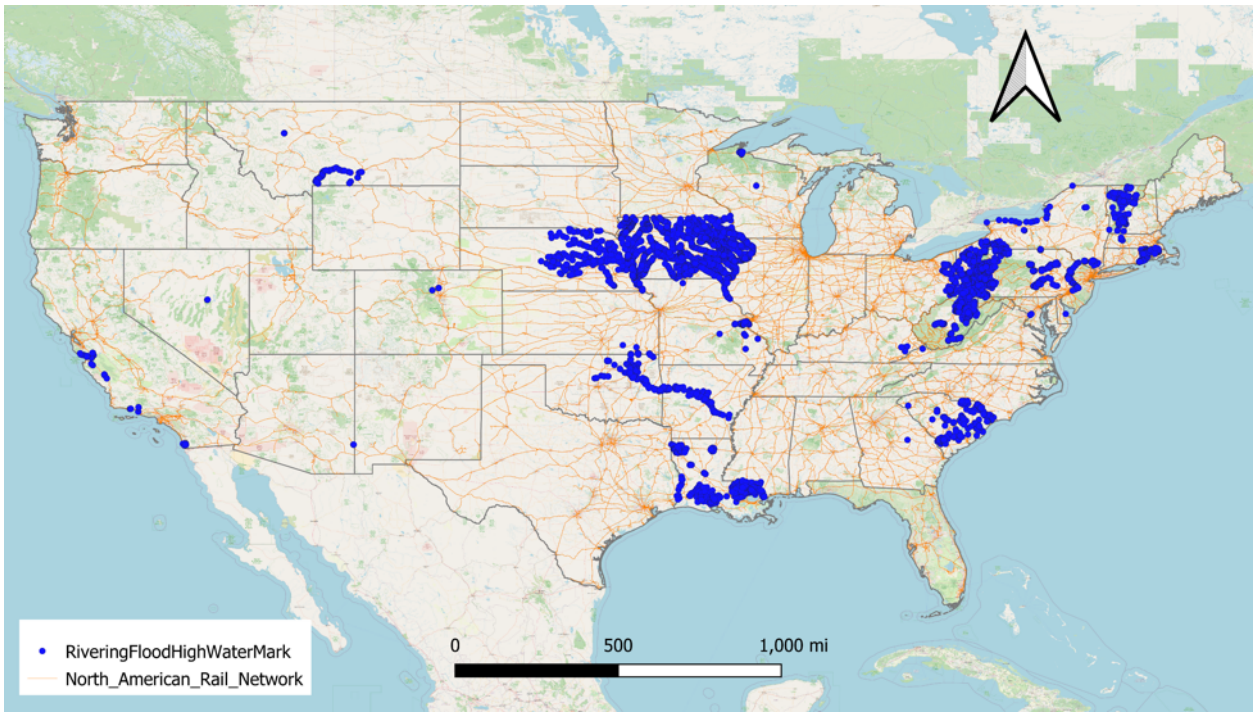

Figure 15. Distribution of Flood Points Across States (1903-2024)

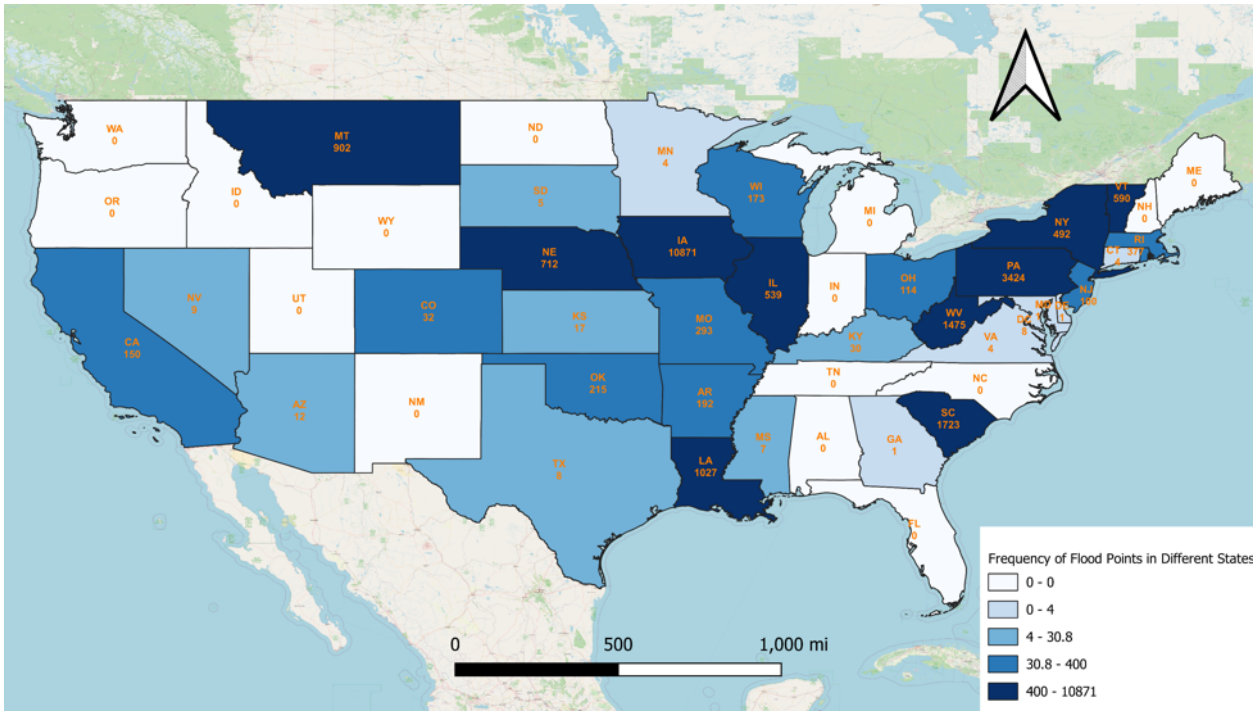

Figure 16. USGS Flood Event Points with State-Wise Breakdown Highlighting the Top 10 States (1903 to 2024)

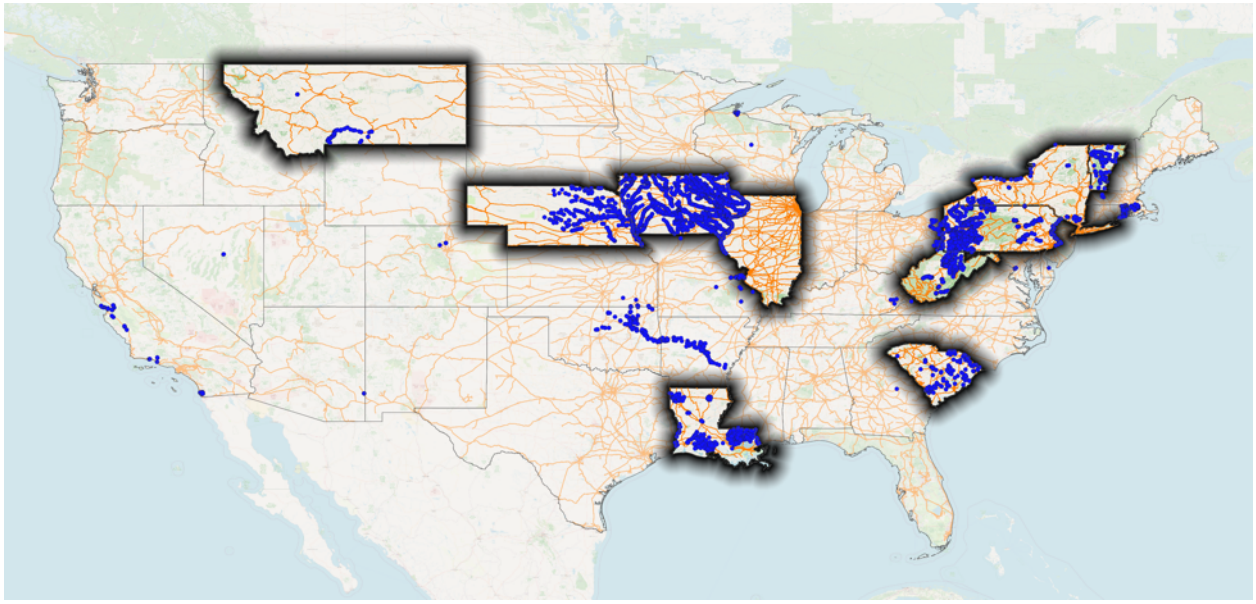

This section of the report focuses on HWMs data collected between 2000 and 2024. Based on the most recent changes in climate patterns, this timeframe leverages the most accurate and technologically advanced data available. Figures 17 and 18 showcase riverine flood HWMs data from 2000 to 2024 across the United States, highlighting key locations where significant flooding events have been recorded. The key insights from this map are:

- **Total HWM Points:** There are 8,904 HWM points recorded, predominantly located in the Mississippi, Missouri, and Arkansas river valleys, while some points were recorded from other flooding events in the northeast. It should be noted as well that this is not an entire collection of flood events; however, these are extensive collections of several flood events, in which a single event may have over 1000 data points.

- **Geographic Distribution:** The distribution is similar to the data from 1903 to 2024, but the frequency of HWM points is notably higher in the central United States, particularly around the Mississippi River.

Figure 17. Distribution of Flood HWMs Across States (2000-2024)

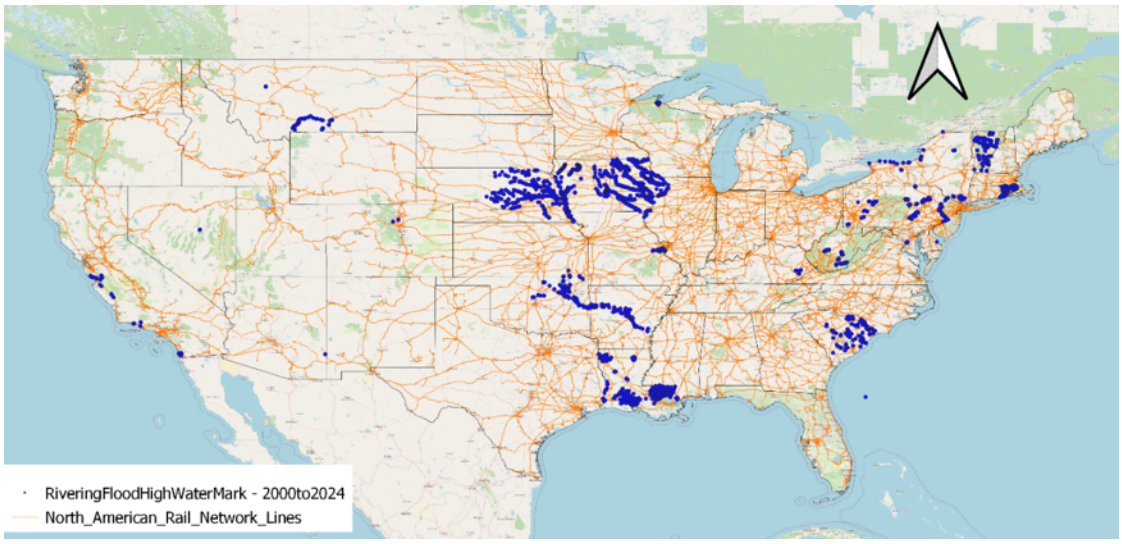

Figure 18. Frequency of Flood HWMs Across States (2000–2024)

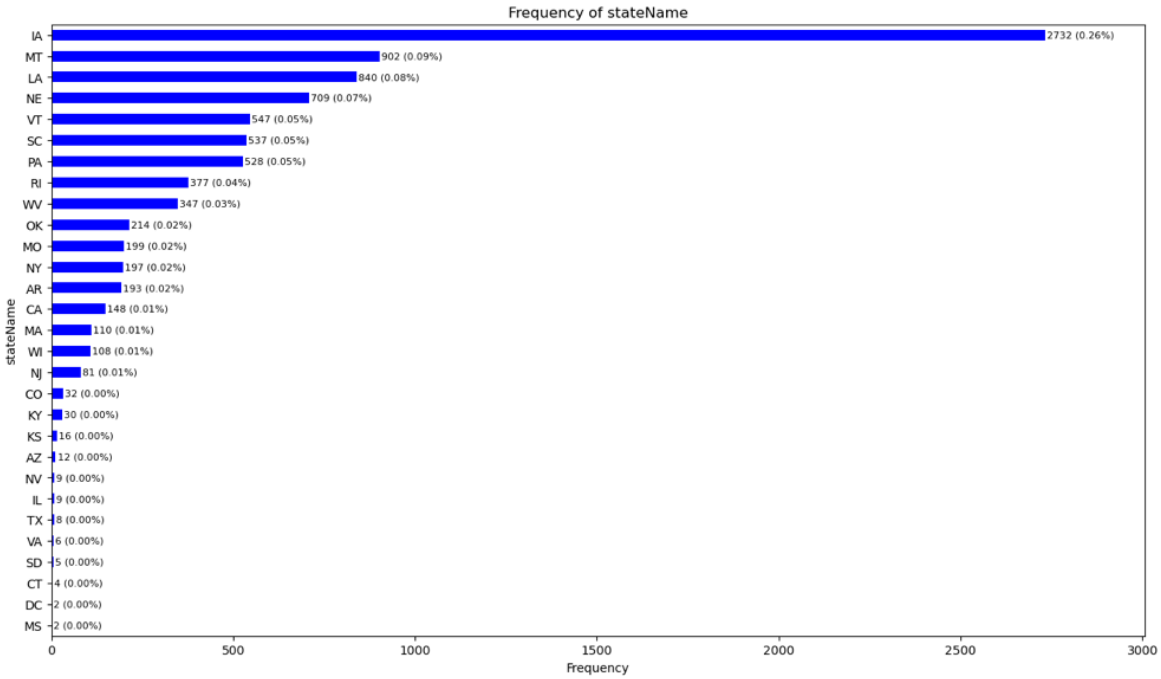

An analysis of various hydrological data collected between 2000 and 2024 is presented in this section of the report. A series of charts provide an overview of data related to (HWMs), Vertical Datum Names, Marker Names, State Names, Event Names, Water Names, and the frequency of survey events. Each chart illustrates different aspects of flood events as recorded by the USGS Flood Event Viewer (FEV). Using these datasets, we can gain a deeper understanding of the

distribution, frequency, and characteristics of flood events over time. This section of the report is structured to discuss each of these aspects in detail, beginning with HWM Type and Quality, followed by an analysis of Vertical Datum and Method Names, and so forth.

Analysis of HWM Types and Quality Distributions

Figure 19 shows the frequency of different types of HWMs observed. Below is a description of each of the variables captured from this dataset.

1. **Debris:** Is a type of HWM generated by lines left by water indicating the high-water levels on the surface or object.

2. **Seed Line:** The second most frequent, with 2,645 occurrences, making up 29.71% of the data. Seed lines, formed by seeds deposited by receding waters, also serve as significant evidence of high-water points.

3. **Mud:** Recorded 1,256 times, representing 14.11% of the observed HWMs. Mud lines indicate areas where sediment was deposited as water levels decreased.

4. **Other (Note in Description Box):** This category, with 1,233 entries (13.85%), includes various unspecified types that would require further detail from descriptions.

5. **Stain Line:** With 808 observations (9.07%), these are marks left by water on structures or vegetation indicating the height of water.

6. **Vegetation Line:** Accounted for 123 observations or 1.38%. These are formed by materials like leaves and twigs deposited at the highest reach of water.

7. **Present at Peak (direct observation):** Observed 93 times (1.04%), where the observer was present at the time the peak water level occurred.

8. **Wash Line:** These marks, seen 51 times (0.57%), are created by small waves washing up debris and other materials, indicating transient high-water.

9. **Clear Water:** Least frequently observed with 9 occurrences (0.10%), these are likely areas where water was clear enough to see the actual depth.

Figure 19. Distribution of HWM Types in Flood Analysis (2000-2024)

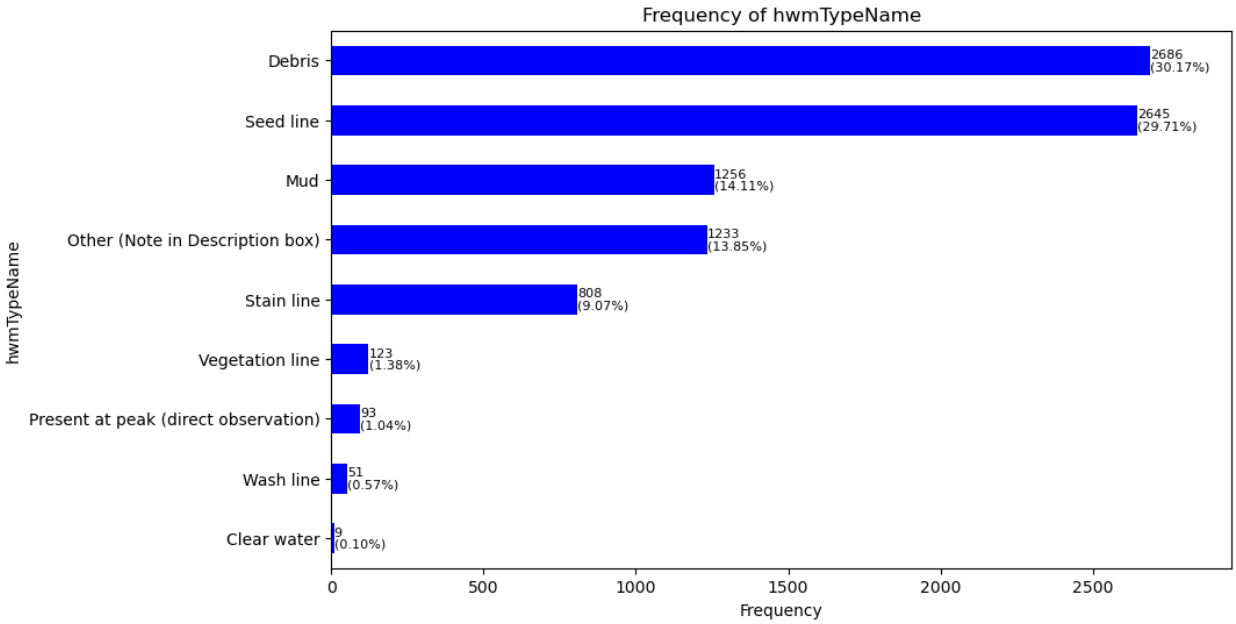

This distribution provides insight into the common physical indicators of flood extents. Each type of HWM offers different levels of reliability and may be influenced by environmental factors. Figure 20 presents the distribution of the quality ratings for HWMs, where the quality type is a function of the available equipment used in reference to elevation datums, and clear evidence provided from Figure 19.

Figure 20. Quality Distribution of HWMs

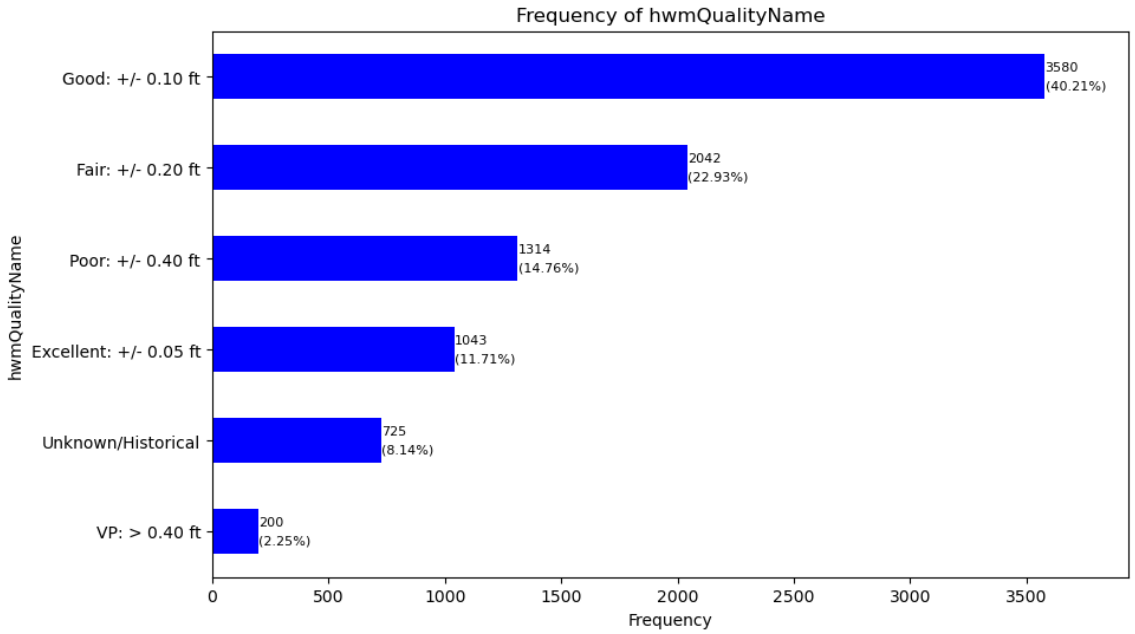

Figure 21 provides an overview of the types of markers used in documenting HWMs. The types of markers used are described below:

1. **Nail and HWM Tag:** The most prevalent marker, used 1,808 times, representing 20.31% of all instances. This method typically involves using both a nail and a specific tag designed to indicate high-water levels, providing a durable and easily identifiable mark.

2. **Marker:** A general category, possibly referring to any standard marking tool, noted 1,175 times, representing 13.20% of all instances.

3. **Not Marked:** Surprisingly, 1,048 instances (11.77%) were recorded where no physical marker was used. This could suggest observational records or instances where marking was not possible.

4. **Nail:** Similar to the "Nail and HWM Tag" but using only a nail, found in 1,047 cases (11.76%). This method is simple and quick, providing a semi-permanent mark.

5. **Stake:** Used 547 times (6.14%), stakes are a traditional method for marking boundaries and levels in field surveys.

6. **Other (Note in Description Box):** Comprises various unspecified methods, totaling 456 occurrences (5.12%).

7. **Tape:** This method was recorded 247 times (2.77%). It typically refers to flagging tape or measuring tape used to indicate specific points in the field. Tape is lightweight, easy to apply, and highly visible, making it suitable for temporary markings.

8. **Paint:** With 226 instances (2.54%), this involves marking with paint, which can be visible and durable but may degrade over time.

9. **Chiseled Mark:** Used 22 times (0.25%), this is a very permanent method, involving chiseling onto a hard surface, such as a road, bridge, or curb.

10. **Chalk Test:** The least frequent, noted 17 times (0.19%), which might be used for temporary or preliminary marking.

Figure 21. Frequency of Marker Types Used in HWMs Documentation

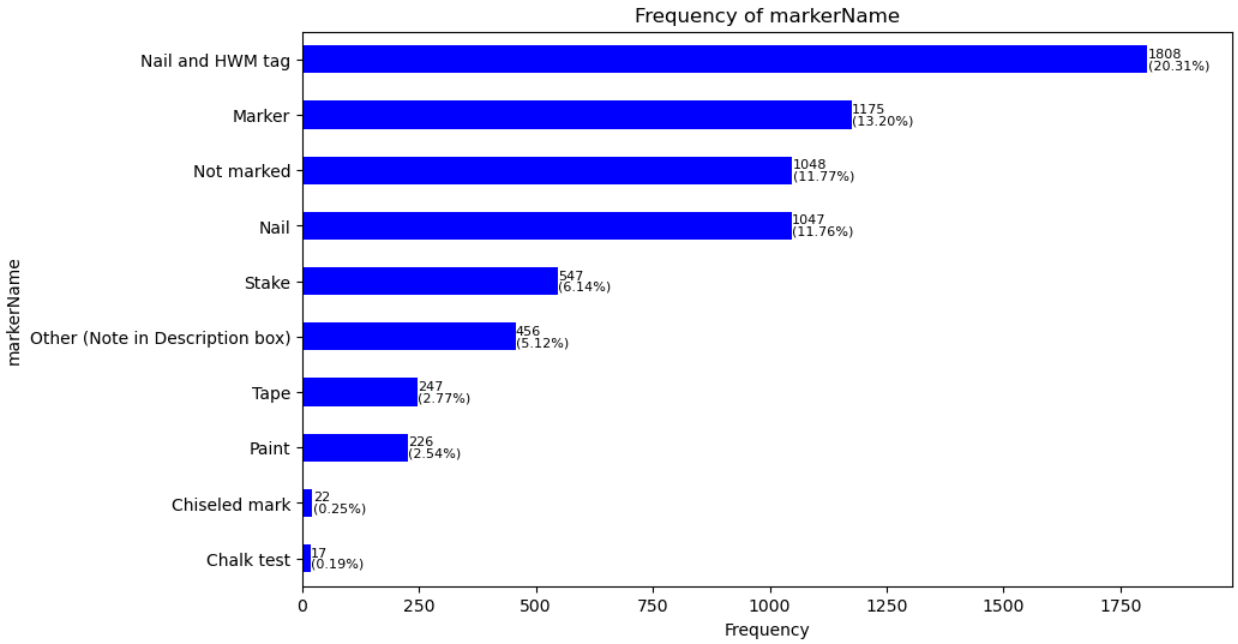

Moving from a review of the marker types used within the highwater mark dataset, the specific and most frequent events that have associated water marks are described below and shown in Figure 22:

- Central U.S. Spring 2019 Flood: 1,549 HWMs (17.40%)
- 2022 June MT Flood: 852 HWMs (9.57%)
- 2023 July MA NV VT Flood: 717 HWMs (8.05%)
- 2008 May IA Flood: 702 HWMs (7.88%)
- 2016 August LA Flood: 586 HWMs (6.58%)

Other significant flood events with notable HWM counts are:

- 2010 March–April RI MA Flood: 491 HWMs (5.51%)
- 2016 June WV Flood: 347 HWMs (3.90%)
- 2018 June–July IA Flood: 280 HWMs (3.14%)
- 2015 October SC DOT Bridge: 326 HWMs (3.66%)

Additionally, the chart captures various less frequent flood events, such as:

- 2022 December–2023 January CA Flood: 78 HWMs (0.88%)
- 2016 August IA Flood: 64 HWMs (0.72%)
- 2023 March Atmospheric Rivers Flood: 32 HWMs (0.36%)
- Flood Shakedown Test 2015: 19 HWMs (0.10%)
- 2006 June NY PA DE MD NJ VA Flood: 3 HWMs (0.03%)

This comprehensive overview illustrates the varied frequency of HWMs across different flood events over the years, highlighting both significant and less frequent occurrences, with a particular focus on major flood incidents and their impact on data collection efforts.

Figure 22. Frequency of HWMs in Flood Events (2000–2024)

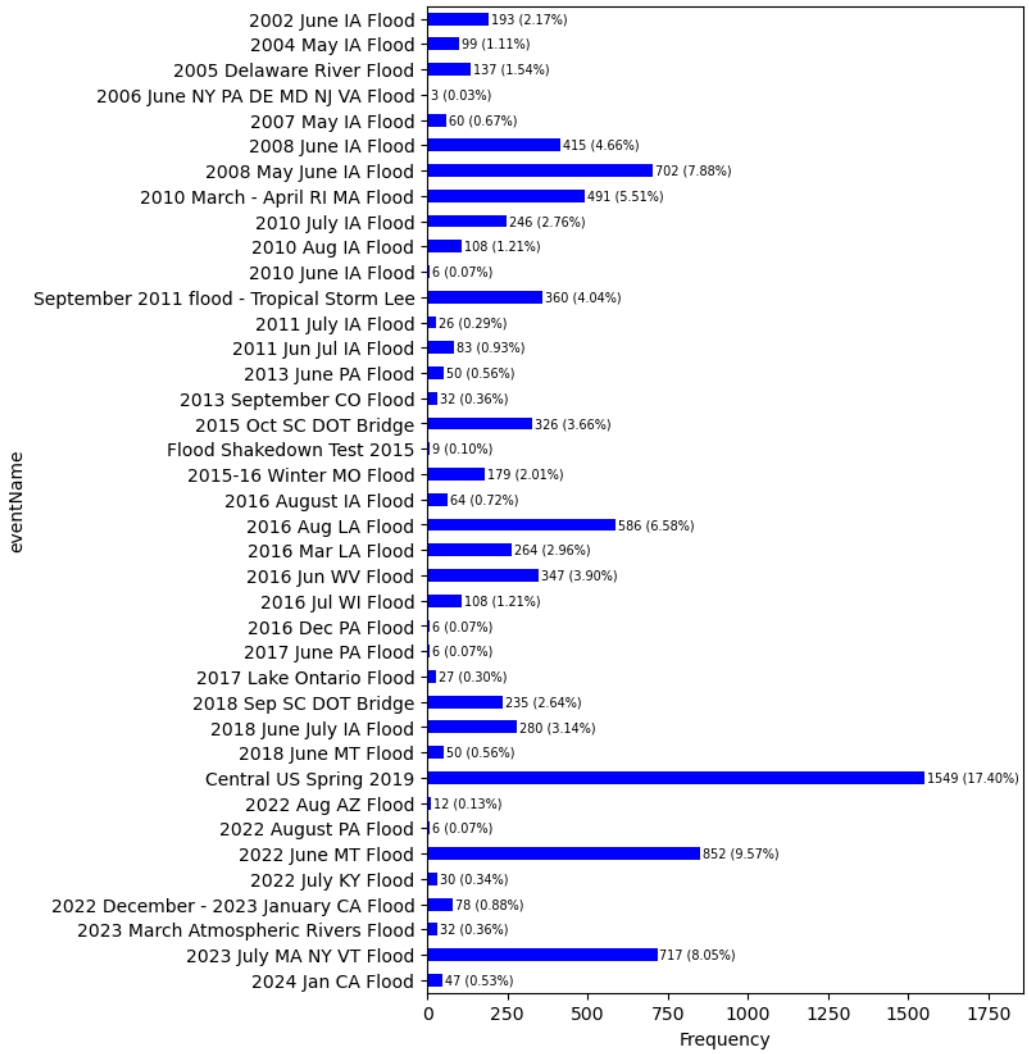

Moving to Figure 23, the majority of survey observations occurred during the spring and summer months, with notable peaks in May, June, and July. The elevated frequency in these months reflects seasonal flooding patterns, including both springtime snowmelt and summertime precipitation events.

Figure 23. Monthly Frequency of Survey (2000–2024)

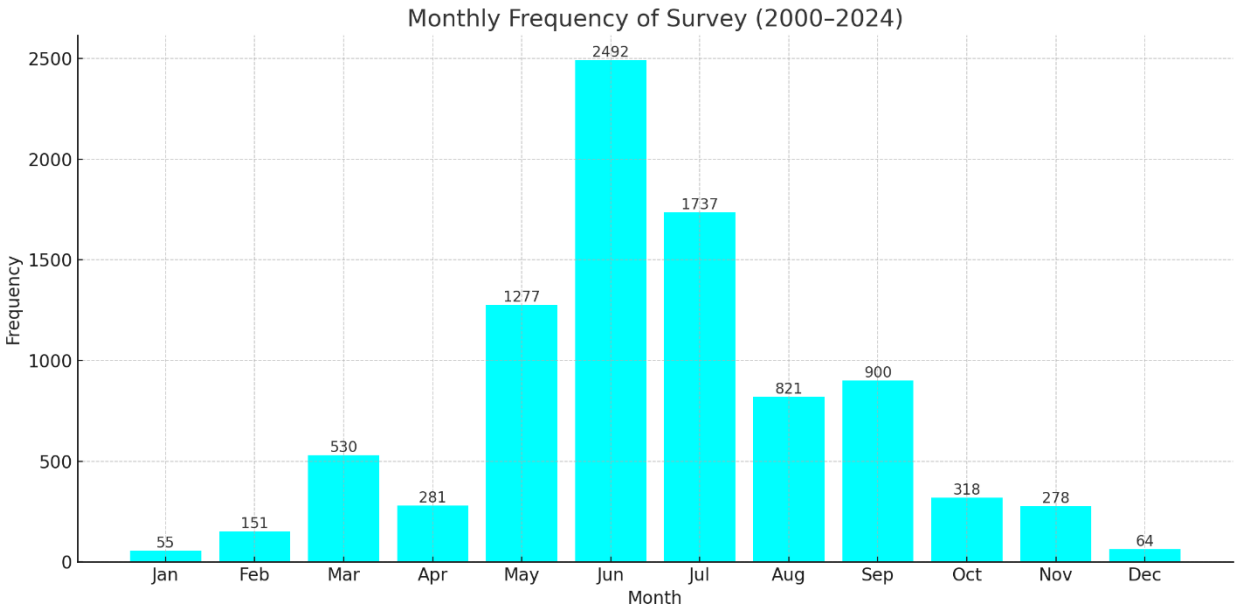

Lastly, the HWMs dataset includes the recorded height of each watermark above ground level (Figure 24). The majority of HWMs are recorded at the following heights:

- **Zero & under 0 feet:** 731 instances (16.0%)
- **0–3 feet:** 1,851 instances (40.6%)
- **3–6 feet:** 1,468 instances (32.2%)
- **6–9 feet:** 385 instances (8.4%)

There are significantly fewer records at heights above 9 feet, with only 94 instances (2.1%) for 9–12 feet, and even fewer at higher intervals. This distribution indicates that most HWMs are recorded at lower elevations, with a sharp decline in frequency as the height increases. This output is important and will be used in future methods to link water levels with physical features near the track—such as estimating how deep the water was and how fast it was moving, both of which can help assess the risk of damage to the railway substructure.

Figure 24. Frequency of Height Above Ground (2000–2024)

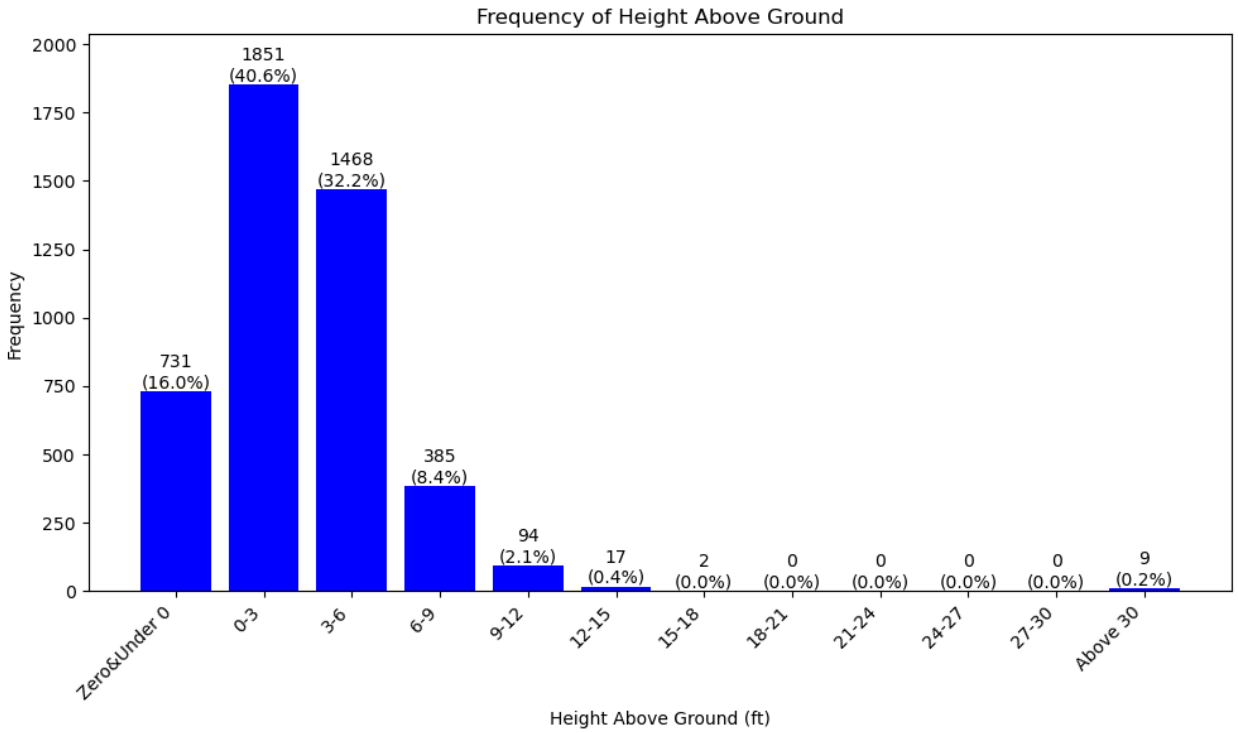

Assigning the USGS Flood Events to the U.S. Rail Network

As mentioned in earlier sections, there are 39 distinct flood events from 2000 to 2024 in the USGS dataset. In this context, "assigning" refers to the process of establishing a geospatial connection between recorded natural hazard events and the rail network, based on spatial overlap or proximity within defined geographic units (e.g., HUC boundaries, forecast zones). This approach enables the identification of rail segments that were likely exposed to each hazard event. The goal of this section is to assign each flood event to the rail network, using the 12-digit HUC maps for this purpose. The 12-digit HUC represents the sub-watershed and has an average size of 10,000 to 40,000 acres (15–60 sq. mi.). The intent of these watersheds is to provide delineation on the potential flow paths within each watershed, where all the water that enters or accumulates from rainfall will exist and drain out to singular locations within the 12-digit HUC itself. This realization allowed the research team to use the HUC as an indicator that flooding would have also existed in close relation to the rail track itself. There are approximately 100,000 such units across the entire USA.

For flood events, there are some points in different locations within the flooding area in the USGS dataset. It is assumed that if there is any recorded flood point within a 12-digit HUC, the entire HUC will be considered flooded. With this assumption, we assigned the specific flood within a particular HUC to the specific length of the rail network.

Figures 25 to 28 represent the rail network that USGS flood events have been assigned to, providing a comprehensive visualization of the data. In Figure 25, the rail network is illustrated alongside the 39 different recorded flood events from the USGS dataset, highlighting the specific locations affected by flooding. Figure 26 presents a binary version of the assigned floods, categorizing the data into two distinct groups: No Flood and At Least One Flood. This binary classification helps in understanding the extent of flooding across the rail network. Figures 27 and 28 further elaborate on this by showing the rail network for At Least One Flood and No Flood, respectively. Furthermore, these maps will also be attached as shapefiles for the FRA, academia, and industry to leverage.

Figure 25. Distribution of Flooding Events (USGS Dataset) Across the Rail Network

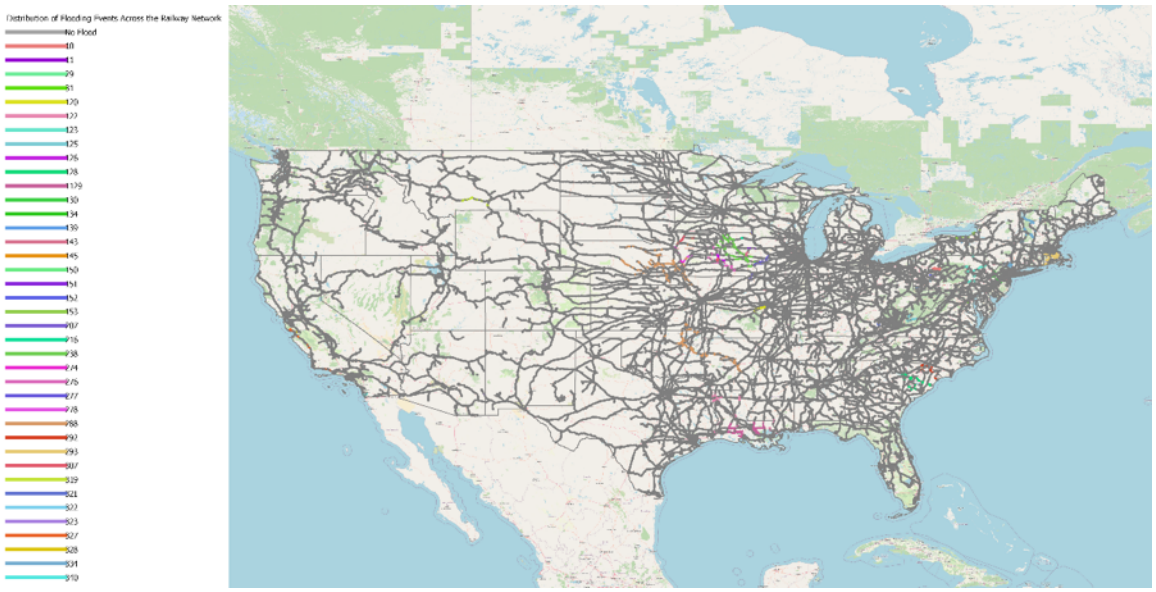

Figure 26. Rail Network Segments with No Flood and Recorded Flood Events (USGS Dataset)

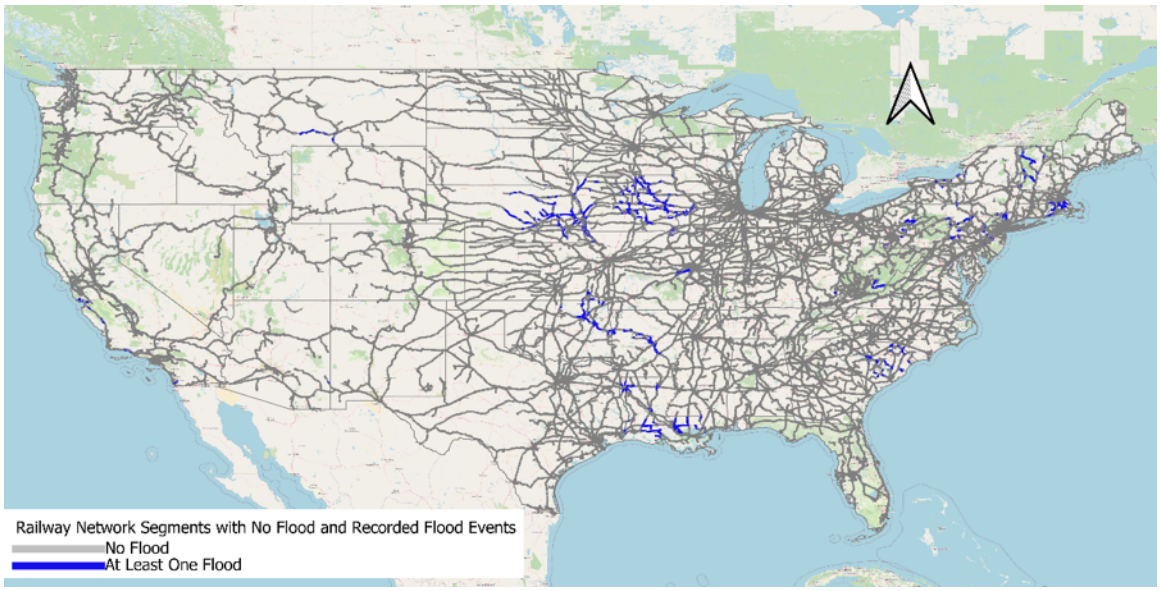

Figure 27. Rail Network Segments with Recorded at Least One Flood Event (USGS Dataset)

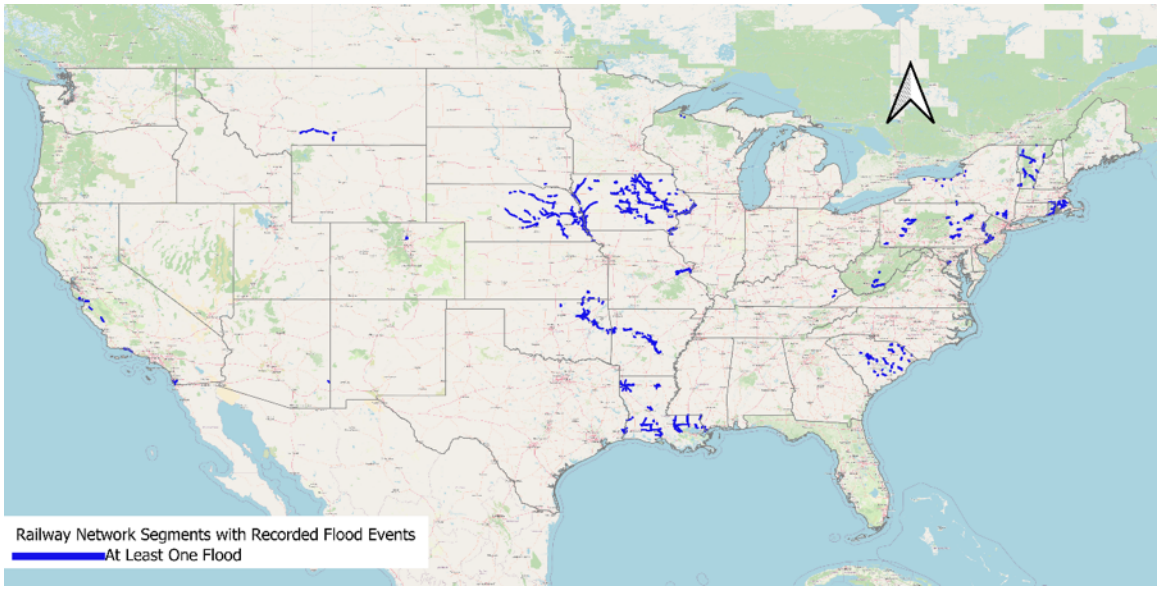

Figure 28. Rail Network Segments with No Flood (USGS Dataset)

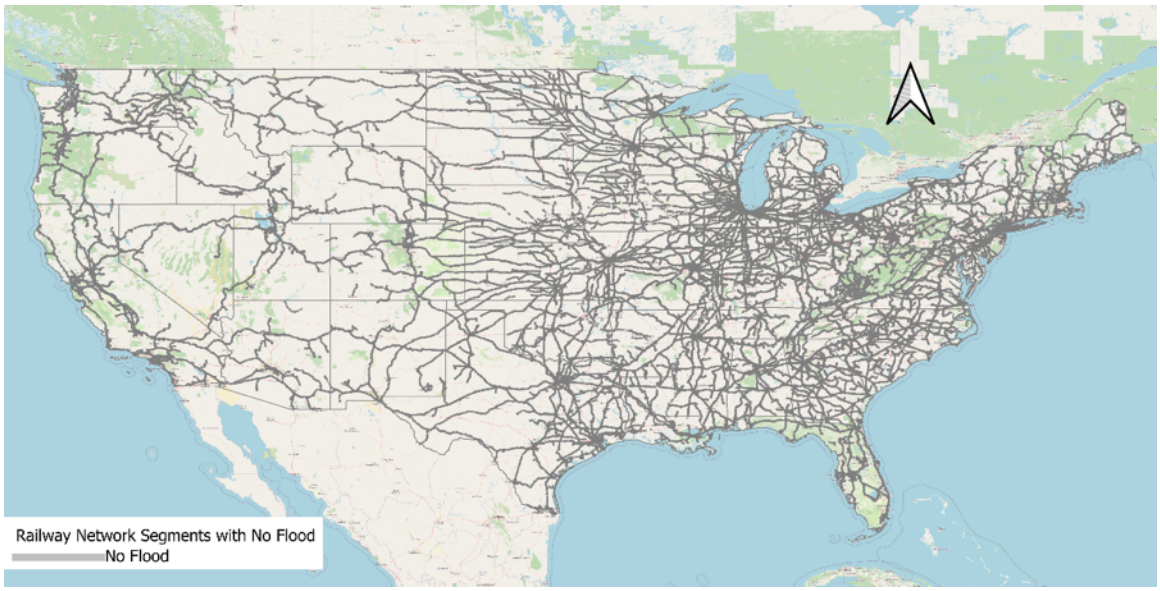

Figure 29 represents a visual display of the distribution of rail lines impacted by flood events in the USGS dataset from 2000 to 2024. The chart classifies the rail lines into two different groups: "No Flood" and "At Least One Flood." According to this pie chart, most of the rails—approximately 96.8%—are under the “No Flood” category, which means they did not intersect with any recorded flood events during this period. Conversely, there was “At Least One Flood” observed on only 3.2% of rail tracks within this data frame, as shown by this graphical presentation. This pie chart highlights the relatively small proportion of rail lines affected by flooding compared to the total rail network, emphasizing the need to focus flood resilience efforts on the segments that are more vulnerable to flooding; however, as this dataset is indeed one where there are extreme levels of accuracy per event, its coverage on all events is limited, which is why the research team investigated a secondary dataset that also tracks flood events, though with less additional information on each event.

Figure 29. Distribution of Rail Lines by USGS Flood Frequency (2000–2024)

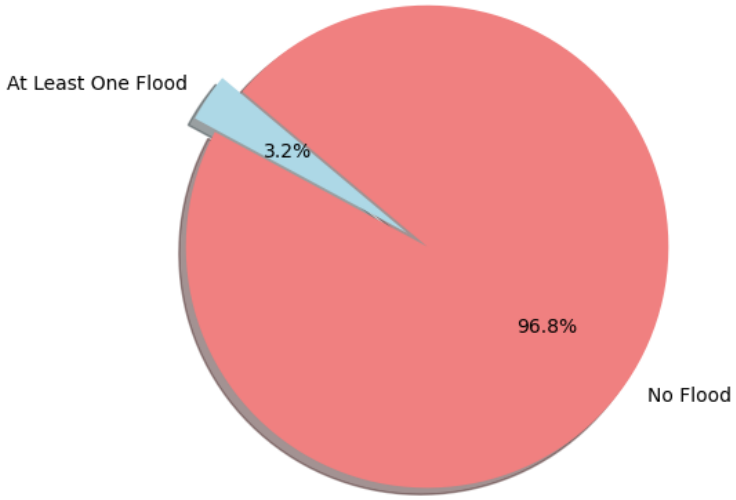

2.4 National Centers for Environmental Information (NCEI) Database

The National Oceanic and Atmospheric Administration (NOAA) has merged its three main data centers into one organization called the National Centers for Environmental Information (NCEI). The integration includes the following:

1. National Climatic Data Center (NCDC)
2. National Geophysical Data Center (NGDC)
3. National Oceanographic Data Center (NODC), which also encompasses the National Coastal Data Development Center (NCDDC)

The National Centers for Environmental Information (NCEI) plays a crucial role in managing and providing access to a vast collection of oceanic, atmospheric, and geophysical data. The purpose of this integration is to optimize data management and enhance the accessibility and usefulness of environmental information for research, policy formulation, and public utilization (*NOAA* n.d.c; *NOAA* n.d.d).

Figure 30 illustrates the geographic distribution of the National Centers for Environmental Information (NCEI) field locations, headquarters, regional climate centers (RCC), regional climate services directors (RCSD), and cooperative institutes across the United States. Here is a detailed breakdown (*NOAA* n.d.c):

- **Orange Stars**: Indicate the locations of the NCEI headquarters and significant field locations, which include:

- Asheville, North Carolina (Headquarters)
- Boulder, Colorado
- Silver Spring, Maryland
- Stennis Space Center, Mississippi

- **Blue Triangles**: Represent the NCEI field locations and the Regional Climate Services Directors (RCSD), who oversee regional climate services.
- **Red Squares**: Denote the locations of Cooperative Institutes that collaborate with NCEI on various research initiatives.
- **Brown Ovals**: Mark the Regional Climate Centers (RCC), which are essential for providing localized climate services and support.

Figure 30. National Centers for Environmental Information

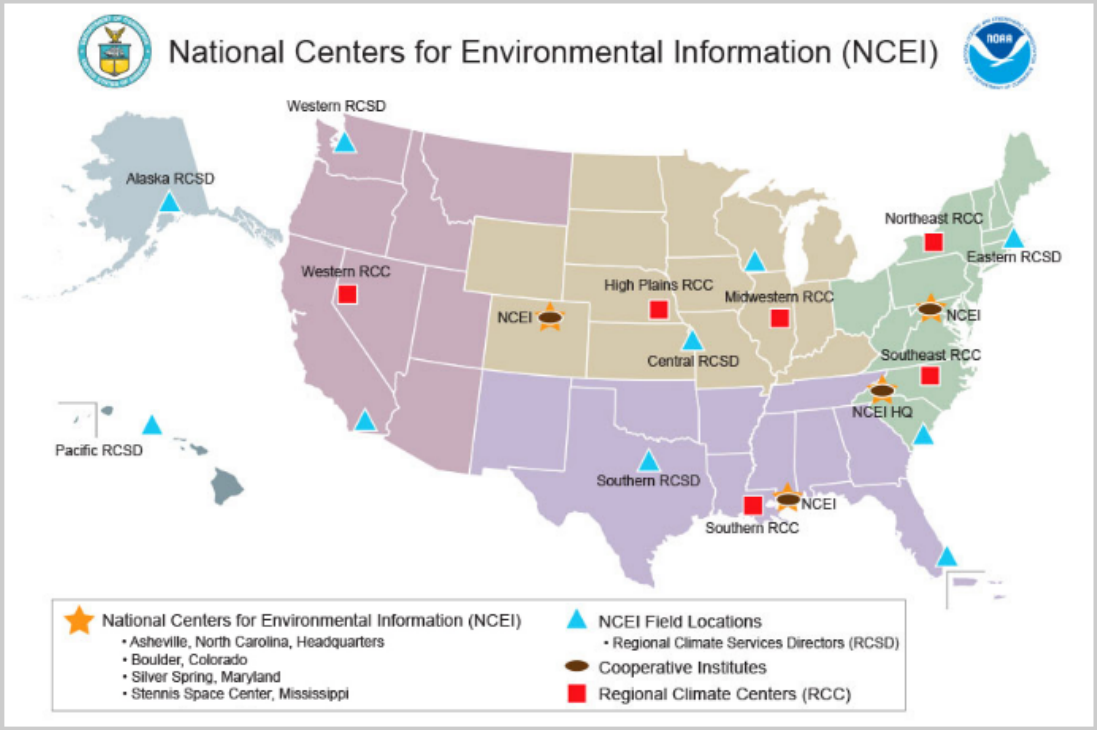

This map was specifically created to illustrate the comprehensive network of the National Centers for Environmental Information (NCEI) throughout the United States. The text emphasizes the strategic positioning of NCEI's facilities and partner institutions, which demonstrates the organization's comprehensive method of handling and distributing environmental data.

The NCEI contains the extensive **Storm Events Database**, which carefully documents several noteworthy weather phenomena across the country. This database plays a critical role in understanding storm patterns and their impacts.

Key Features of the NCEI Storm Events Database:

The Storm Events Database records the following types of events:

1. **Storm Occurrences:** It includes detailed records of storms and significant weather phenomena that have had a considerable impact, such as causing loss of life, injuries, significant property damage, or disrupting commerce.

2. **Rare and Unusual Weather Phenomena:** This category covers exceptional weather events that generate media attention, including unusual snow flurries in typically warm regions such as South Florida or the San Diego coastal area.

3. **Meteorological Extremes:** The database also captures other significant meteorological events, including record maximum or minimum temperatures or unusual precipitation patterns that occur in connection with another weather event.

Data from January 1950 to March 2024, as reported by NOAA's National Weather Service (NWS), is currently accessible through the database. The types and durations of data that are accessible have varied over time due to modifications in data gathering and analysis processes. To ensure consistency, NCEI has standardized event classifications and structured data, but the real numbers for locations, fatalities, injuries, damage, and narratives have not changed.

The NCEI's Storm Events Database is an extensive repository that records significant weather phenomena. The database includes detailed information about the occurrence, duration, and impacts of various storm events. This data is crucial for studying weather patterns, assessing the risks associated with different types of storms, and formulating strategies for disaster preparedness and response. In this report, all the events have been categorized into main categories and sub-categories based on their nature, providing a structured overview of the diverse weather phenomena recorded in the database. Table 9 represents the different types of storm events classification (NOAA, n.d.e):

Table 9. Categorization of Storm Events Data (NCEI)

Main Category	Sub-Category	Event Type
Natural Phenomena	Astronomical Events	Astronomical Low Tide, Northern Lights
	Geophysical Events	Avalanche, Debris Flow, Tsunami, Volcanic Ash, Volcanic Ashfall
Weather Events	Winter Weather	Blizzard, Lake-Effect Snow, Heavy Snow, Winter Storm, Winter Weather
	Coastal and Marine Events	Coastal Flood, Marine Dense Fog, Marine Hail, Marine High Wind, Marine Hurricane/Typhoon, Marine Lightning, Marine Strong Wind, Marine Thunderstorm Wind, Marine Tropical Depression, Marine Tropical Storm, Storm Surge/Tide, High Surf, Sneaker Wave
	Cold Weather Events	Cold/Wind Chill, Extreme Cold/Wind Chill, Freezing Fog, Frost/Freeze
	Dust and Fog Events	Dense Fog, Dense Smoke, Dust Devil, Dust Storm
	Floods and Rain Events	Flash Flood, Flood, Heavy Rain, Lakeshore Flood, Seiche
	Heat Events	Excessive Heat, Heat
	Hurricane and Tropical Storms	Hurricane, Hurricane/Typhoon, Tropical Depression, Tropical Storm
	Ice and Sleet Events	Ice Storm, Sleet
	Lightning Events	Lightning
	Tornado and Wind Events	High Wind, Strong Wind, Thunderstorm Wind, Tornado, Waterspout, Funnel Cloud
	Drought Events	Drought
	Hail Events	Hail
Fire Events	Wildfire Events	Wildfire
Other Events	Miscellaneous Events	Rip Current

Each weather event in the Storm Events Database is documented with comprehensive information. The details are categorized into various sections to provide a structured overview of the data. Table 10 outlines the categorization used in this report (NOAA, n.d.c):

Table 10. Event Information Categorization

Category	Field Name	Description	Example
Event Details	begin_yearmonth	Year and month when the event began (YYYYMM)	201212
	begin_day	Day of the month when the event began (DD)	31
	begin_time	Time of day when the event began (hhmm)	2359
	end_yearmonth	Year and month when the event ended (YYYYMM)	201301
	end_day	Day of the month when the event ended (DD)	1
	end_time	Time of day when the event ended (hhmm)	1
	episode_id	ID for the storm episode	61280
	event_id	ID for the individual storm event	383097
Geographical and Temporal Information	state	State where the event occurred (ALL CAPS)	GEORGIA
	state_fips	State FIPS number	45
	year	Year of the event	2000
	month_name	Name of the month of the event	January
	cz_type	Event location type: County/Parish (C), Zone (Z), Marine (M)	C
	cz_fips	County FIPS number	245
	cz_name	County/Zone/Marine name	AIKEN
	wfo	NWS Forecast Office's area of responsibility	CAE
	begin_date_time	Start date and time of the event (MM/DD/YYYY hh:mm)	04/01/2012 20:48
	cz_timezone	Time zone for the event location	EST-5
Impact Data	injuries_direct	Number of direct injuries	1
	injuries_indirect	Number of indirect injuries	0
	deaths_direct	Number of direct deaths	0
	deaths_indirect	Number of indirect deaths	4
	damage_property	Estimated property damage	10.00K
	damage_crops	Estimated crop damage	500.00K
Event Characteristics	event_type	Type of weather event	Hail
	source	Source reporting the event	Public
	magnitude	Measured extent of the event (e.g., wind speed in knots, hail size in inches)	0.75
	magnitude_type	Type of magnitude measurement (EG for Estimated Gust)	EG
Flood and Tornado Details	flood_cause	Cause of the flood event	Heavy Rain
	tor_f_scale	Enhanced Fujita Scale rating for tornado events (e.g., EF0 for Light Damage)	EF0
	tor_length	Length of the tornado path (miles)	0.66

Category	Field Name	Description	Example
	tor_width	Width of the tornado path (feet)	25
	tor_other_* fields	Information about continuing tornado segments as they cross from one area to another	KS, NE, OK
Narratives	episode_narrative	General description of the weather episode	A strong upper level...
	event_narrative	Detailed description of the individual weather event	

In this section of the report, the analysis of various types of flood events—including Flood, Flash Flood, Lakeshore Flood, and Coastal Flood—has been conducted. The results of this analysis are detailed below.

Flood Events Analysis in the United States (NCEI)

This section of the report presents the analysis of flood event frequency across different states in the United States. A flood is defined as any high flow, overflow, or inundation by water that causes or threatens damage (*NOAA n.d.e*). Figure 31 illustrates the frequency of flood events in each state, categorized into five ranges to highlight the variation in flood occurrences.

Figure 31. Flood Event Frequency Analysis in the United States (NCEI)

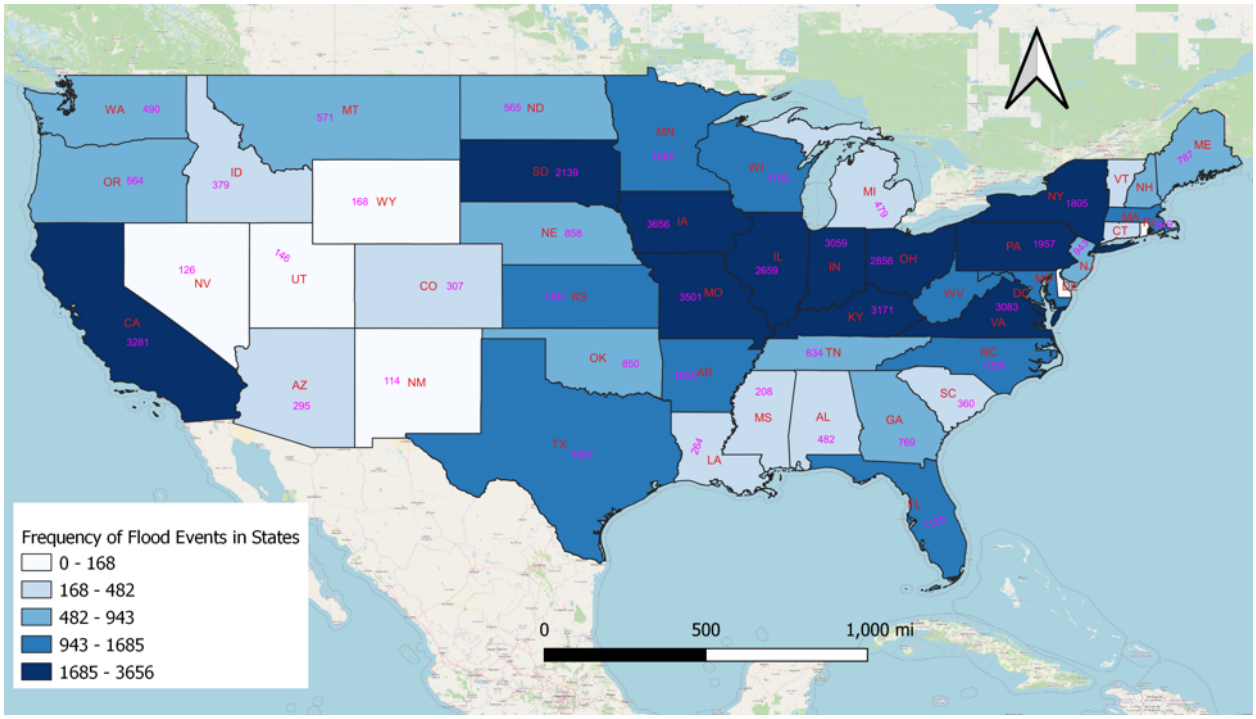

Figure 32 illustrates the frequency of flood events reported by various sources. Total event frequency is about 57,831 and the most significant contributors are River/Stream Gage data, accounting for 17.00% (9,830 events), followed by Emergency Manager at 16.27% (9,410 events), and Law Enforcement at 14.75% (8,532 events). Other notable sources include the Department of Highways and Official NWS Observations, contributing 6.97% (4,031 events) and 5.54% (3,206 events), respectively.

Figure 32. Frequency of Flood Events by Source 2000–2024 (NCEI)

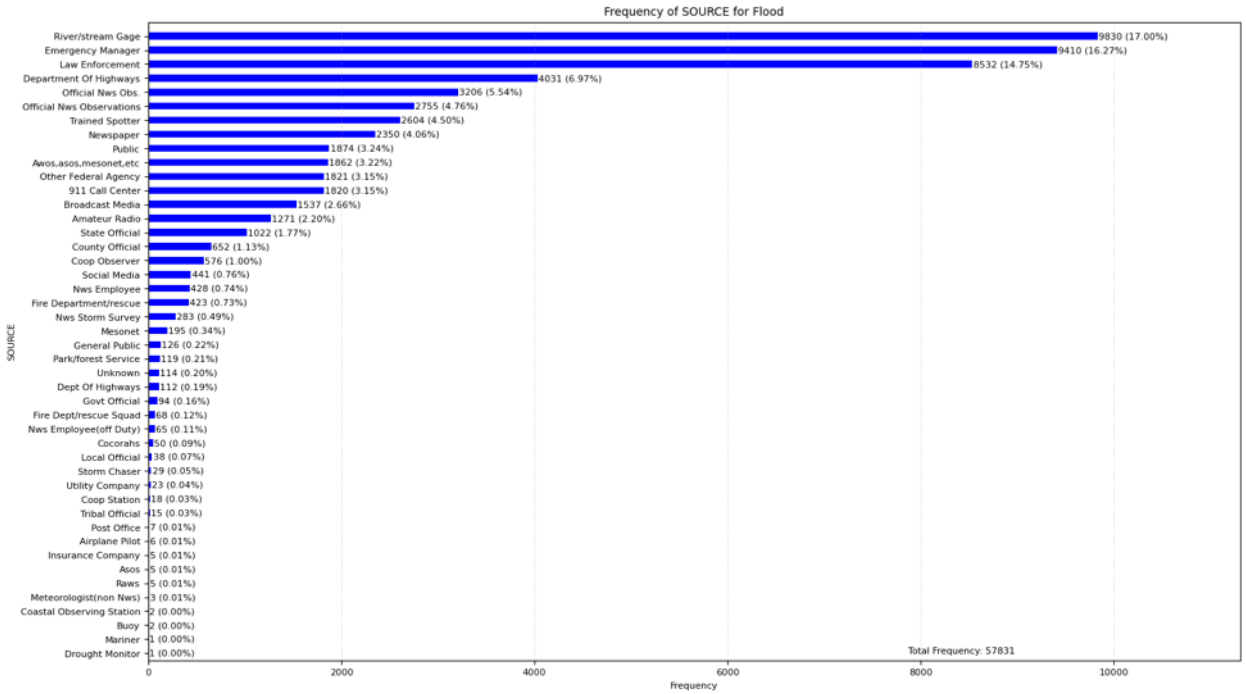

The analysis of flood event durations from 2000 to 2024 provides insights into the frequency and average duration of flood events, which are critical for understanding their impact on rail infrastructure. By examining the distribution and yearly trends of flood durations, we can better assess the potential risks and necessary measures for maintaining and protecting rail systems.

Figure 33 illustrates the frequency of flood events by year from 2000 to 2024, showing significant variability over the years. The highest frequency of flood events occurred in 2018 and 2019 with 4,824 events (8.34%) and 4,949 events (8.56%), respectively. Other notable peaks include 2011 with 3,729 events (6.45%). In contrast, 2012 experienced the lowest frequencies, with 993 events (1.72%). This fluctuation indicates periods of increased flood activity, which may correlate with extreme weather patterns and may also follow the extremes of El Nino and La Nina process; however, this still needs further exploration.

Figure 33. Frequency of Flood Events by Year 2000–2024 (NCEI)

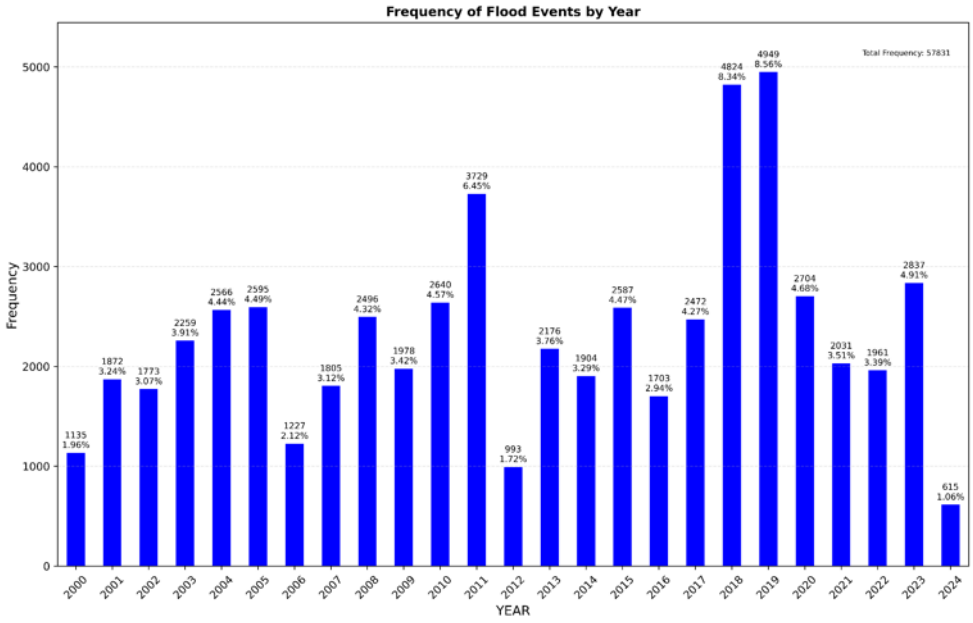

Figure 34 displays the frequency of flood events by month, revealing distinct seasonal patterns in flood occurrences. The peaks of the figures suggest a higher incidence of flooding during the late spring and early summer months, likely due to seasonal heavy rainfall and snowmelt. Conversely, November has the lowest frequency of flood events, indicating fewer flood occurrences in the late autumn. This seasonal variation highlights the importance of preparing rail infrastructure for heightened flood risks during specific times of the year to ensure resilience and minimize disruption.

Figure 34. Frequency of Flood Events by Month 2000-2024 (NCEI)

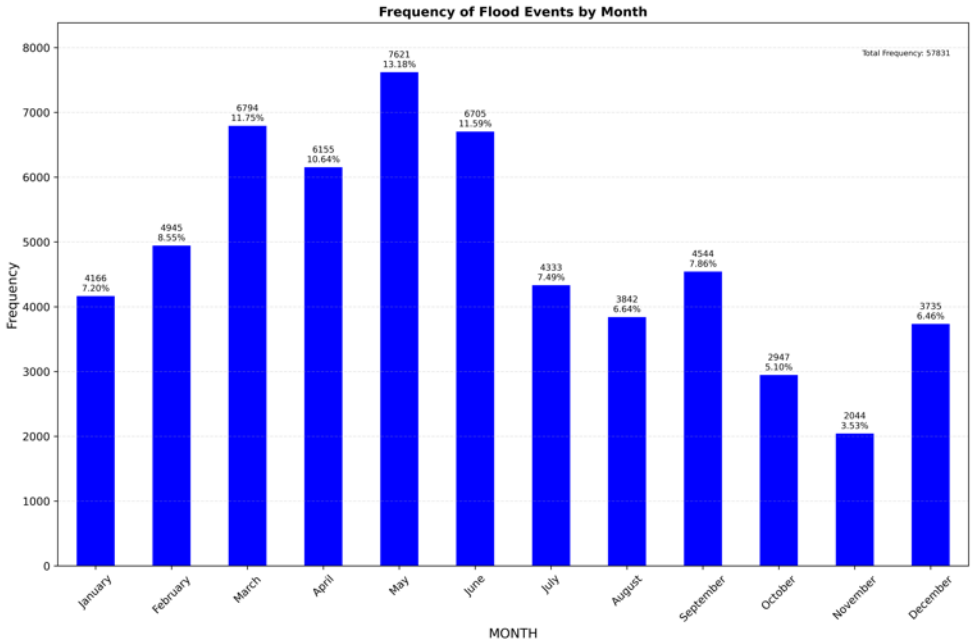

Figure 35 illustrates that many flood events are short-lived, with 1-day events being the most common at 50.35%, followed by 2-day events at 19.46%, and 3-day events at 7.22%. As the duration increases, the frequency of flood events decreases significantly, with events lasting longer than 10 days being relatively rare. This pattern indicates that while prolonged flooding does occur, it is much less common than shorter, more transient flood events.

Figure 35. Duration for Flood Events in Days 2000–2024 (NCEI)

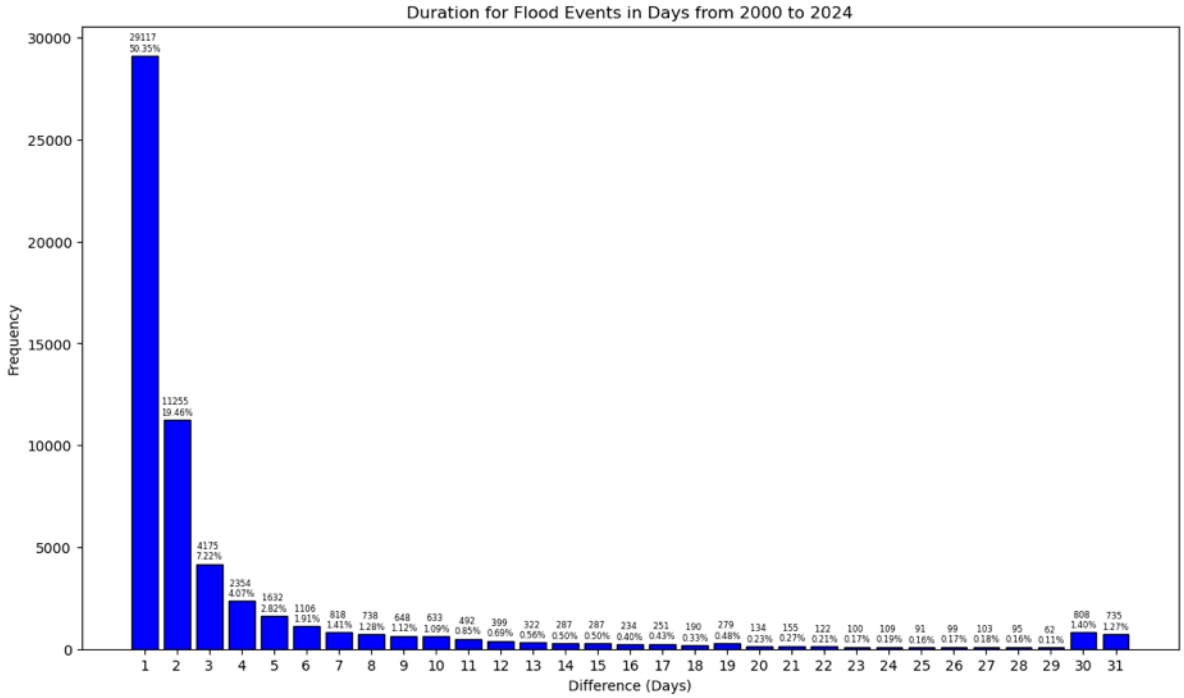

Figure 36 shows the average duration of flood events for each year from 2000 to 2024. Notably, 2011 stands out with the highest average duration of 6.93 days, followed by 2019 at 6.39 days and 2001 at 5.77 days. These fluctuations suggest that some years experience more prolonged flood events, potentially leading to extended disruptions and increased maintenance demands on rail infrastructure.

Figure 36. Average Duration of Flood Events per Year 2000–2024 (NCEI)

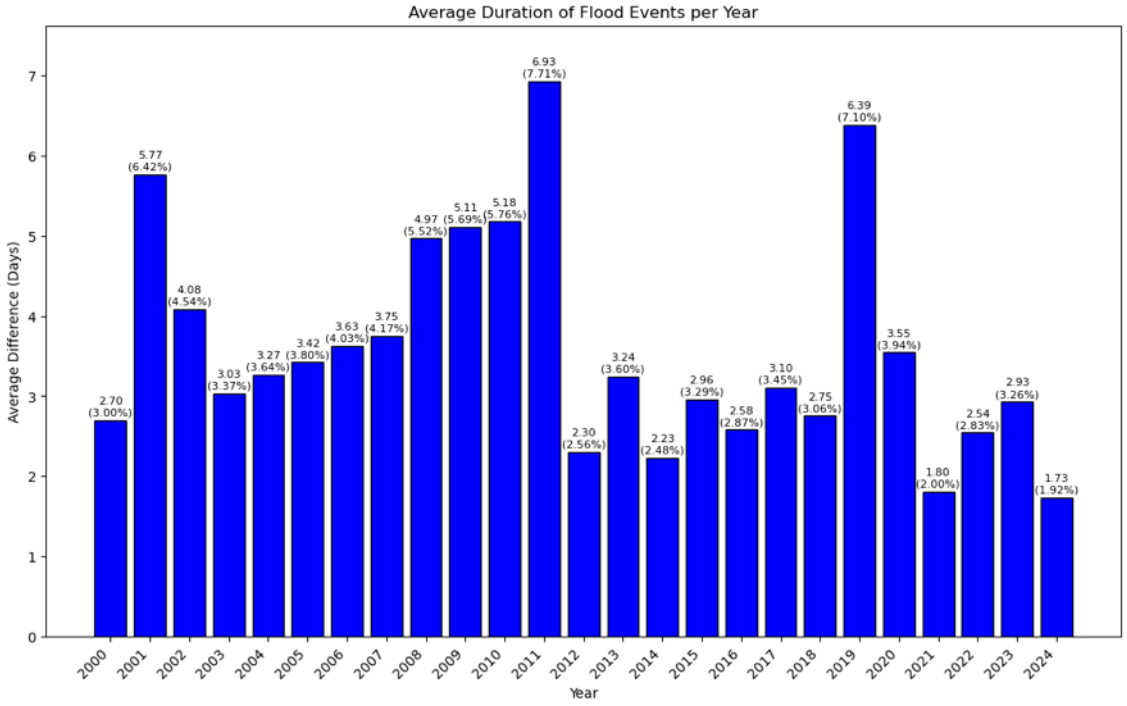

Assigning the NCEI Flood Events to the U.S. Rail Network

As mentioned in Section 1.1.1.3.2, "Assigning the USGS Flood Events to the U.S. Rail," the goal here is to assign each flood event to the rail network, using the 12-digit HUC maps for this purpose. For the NCEI flood events, there is one specific point for each flood event. It has been assumed that if there is any recorded flood point within a 12-digit HUC, the entire HUC will be considered flooded. With this assumption, we assigned the specific flood within a particular HUC to the specific length of the rail network.

Figures 37 to 40 illustrate the rail network to which NCEI flood occurrences have been allocated. In Figure 37, the rail network is illustrated with 46,436 different recorded flood events (out of 57,831 recorded flood events) that have coordinates from the NCEI dataset, highlighting the specific locations affected by flooding. In this figure, the labels show the number of distinctive flood events within the 12-digit HUC boundary. Notably, the boundary with the maximum distinct flood points contains 195 different points.

Figure 38 presents a binary categorization of the assigned floods, classifying the data into two distinct groups: "No Flood" and "At Least One Flood." Figures 39 and 40 provide further clarification by separately illustrating the rail network for "At Least One Flood" and "No Flood," respectively.

Figure 37. Distribution of Flooding Events (NCEI Dataset) Across the Rail Network

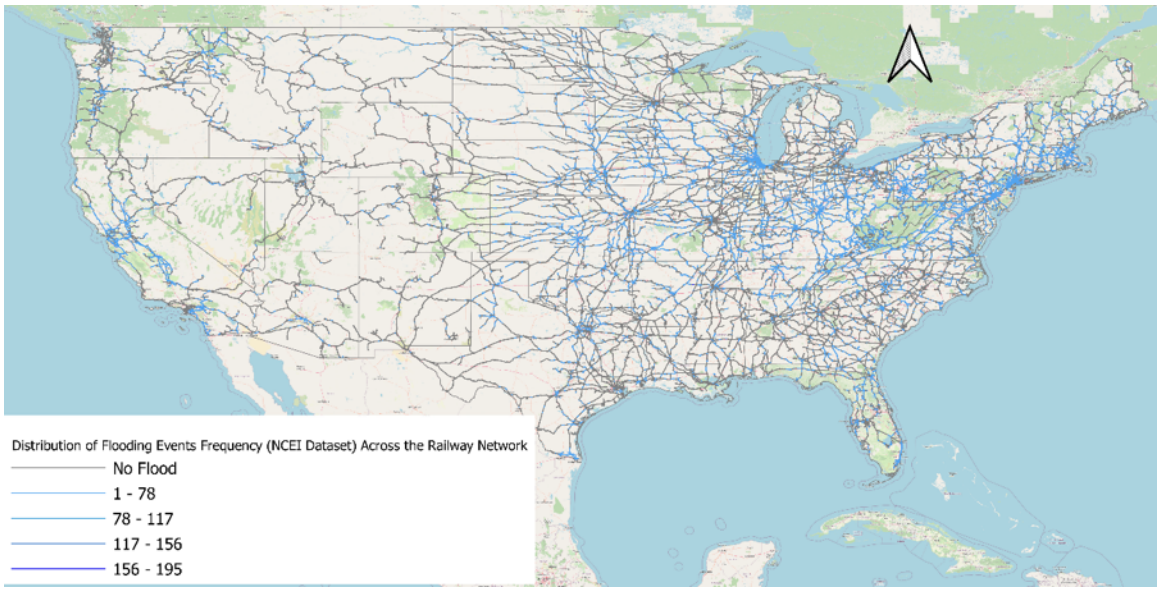

Figure 38. Rail Network Segments with No Flood and Recorded Flood Events (NCEI Dataset)

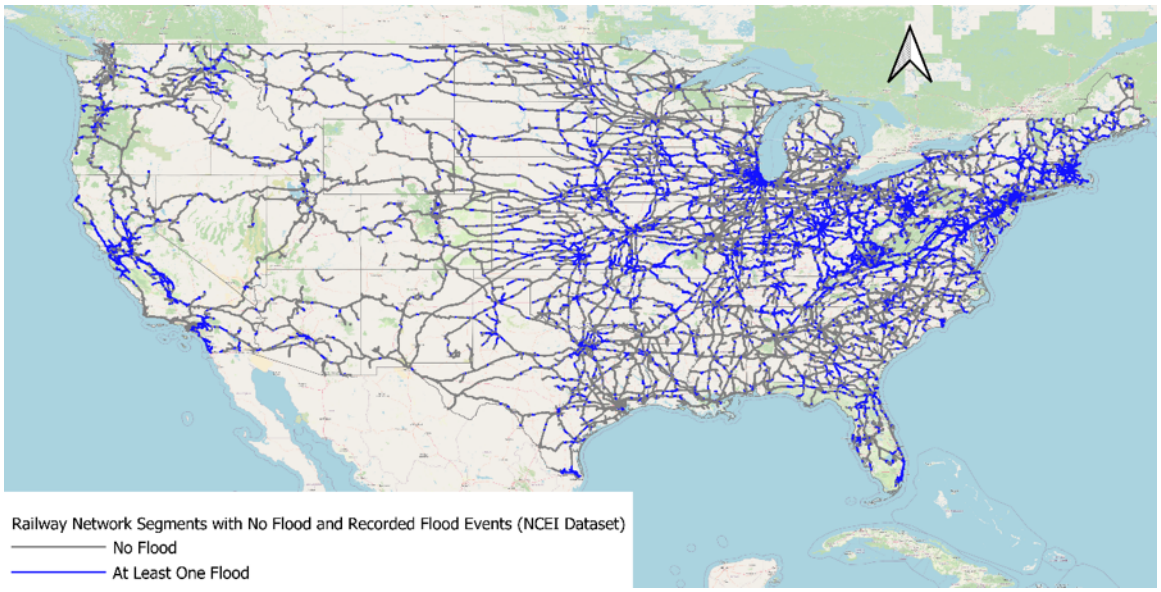

Figure 39. Rail Network Segments with Recorded at Least One Flood Event (NCEI Dataset)

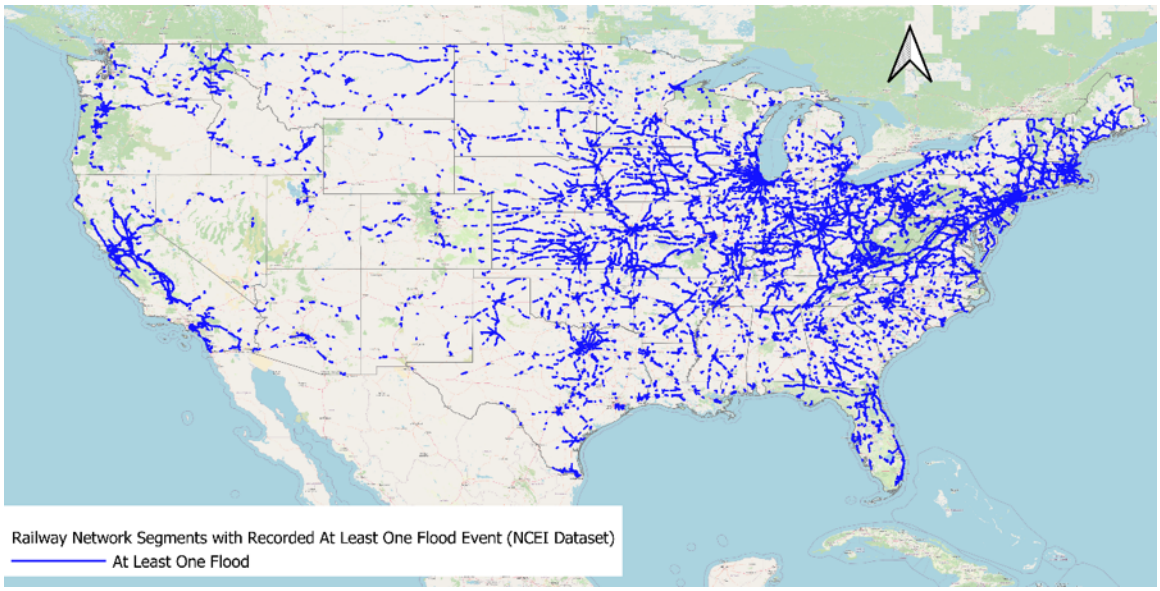

Figure 40. Rail Network Segments with No Flood (NCEI Dataset)

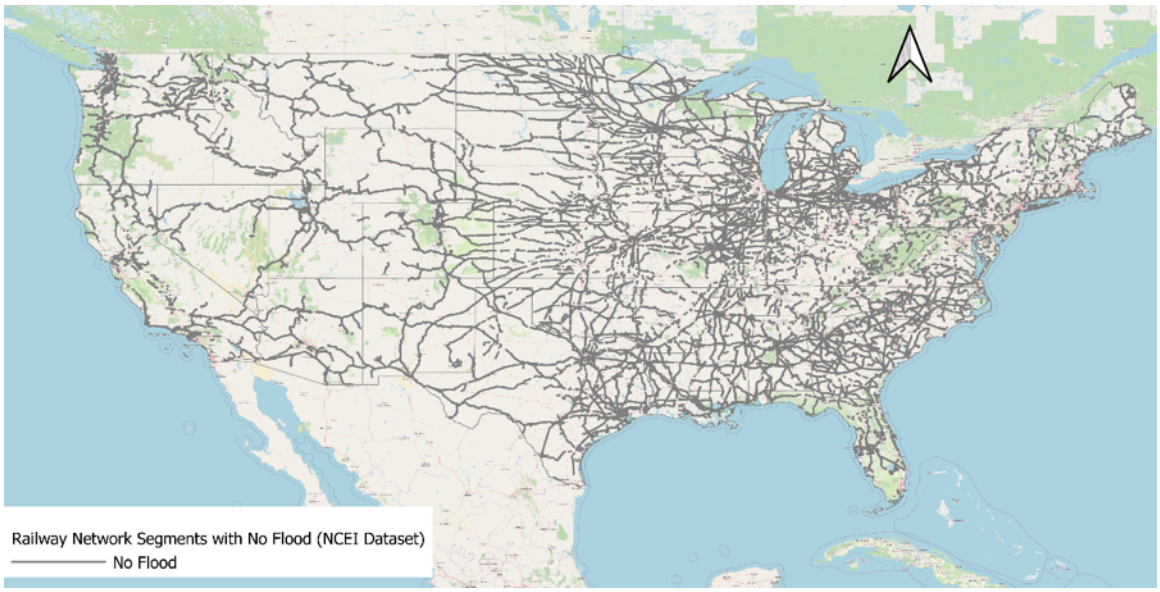

Figure 41 illustrates the distribution of rail segments affected by flood events based on the NCEI dataset. It categorizes the network into two groups: segments with "No Flood" events, comprising 58.9% of the total and shown in red, and segments with "At Least One Flood" event, comprising 41.1% of the total and shown in blue. This visual representation highlights that a significant portion of the rail network (41.1%) has experienced flooding, indicating areas where flood resilience measures may be necessary to protect infrastructure.

Figure 41. Distribution of Rail Lines by NCEI Flood Frequency (2000–2024)

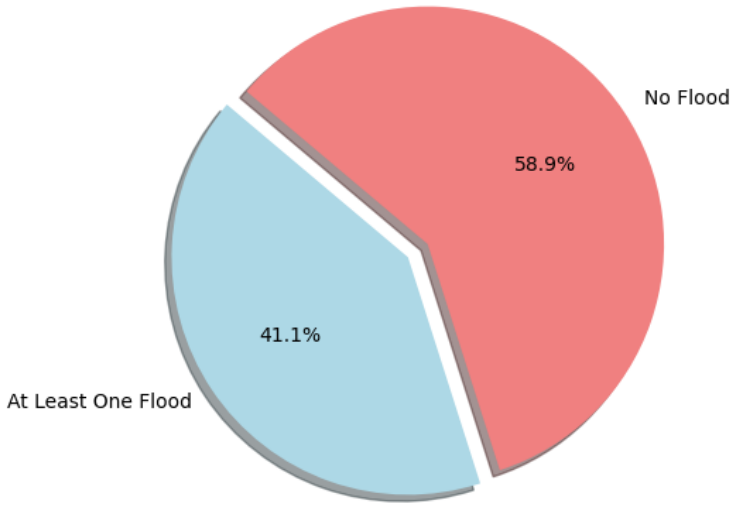

Figure 42 depicts the total length of the rail miles classified by the number of flood events. The x-axis and y-axis show the flood frequency ranges and the sum of rail length in miles. The largest category is “No Flood,” comprising 115,708 miles (58.9%) of rail length. The second bar displays the "0–10" flood category, which represents the 71,814 miles (36.6%) of the rail that experienced one to ten flood incidents. The remaining bars represent the section of the rail that experiences more frequent flooding.

Figure 42. Sum of Rail Length by Flood Frequency Events (NCEI)

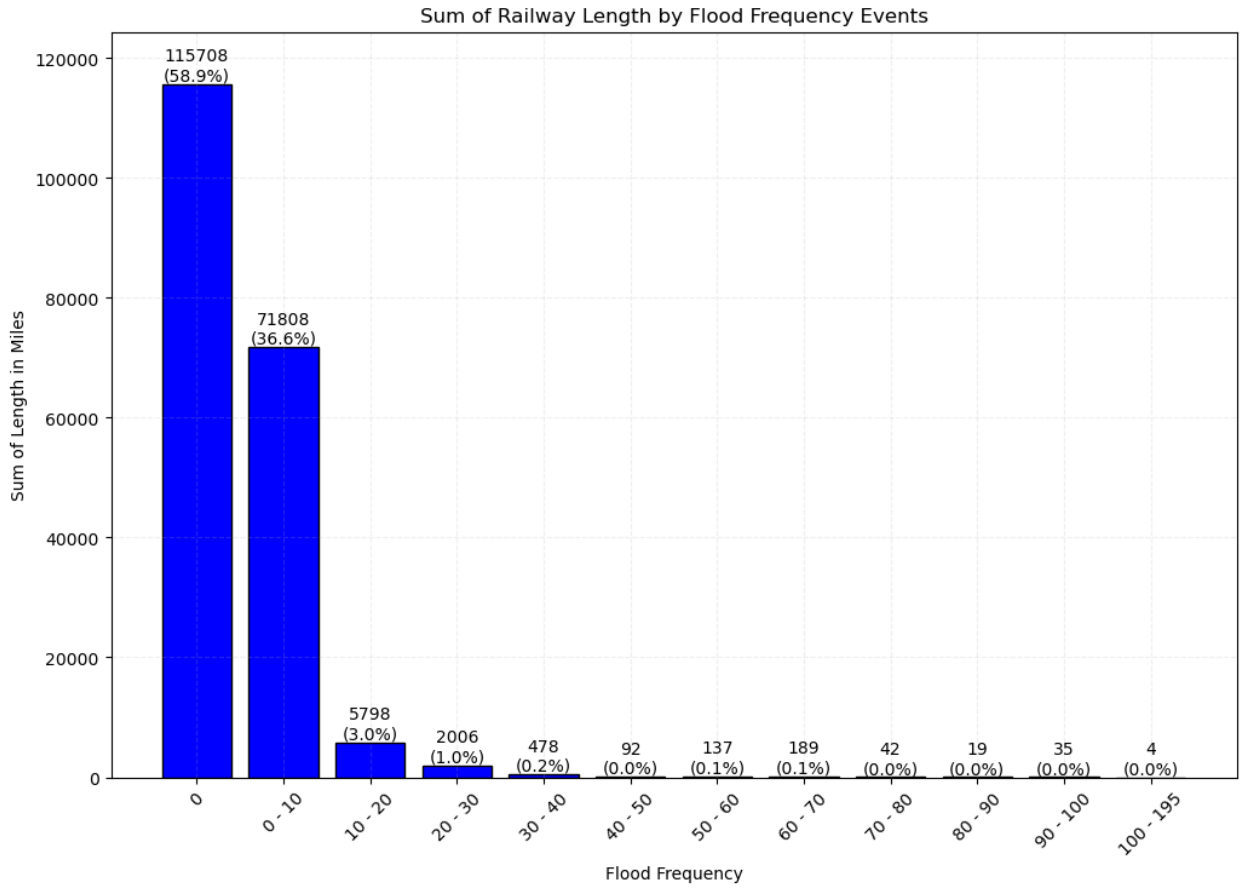

Figure 43 demonstrates the total rail lengths in miles for flood frequencies ranging from one to ten incidents. The y-axis displays the total miles of rail, and the x-axis displays the number of flood events that happened along specific lengths of the rail. The figure indicates that rail segments that have encountered only one flood occurrence have the highest cumulative length of 31,558 miles (43.2%), while parts with two flood episodes have a total length of 14,339 miles (19.6%). As flood frequency increases, the total affected rail length decreases sharply, with just 1,241 miles (1.7%) exposed to ten flood events. This is a further depiction of Figure 42, where the purpose behind both plots is to begin an effort to potentially isolate sections that are receiving higher flood frequencies of occurrences. Thus, the locations with the highest frequency will be the starting links for risk assessments, once tied to the latter methodological approaches in the remaining sections of the report.

Figure 43. Sum of Rail Length by Flood Frequency Between 1–10 (NCEI)

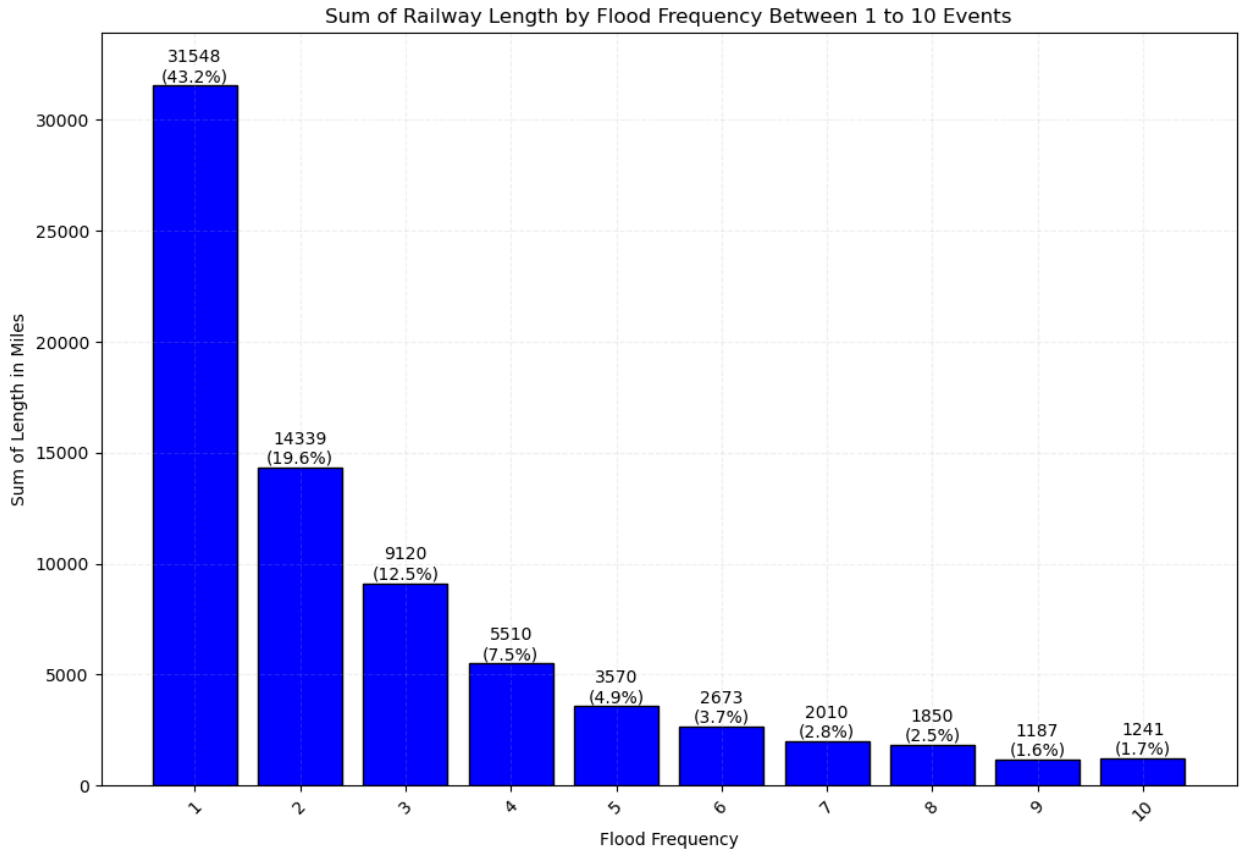

Flash Flood Events Analysis in the United States (NCEI)

Figure 44 presents the frequency of flash flood events across different states in the United States. A flash flood is a rapid and extreme flow of high-water into a normally dry area, or a rapid water level rise in a stream or creek above a predetermined flood level, beginning within six hours of the causative event (e.g., intense rainfall, dam failure, ice jam). However, the actual time threshold may vary in different parts of the country. Ongoing flooding can intensify to flash flooding in cases where intense rainfall results in a rapid surge of rising flood waters (*NOAA* n.d.a).

Figure 44 reveals considerable variation in the number of recorded flash flood events across the United States. The total number of recorded events is approximately 88,094 and Texas experiences the highest number of flash flood events, with a staggering 10,384 occurrences, highlighting both the state's vulnerability to intense and sudden rainfall and its numerous approaches to relaying flood events. States such as Missouri (5,143), Kentucky (3,621), and Arizona (2,969) also show high frequencies, indicating significant risks to infrastructure. In contrast, states such as Oregon (87), Washington (171), and Rhode Island (84) have much lower frequencies, suggesting fewer instances of flash flooding.

Figure 44. Flash Flood Event Frequency Analysis in the United States (NCEI)

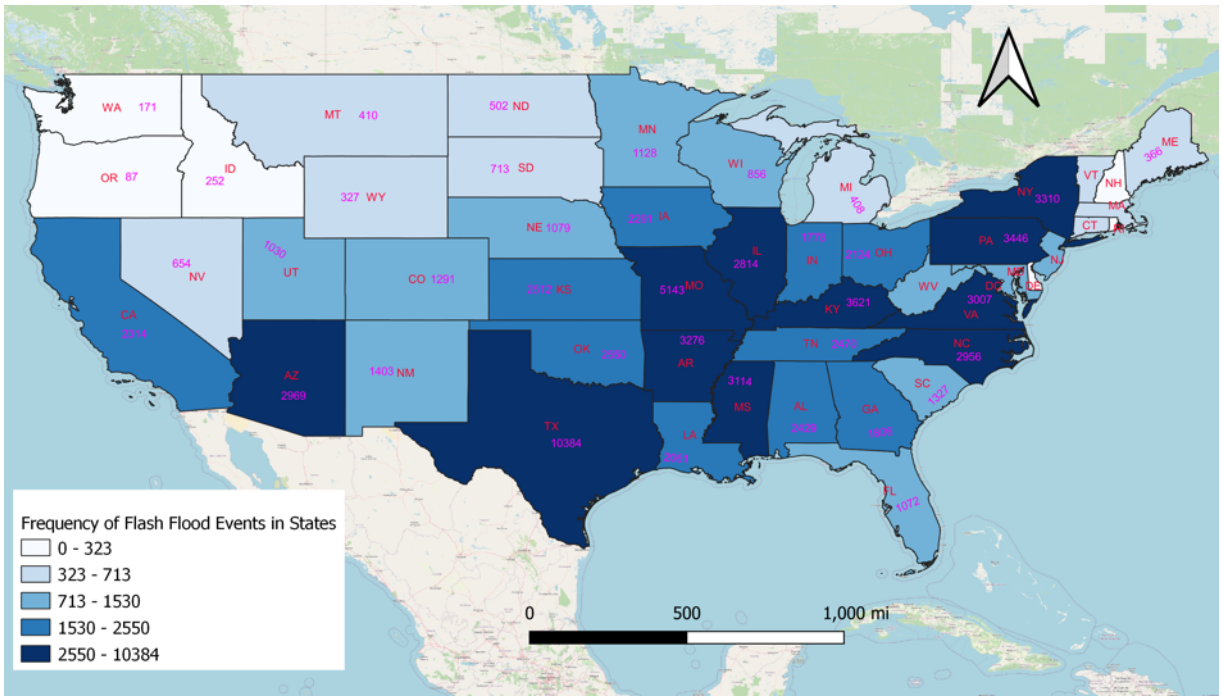

Figure 45 shows the frequency of flash flood events by source. Law Enforcement reports the most events at 28.67% (25,255 events), followed by Emergency Managers at 22.47% (19,794 events). Despite their importance, River/Stream Gage reports only 0.97% (857 events) of flash floods.

Figure 45. Frequency of Flash Flood Events by Source 2000–2024 (NCEI)

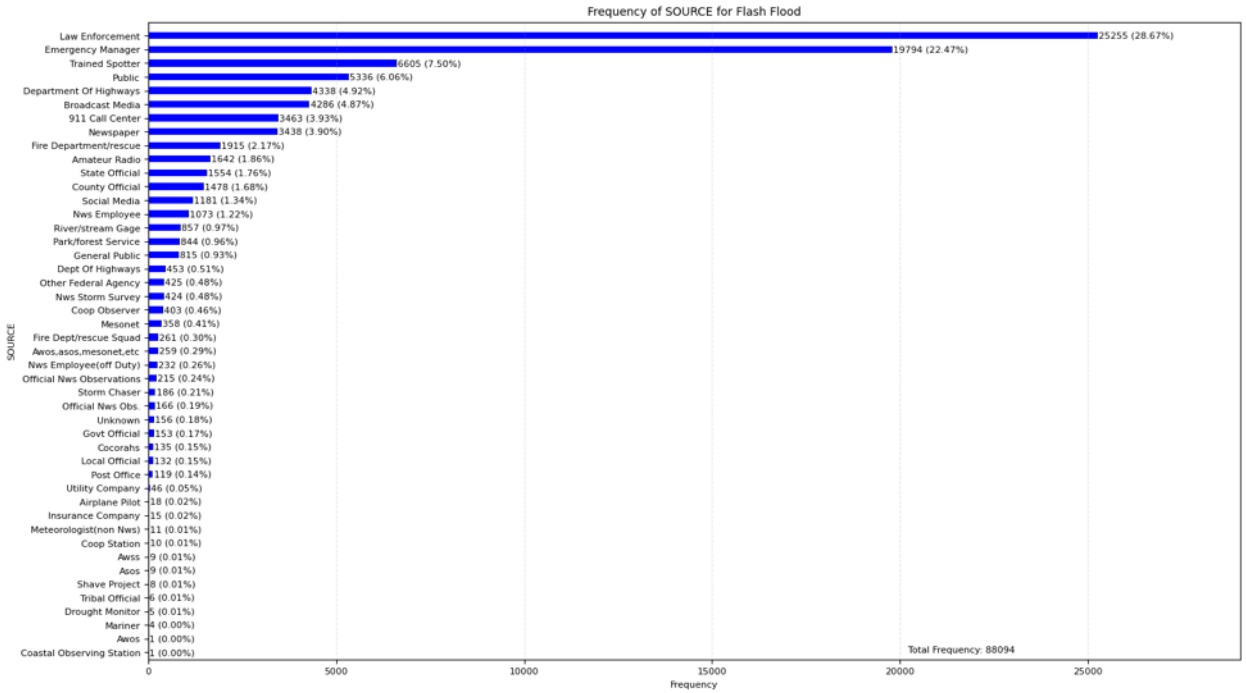

Figure 46 shows the frequency of flash flood events by year from 2000 to 2024. The highest frequency occurred in 2015 with 5,063 events (5.75%), followed by 2021 with 4,797 events (5.45%) and 2003 with 2018 events (4.97%). The lowest frequency was in 2012, with only 2,304 events (2.62%), and the events frequency for 2024 is not for the whole year.

Figure 46. Frequency of Flash Flood Events by Year 2000-2024 (NCEI)

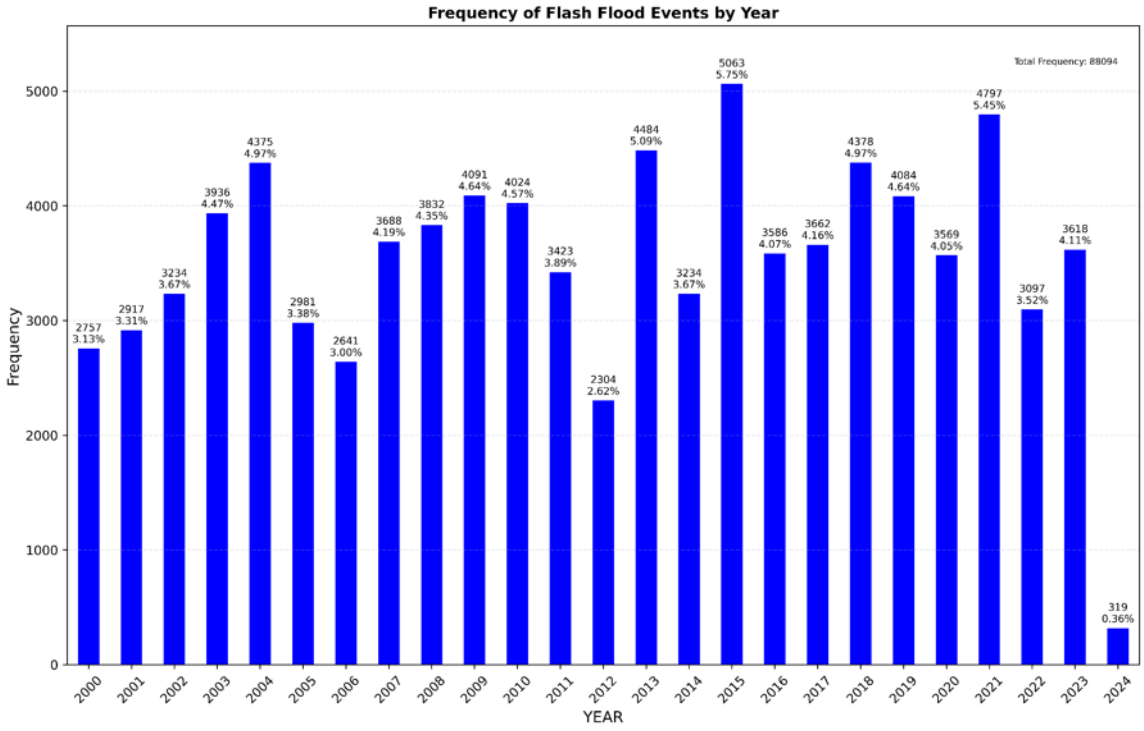

Figure 47 shows the frequency of flash flood events by month. July has the highest frequency with 16,441 events (18.66%), followed by June with 14,146 events (16.06%) and August with 14,069 events (15.97%). The lowest frequencies occur in November (1,880 events, 2.13%) and January (2,328 events, 2.64%). This pattern highlights the peak flash flood season during the summer months, which may provide incentives on when to conduct resilience-based infrastructure improvements, in preparation for rain seasons.

Figure 47. Frequency of Flash Flood Events by Month 2000–2024 (NCEI)

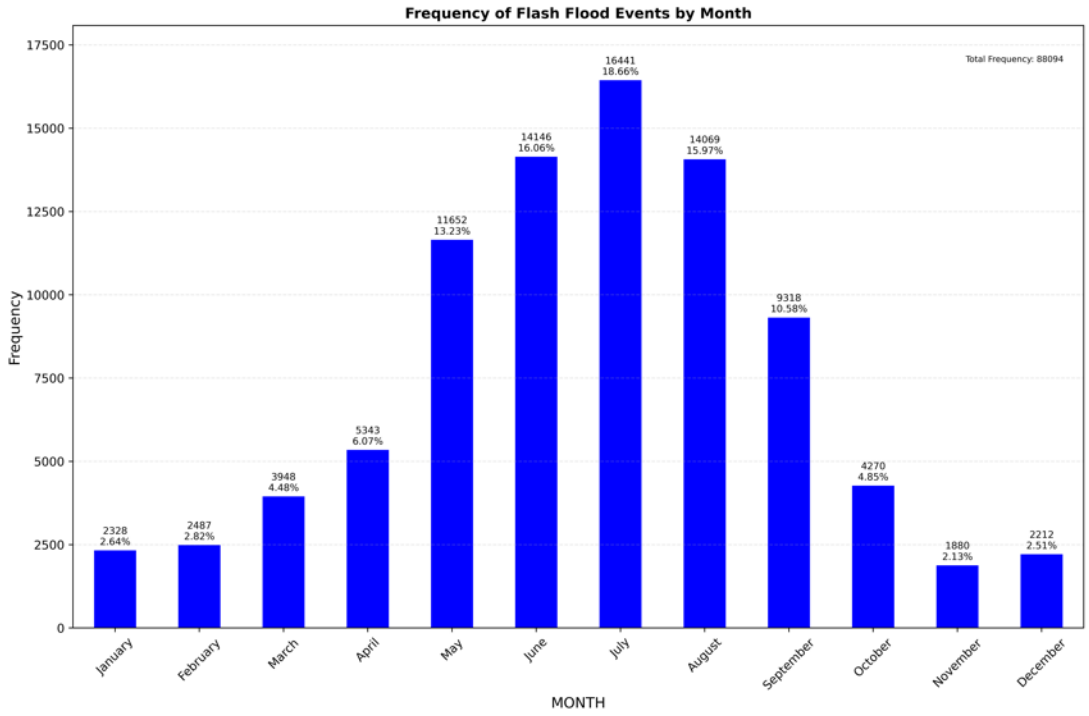

Figure 48 shows that most flash flood events are short-lived, with 88.20% lasting only one day (77,698 events) and 11.44% lasting two days (10,077 events). Events lasting more than two days are extremely rare, highlighting the typical brief duration of flash floods.

Figure 48. Duration for Flash Flood Events in Days 2000–2024 (NCEI)

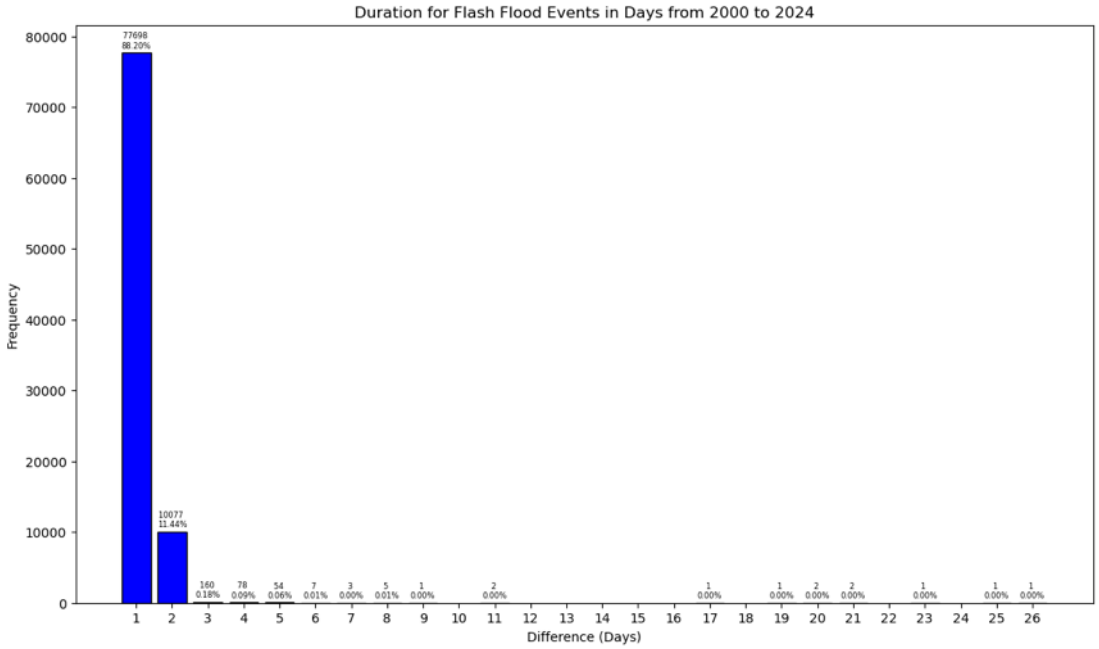

Figure 49 displays the average duration of flash flood events per year from 2000 to 2024. The average duration remains consistently around 1.1 to 1.2 days each year, with minor fluctuations. This consistency underscores the generally short-lived nature of flash floods across different years.

Figure 49. Average Duration of Flash Flood Events per Year 2000–2024 (NCEI)

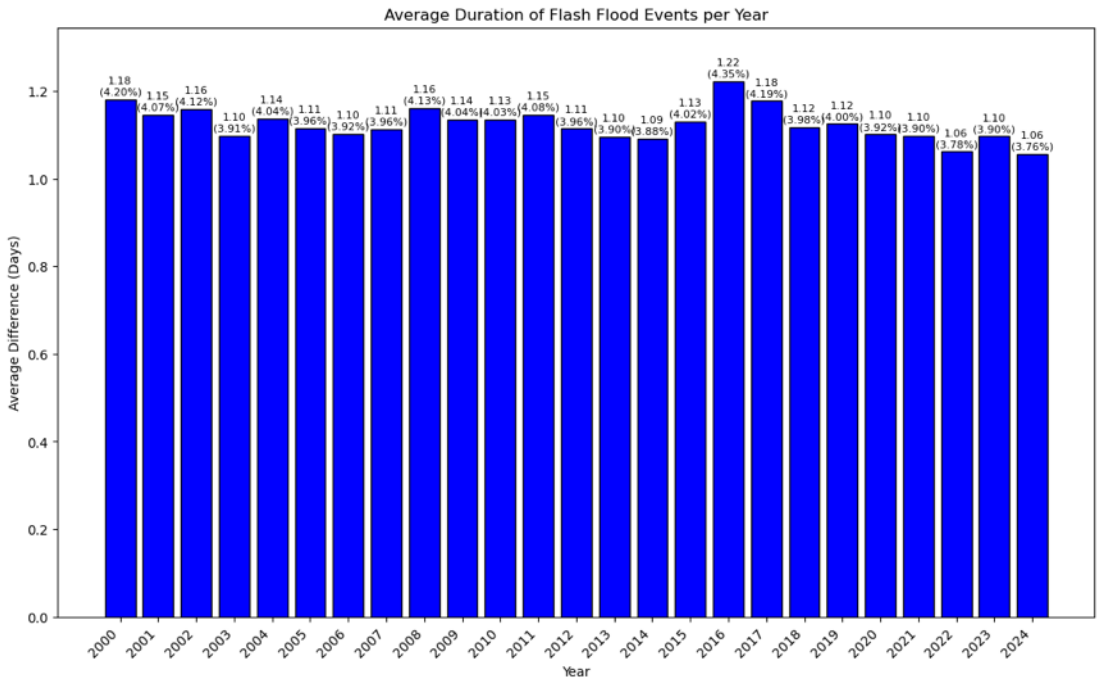

Assigning the NCEI Flash Flood Events to the U.S. Rail Network

For the NCEI flash flood events, each flash flood event is represented by a specific point. If there is any recorded flash flood point within a 12-digit HUC, the entire HUC is considered flooded. The methodology applied here is consistent with that used in the flood section. Figures from 50 to 53 illustrate the rail network to which NCEI flash flood occurrences have been allocated. This will also be an additional shapefile provided to the FRA from this report providing a flood-based rail dataset bound to historic events from the NCEI dataset. In Figure 51, the rail network is illustrated with 69,547 different recorded flood events (out of 88,094 recorded flood events) that have coordinates from the NCEI dataset, highlighting the specific locations affected by flooding.

Figure 50. Distribution of Flash Flooding Events (NCEI Dataset) Across the Rail Network

Figure 51. Rail Network Segments with No Flash Flood and Recorded Flash Flood Events (NCEI Dataset)

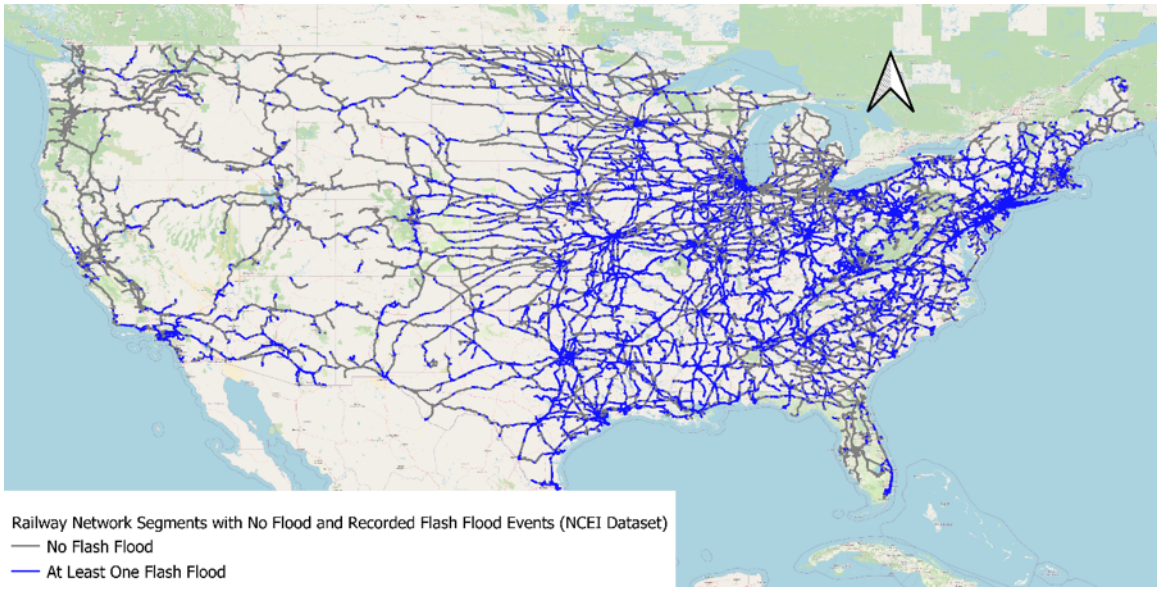

Figure 52. Rail Network Segments with Recorded at Least One Flash Flood Event (NCEI Dataset)

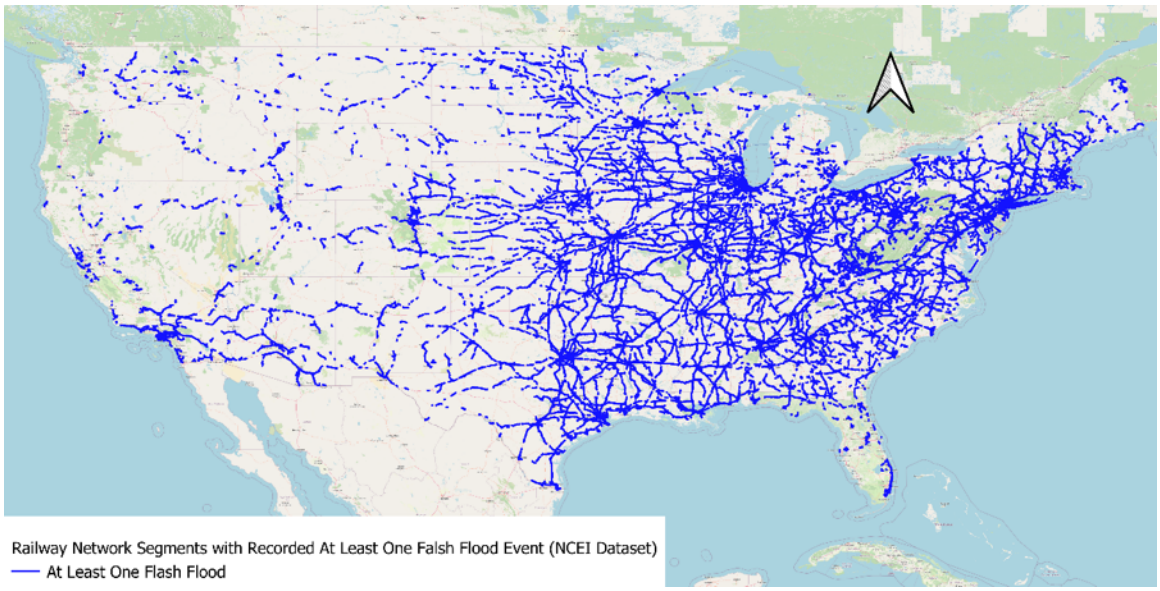

Figure 53. Rail Network Segments with No Flash Flood (NCEI Dataset)

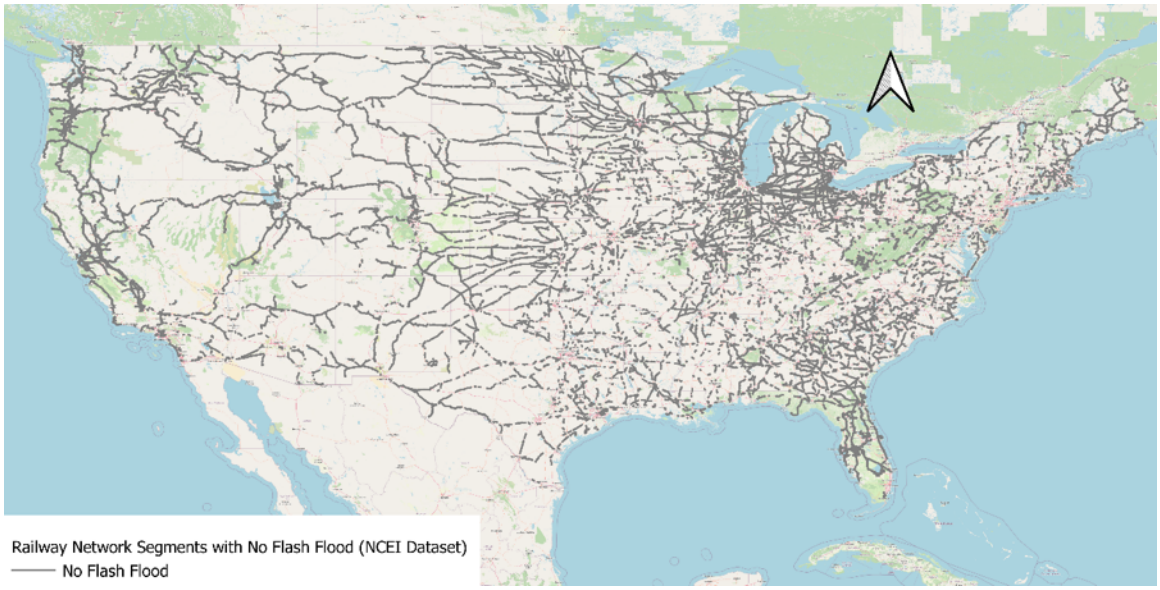

The network is divided into two categories: segments with "No Flash Flood" incidents, which comprise 43.1% of the total and are displayed in red, and segments with "At Least One Flash Flood" incidents, which make up 56.9% of the total and are displayed in blue.

Figure 54. Distribution of Rail Lines by NCEI Flash Flood Frequency (2000–2024)

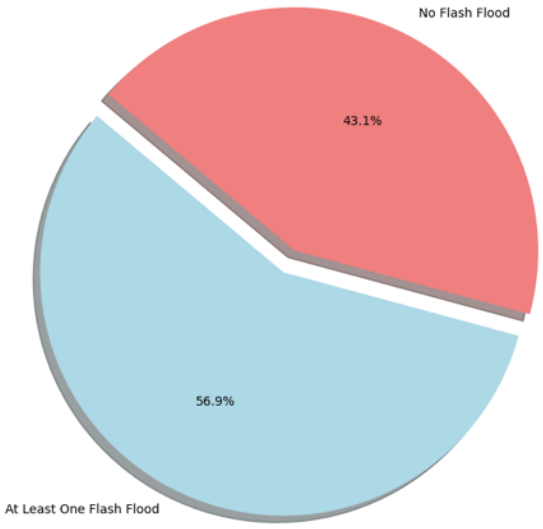

Figures 55 and 56 depict the classification of rail length by flash flood frequency events.

Figure 55. Sum of Rail Length by Flash Flood Frequency Events (NCEI)

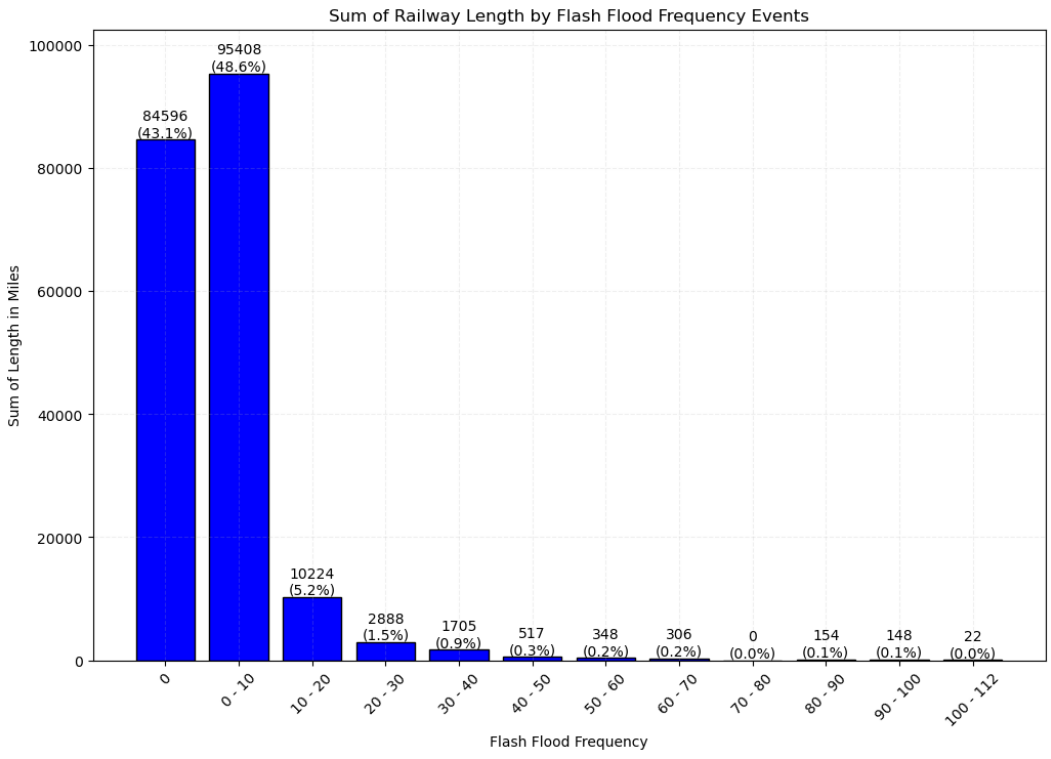

Figure 56. Sum of Rail Length by Flash Flood Frequency Between 1–10 (NCEI)

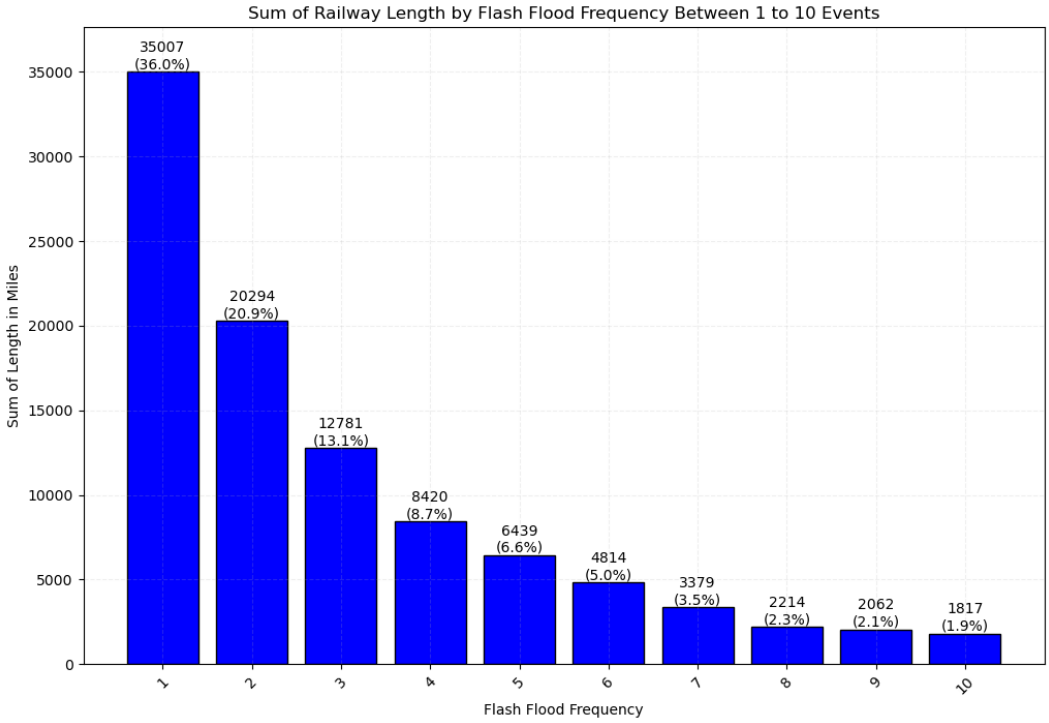

Coastal Flood Events Analysis in the United States (NCEI)

Figure 57 presents the frequency of coastal flood events across different states in the United States. Coastal flooding occurs when water is driven onto land from an adjacent body of water. This generally occurs when there are significant storms, such as tropical and extratropical cyclones (NOAA, n.d.e). Total coastal flooding event frequency is about 3617 and New Jersey experiences the highest frequency with 665 events, followed by Florida with 318 events, South Carolina with 307 events, and New York with 267 events. States such as California (87), North Carolina (111), and Texas (77) also show notable frequencies. In contrast, many inland states have no recorded coastal flood events. While the following sections describe a process similar to that used with the data from NCEI for flooding and flash flooding, the events themselves did not have specific coordinates, so a general review of the data is described; however, the generation of a shapefile with events assigned to segments of track could not be accomplished. While assigning coastal flood events could follow the same methodology used for extreme and excessive heat—by utilizing National Weather Service (NWS) forecast zones—this approach may reduce spatial accuracy. Specifically, it may not reflect the precise coastal locations or sub-watersheds where flooding occurs and could **overestimate** the number of events affecting the rail network, especially if rail segments lie inland but still fall within a broad NWS zone. Furthermore, while Figure 57 captures the more prominent types of agencies from which data comes, there are also weather - and station-specific data—specifically river/stream gages and C-man stations—which will provide environmental data

that will be leveraged to assign annual exceedance risk from the events in future chapters of this research.

Figure 57. Coastal Flood Event Frequency Analysis in the United States (NCEI)

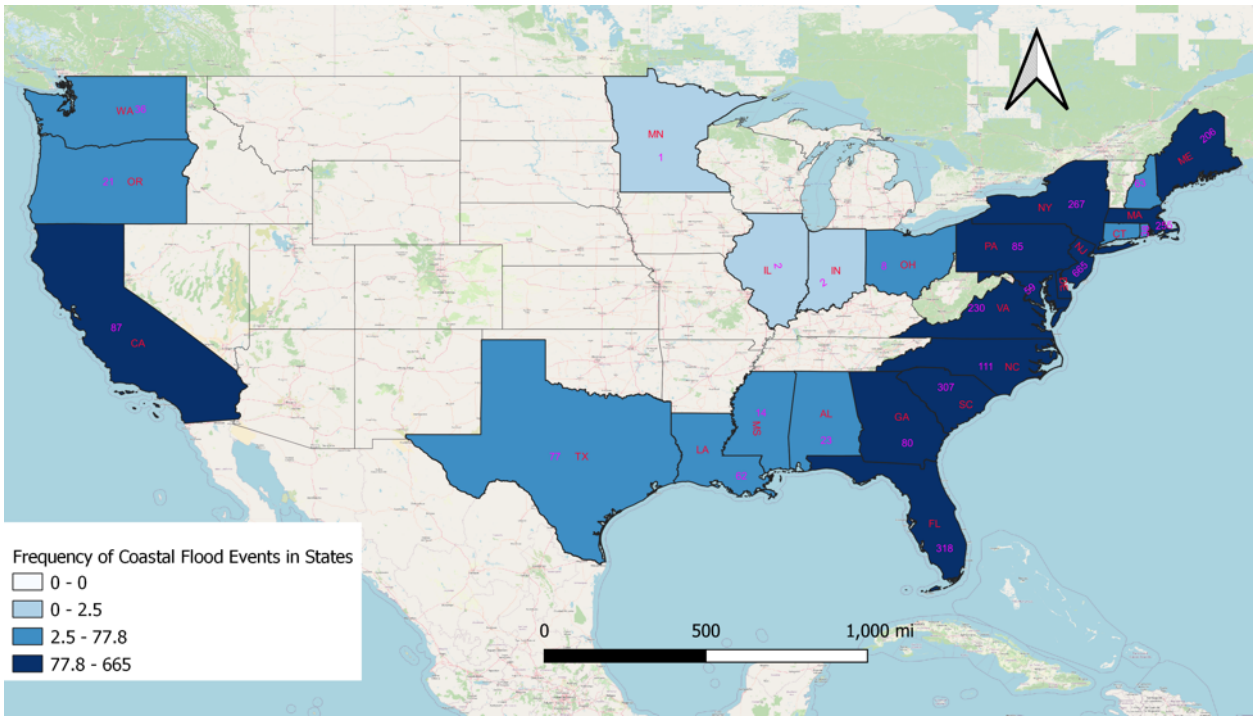

Figure 58 shows the frequency of coastal flood events reported by various sources. River/Stream Gage is the leading source, contributing 17.31% (626 events), followed by Emergency Manager at 14.32% (518 events) and Broadcast Media at 9.79% (354 events). Other notable sources include C-man Station (7.24%) and Amateur Radio (5.78%).

Figure 58. Frequency of Coastal Flood Events by Source 2000–2024 (NCEI)

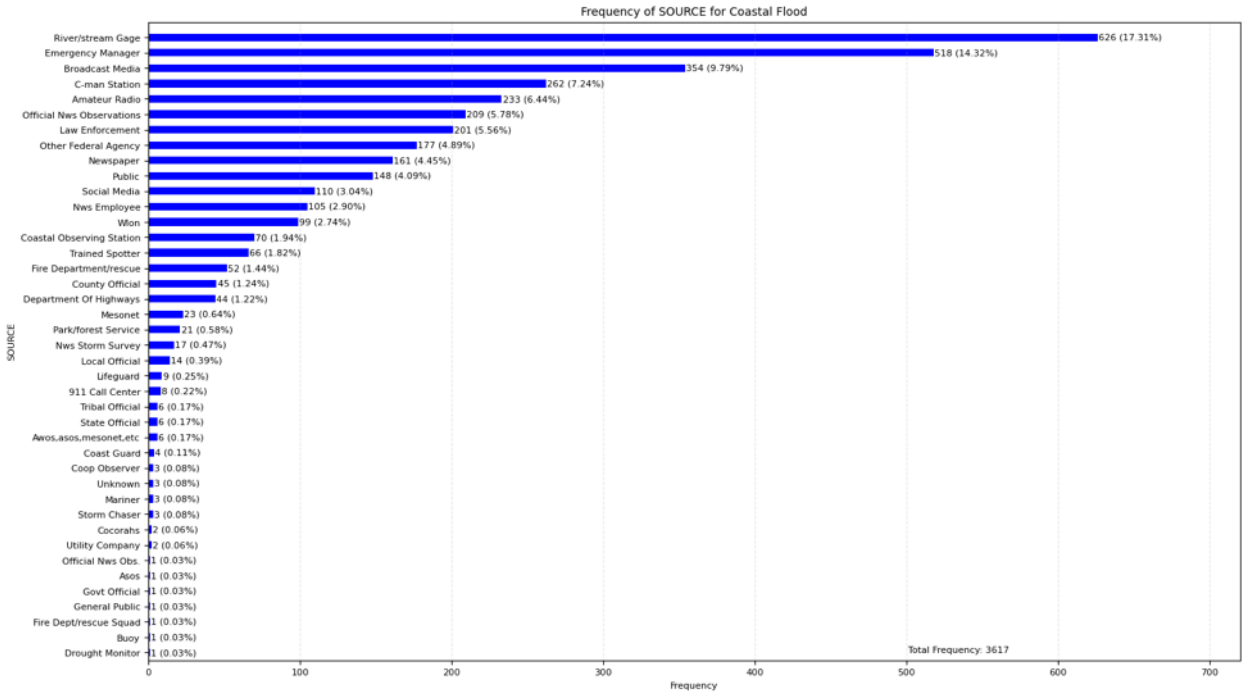

Figure 59 shows the frequency of coastal flood events by year. The highest frequency occurred in 2018 with 321 events (8.87%), followed by 2012 and 2015 with 269 and 270 events (7.46% and 7.44%), respectively. Lower frequencies were observed in 2000 to 2005 with single-digit events. This variability indicates periods of increased coastal flooding activity, emphasizing the need for adaptive measures to protect infrastructure in vulnerable years.

Figure 59. Frequency of Coastal Flood Events by Year 2000–2024 (NCEI)

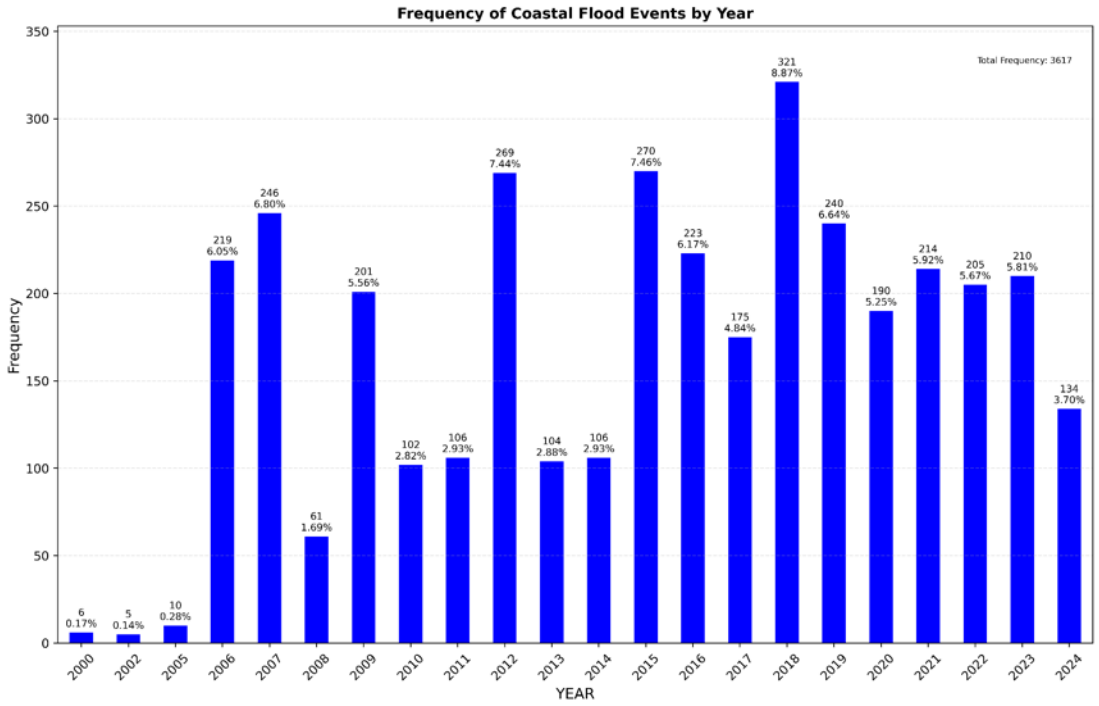

Figure 60 shows the frequency of coastal flood events by month. October has the highest frequency with 838 events (23.17%), followed by September with 422 events (11.67%) and January with 420 events (11.61%). The lowest frequencies occur in July and August with 40 (1.11%) and 90 events (2.49%), respectively.

Figure 60. Frequency of Coastal Flood Events by Month 2000-2024 (NCEI)

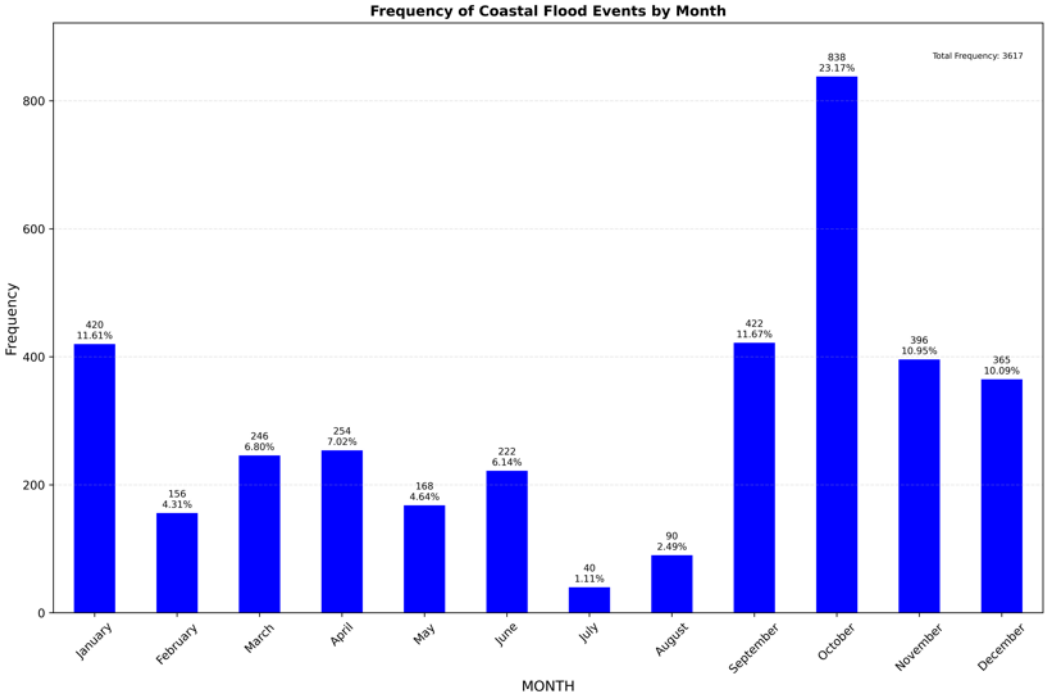

Figure 61 shows the duration of coastal flood events from 2000 to 2024. The majority of events (74.95%) lasted only one day, with 2,711 occurrences. Two-day events account for 16.06% (581 occurrences), and three-day events make up 4.81% (174 occurrences). Events lasting more than three days are rare, highlighting that most coastal floods are short-lived, with a significant drop in frequency for durations longer than two days.

Figure 61. Duration for Coastal Flood Events in Days 2000–2024 (NCEI)

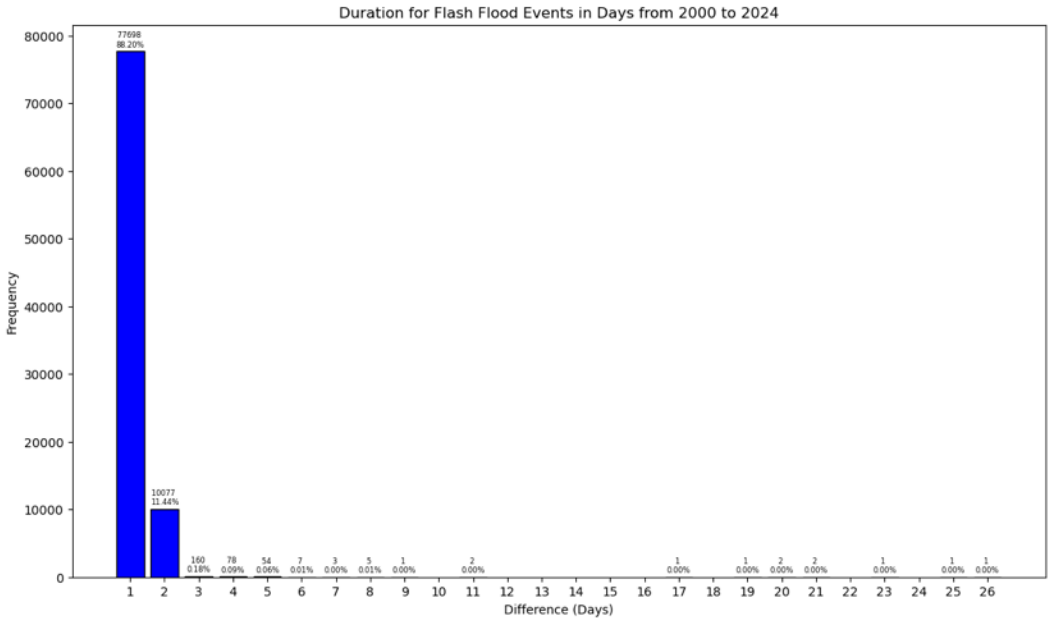

Figure 62 shows the average duration of coastal flood events per year from 2000 to 2024. Most years have an average duration of around 1 to 1.6 days, indicating generally short-lived coastal floods. However, 2017 stands out with a significantly higher average duration of 9.26 days (25.24%). This spike is attributed to events in New York that occurred over different months and lasted for up to one month. This highlights the need for adaptive strategies in flood management to handle both typical short-term and rare prolonged flooding events.

Figure 62. Average Duration of Coastal Flood Events per Year 2000–2024 (NCEI)

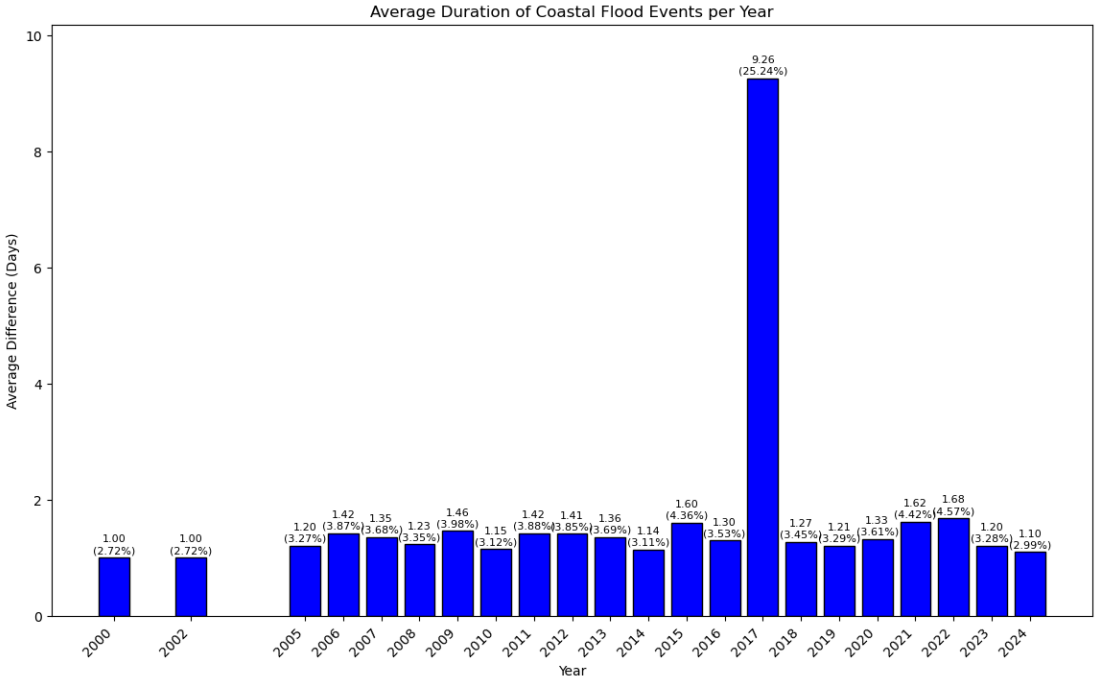

3. Heat and Excessive Heat

Rail infrastructure is vulnerable to various natural hazards, and as the speed and demand on the rail network increases, accounting for the impacts of these hazards becomes critical for minimizing disruptions. While the previous section focused on flooding, this section addresses heat and extreme heat events, another major hazard that can cause widespread damage and service interruptions across the U.S. rail network.

Figure 63 has been developed for the heat events dataset. The process begins with various data sources, including the Rail Equipment Accident/Incident Data (READ), National Weather Forecast Zones (NWS), NCEI (NOAA), and the U.S. Rail Network Shapefile (USRN). First, the financial impact and frequency of rail accidents caused by heat are highlighted. Then, historical heat and excessive heat events are assigned to NWS forecast zones. Afterwards, heat and excessive heat events are mapped to specific rail lengths utilizing the NWS forecast zones. The following sections will elaborate on each of these steps in detail.

Figure 63. Process Flowchart for Assigning Heat Events to Rail Infrastructure

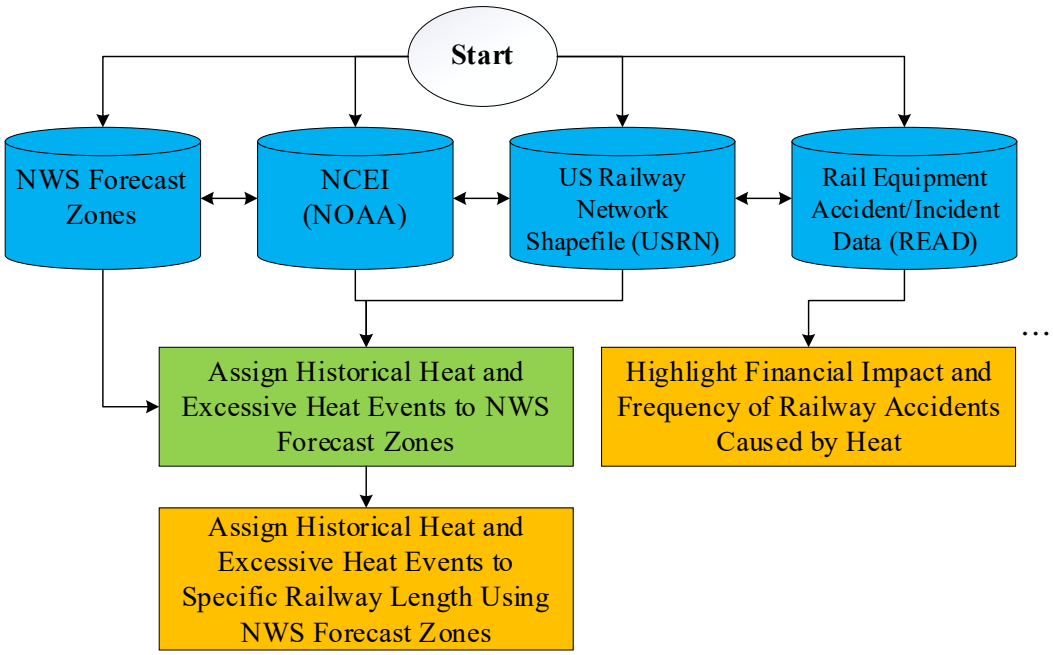

3.1 Train Accident Cause Codes

The accident data pertaining to track damage from irregular track alignment has been examined in this section of the report (T109). This analysis includes detailed information on the types and frequency of related incidents that occurred between 2000 and 2023, helping to better understand the impact of this specific track defect on rail safety.

The review of T109 events revealed a total of 604 instances, with 597 (99%) resulting in derailments and the remaining 7 (1%) contributing to other accident types according to the data's narrative reports. This demonstrates that the vast majority of T109 events resulted in derailments, with just a minor proportion caused by other specific accident types. Figure 64 and Table 11 show the frequency and distribution of different accident types across states, which helps to explain these findings.

Figure 64. The Frequency of T109 Accidents Across States from 2000 to 2023

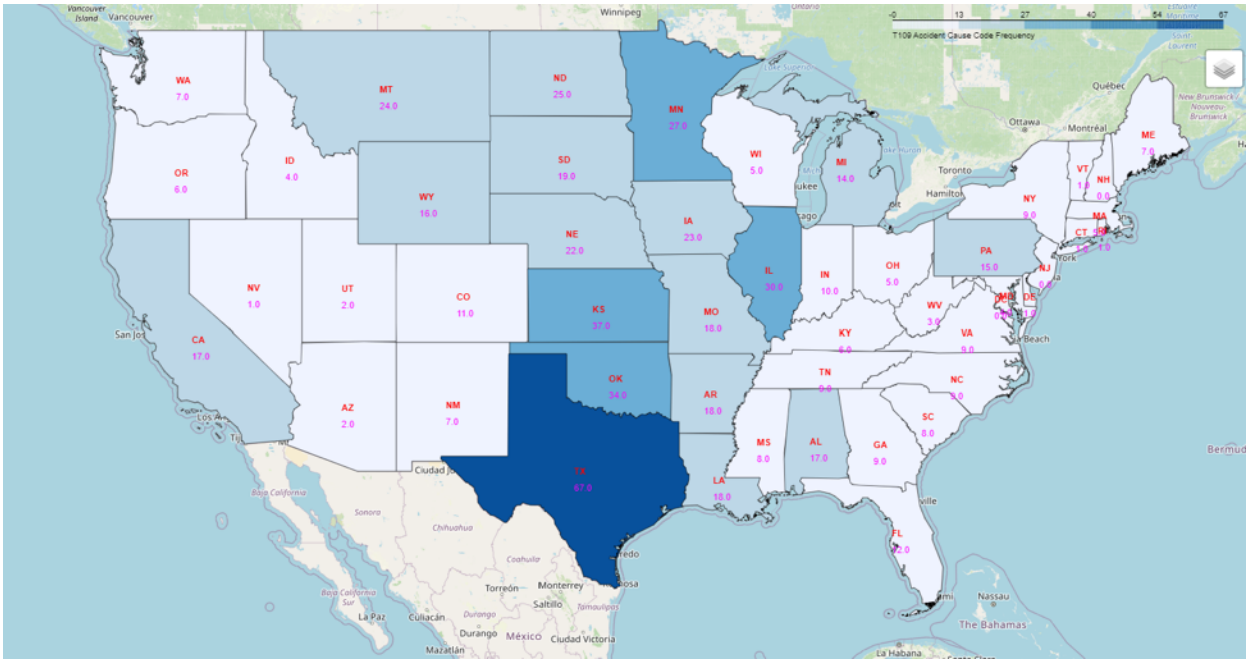

Table 11. The Frequency of T109 Accidents Across States from 2000 to 2023

State Name	T109	State Name	T109	State Name	T109
TEXAS	67	PENNSYLVANIA	15	KENTUCKY	6
KANSAS	37	MICHIGAN	14	OHIO	5
OKLAHOMA	34	FLORIDA	12	MASSACHUSETTS	5
ILLINOIS	30	COLORADO	11	WISCONSIN	5
MINNESOTA	27	INDIANA	10	IDAHO	4
NORTH DAKOTA	25	TENNESSEE	9	MARYLAND	4
MONTANA	24	VIRGINIA	9	WEST VIRGINIA	3
IOWA	23	NEW YORK	9	UTAH	2
NEBRASKA	22	GEORGIA	9	ARIZONA	2
SOUTH DAKOTA	19	NORTH CAROLINA	9	VERMONT	1
LOUISIANA	18	SOUTH CAROLINA	8	DELAWARE	1
ARKANSAS	18	MISSISSIPPI	8	CONNECTICUT	1
MISSOURI	18	NEW MEXICO	7	ALASKA	1
CALIFORNIA	17	WASHINGTON	7	NEVADA	1
ALABAMA	17	MAINE	7	RHODE ISLAND	1
WYOMING	16	OREGON	6		

An examination of T109 accident frequencies between 2000 and 2023 indicates a clustering of higher events in Texas and the Midwest, with Texas taking the lead with 67 accidents. Significant accident statistics are also observed in the Midwest and Southern regions, which encompass Kansas, Oklahoma, and Illinois. Conversely, states in the western and northeastern regions, such as Nevada and Delaware, have the lowest number of accidents. This indicates that there may be either less involvement in T109-related activities or the implementation of successful safety measures. The distribution map emphasizes these patterns, highlighting regional variations and the necessity for focused safety initiatives in areas with elevated risks.

Track alignment irregularities are an area of great concern as they constitute a safety hazard not only to the track but also to the rolling stock and passengers. By analyzing the frequency of track alignment irregularities (i.e., buckled or sun kink tracks) from 2000 through 2023, it was revealed that this trend is quite dynamic with significant peaks (Figure 65). A large peak occurred in 2006 when 53 incidents were recorded, followed by another peak in 2011 with 48 incidents. These peaks suggest that there are periods of greater vulnerability to track alignment problems due to weather conditions acting as external factors on the rail infrastructure. After 2012, there is a significant drop-off in accident frequency, which may be attributed to increased maintenance periods or changes in maintenance regulations. From 2013 to 2020, the trend remains relatively constant

with minor fluctuations, but it is evident that the accident frequency increased from 2021 to 2022. The recent upward turn of events shows how difficult it is to maintain the track in a straight line and makes the case for more monitoring and prevention programs for such problems that can impede rail performance.

Figure 65. Frequency of Track Alignment Irregular (Buckled/Sun Kink) by Year from 2000 to 2023

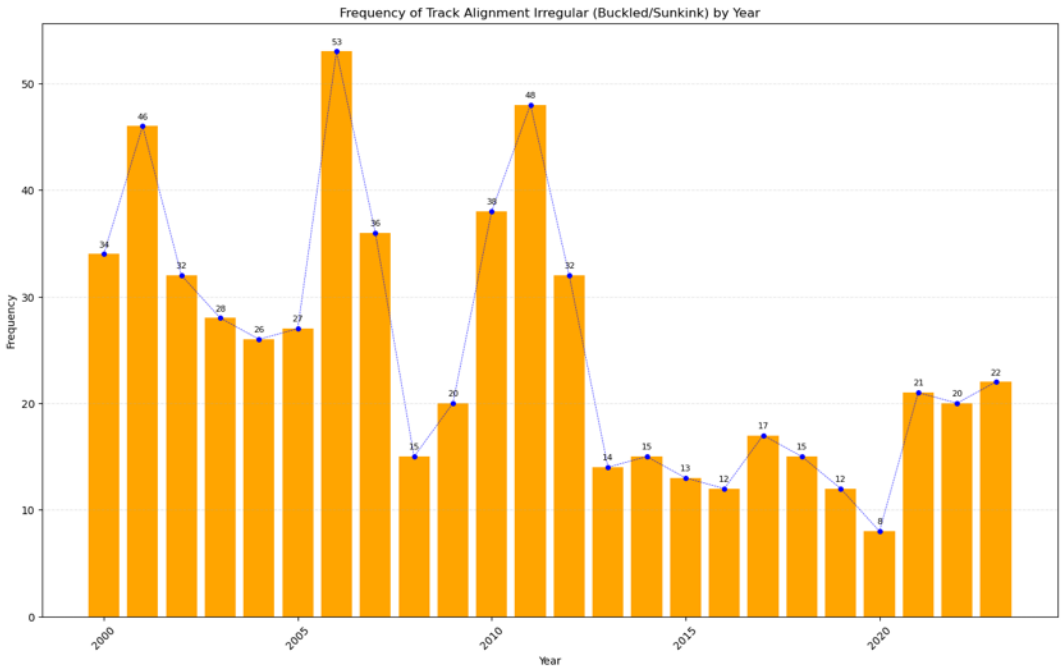

In the accident dataset there are two types of damage cost for each accident: equipment damage and track damage. There are some accident rows in the dataset where the Total Damage Cost (based on the dataset) exceeds the sum of the two types of accidents (sum of equipment and track). It is not explained in the dataset what the source of this difference is, and here it has been considered as other costs. T109 statistics are provided, followed by an accumulated frequency analysis for both categories combined (Table 12 and Figure 66).

Table 12. Breakdown of T109 Accident Damage Costs (2000-2023)

Accident Type	Equipment Damage Cost	Track Damage Cost	Other Costs	Total Damage Cost
Derailment	$189,702,305	$84,973,973	$47,574,176	$322,250,454
Non-Derailment (Other Accidents)	$459,836	$179,400	$448,684	$1,087,920
Total	$190,162,141	$85,153,373	$48,022,860	$323,338,374

Figure 66. (a) Proportion of Damage Costs for Derailments in T109 Accidents, (b) Proportion of Damage Costs for Non-Derailments in T109 Accidents, (c) Proportion of Total Damage Costs for All T109 Accidents

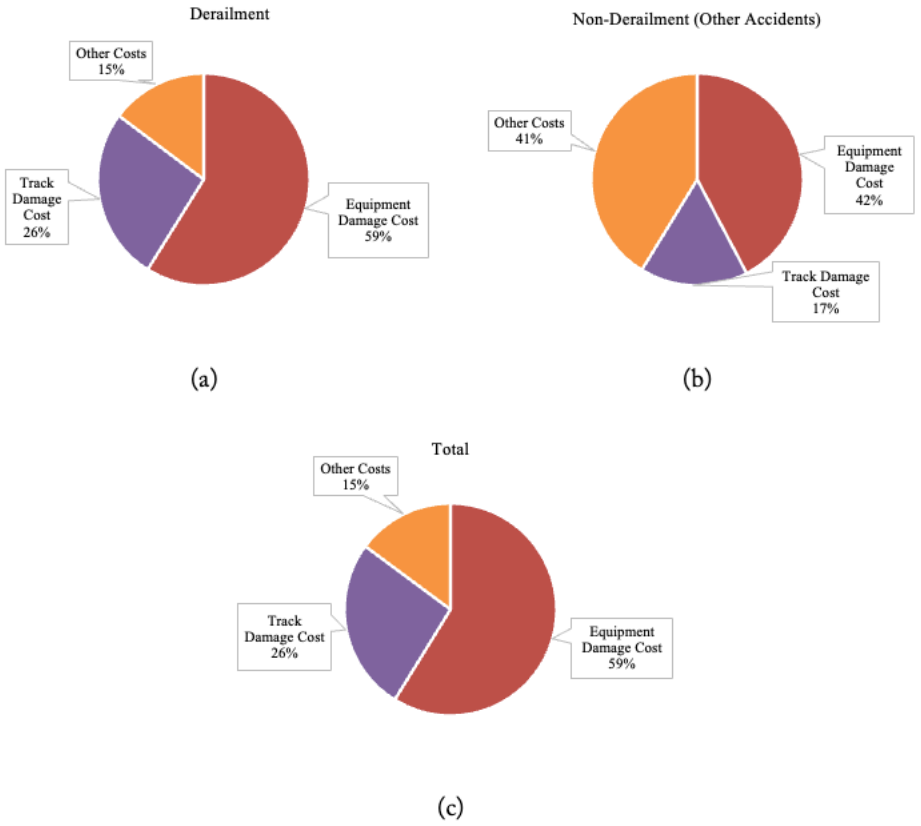

The analysis of T109 accident damage costs from 2000 to 2023 reveals significant insights into the distribution and impact of costs associated with derailments and non-derailment (other) accidents. Table 12's data highlights that the total damage cost for derailments is substantially higher at $322,250,454, compared to $1,087,920 for non-derailment accidents. Equipment damage is the largest contributor to these costs, with derailments accounting for $189,702,305 and non-derailment accidents accounting for $459,836. Track damage costs are also notable, with derailments incurring $84,973,973 compared to $179,400 for non-derailment accidents. Other costs, encompassing miscellaneous expenses related to the accidents, amount to $47,574,176 for derailments and $448,684 for non-derailment accidents.

Figure 66 further illustrates these distributions, indicating that equipment damage constitutes the largest proportion of costs in both derailments and non-derailment accidents. Specifically, equipment damage accounts for 59% of the costs in derailments and 42% in non-derailment accidents. Track damage costs are notably higher in derailments, representing 26% of the total costs, compared to just 17% in non-derailment accidents. Other costs make up 15% of the total costs in derailments and a significant 41% in non-derailment accidents. Overall, the comprehensive analysis emphasizes the critical need for targeted maintenance and preventive

measures to mitigate equipment damage and track damage, particularly focusing on reducing the high costs associated with derailments.

3.2 National Weather Service Forecast Zones

Using a process similar to the flood and flash flood approach, where events were assigned first to basins and then to the track itself, the extreme heat events that were identified were assigned to national weather service zones where it is understood that the environmental features within the zone would be constant. The NWS issues forecasts and some watches and warnings for general areas, which are usually counties but in many cases are subsets of counties. Because of differences in climate within a county due to things like elevation or proximity to large bodies of water, counties are divided into sub-regions to allow for more accurate forecasting (*NWS Public Forecast Zones*, n.d.).

Figure 67 and Table 13 depict the NWS forecast zone throughout the U.S. and shapefile attributes, respectively.

Figure 67. NWS Public Forecast Zones Shapefile

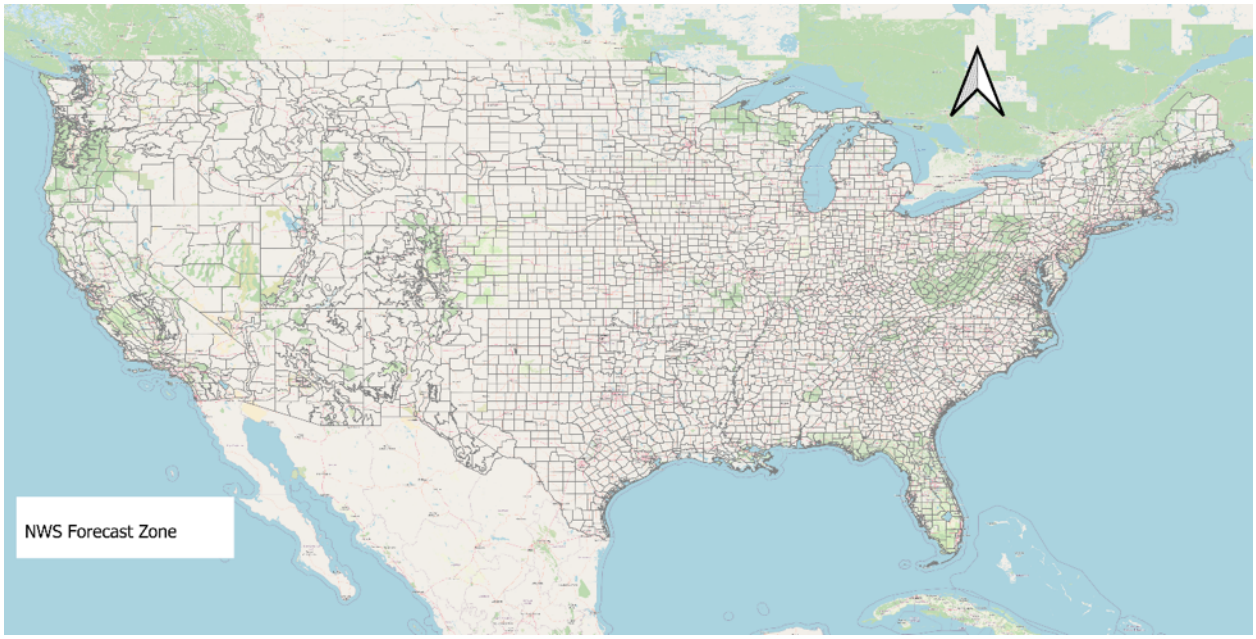

Table 13. Attributes of NWS Public Forecast Zones

Field Name	Type	Width, Decimals	Description
STATE	Character	2	U.S. postal standard two-letter abbreviation
ZONE	Character	3	Zone number from NWSI 10-507
CWA	Character	3	CWA (WFO) abbreviation from NWSI 10-507
NAME	Character	254	Zone name from NWSI 10-507
STATE_ZONE	Character	5	Concatenation of state and zone
TIME_ZONE	Character	2	Time zone abbreviation
FE_AREA	Character	2	Cardinal area of the state
LON	Numeric	10,5	Longitude of centroid (decimal degrees)
LAT	Numeric	9,5	Latitude of centroid (decimal degrees)
SHORTNAME	Character	32	Name truncated to 32 characters

Heat Events Analysis in the United States (NCEI)

This section of the report presents the analysis of heat event frequency across different states in the United States. Figure 68 illustrates the frequency of heat events in each state, categorized into seven ranges to highlight the variation in heat occurrences. The map provides a visual representation of heat event frequencies across the United States. The states are color-coded based on the number of heat events recorded, with darker shades indicating higher frequencies. The data reveals significant regional differences in heat event occurrences.

Figure 68. Heat Event Frequency Analysis in the United States (NCEI)

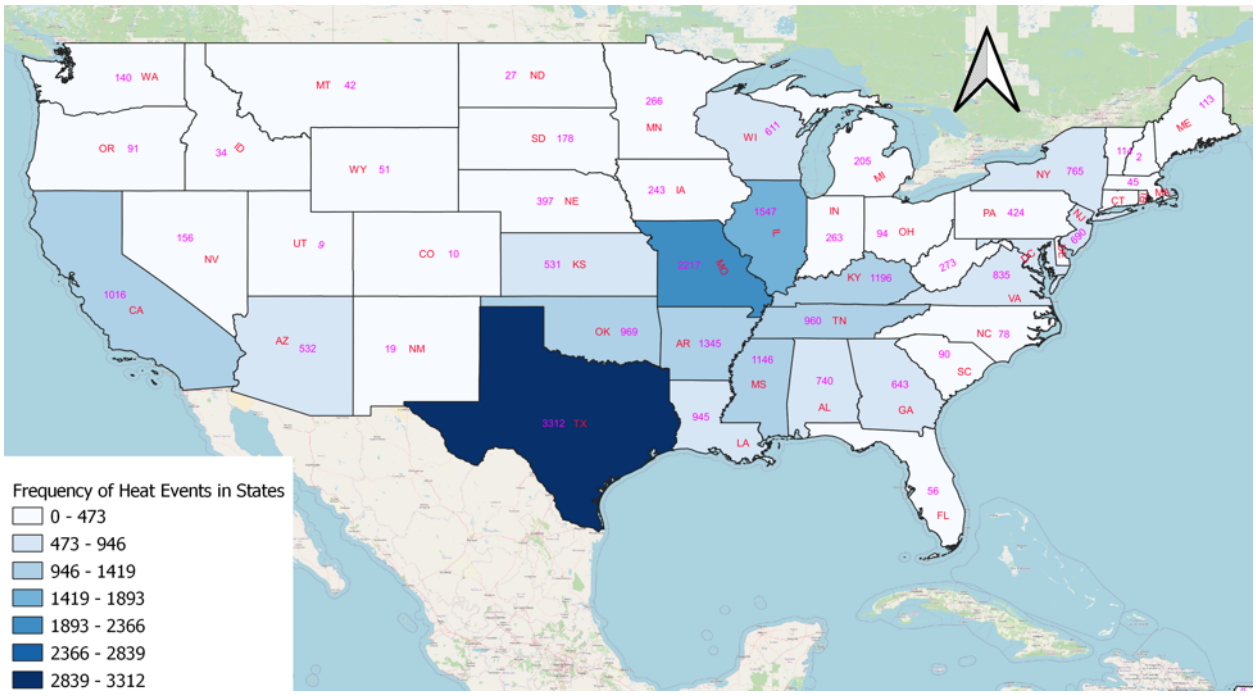

The map provides a visual representation of the frequency of heat events across different states in the United States. The data is color-coded to indicate the number of events, ranging from white (0–473 events) to dark blue (2,839–3,312 events). Texas experiences the highest number of heat events with a frequency of 3,312, while states such as Utah and New Mexico have some of the lowest frequencies, at 9 and 19, respectively. However, it should be noted that this number could be the result of a lack of reporting procedures at the state level. The total frequency of heat events recorded in this dataset is 24,188 and the highest and lowest states are as follows:

- **Texas** leads significantly with 3,312 events.
- **Missouri**, **Illinois**, **Arkansas**, **Kentucky, Mississippi,** and **California** follow with 2,217, 1,547, 1,345, 1,196, 1,146, and 1,016 events, respectively.
- **Alaska** (1), **New Hampshire** (2), and **Rohde Island** (8) are among the states with the fewest heat events.

Figure 69 illustrates the frequency of heat events reported by various sources. The NCEI dataset shows that automated weather observing systems (ASOS and AWOS) are the primary sources for heat event reports, contributing over 50% of the data. There are other sources as well and this diverse range ensures comprehensive data collection for analyzing heat events. The total frequency of heat events reported across all sources is 24,444.

Figure 69. Frequency of Heat Events by Source 2000–2024 (NCEI)

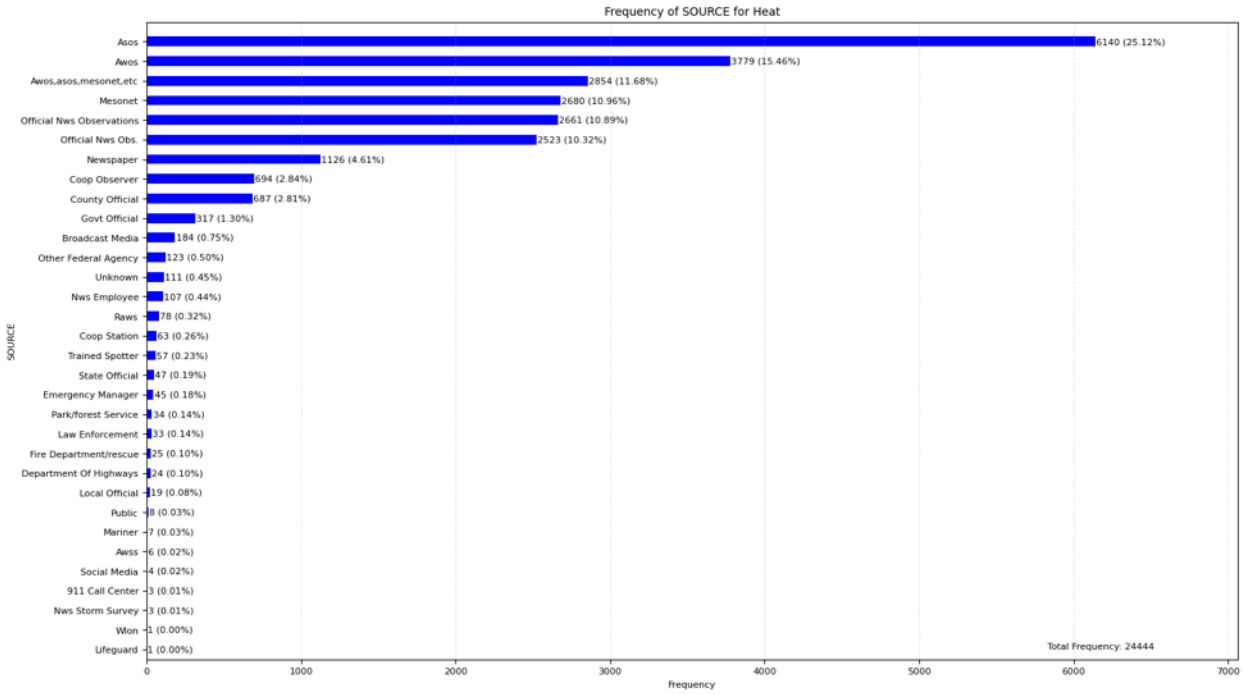

These recorded high-temperature events can be particularly useful in identifying significant locations for track buckling in rail infrastructure. By correlating the frequency and intensity of heat events with occurrences of track buckling, the risk of such incidents can be better predicted and mitigated.

The frequency of heat events has generally increased over the years, with notable spikes in 2001, 2006, 2002, 2022, and particularly in 2023, which saw the highest number of events. This rising trend underscores the growing occurrence of high-temperature events, which are critical for identifying significant locations for track buckling in rail infrastructure. The data from these recorded high-temperature events can provide a valuable basis for developing preventive measures and enhancing the resilience of rail systems against extreme heat.

Figure 70. Frequency of Heat Events by Year 2000–2024 (NCEI)

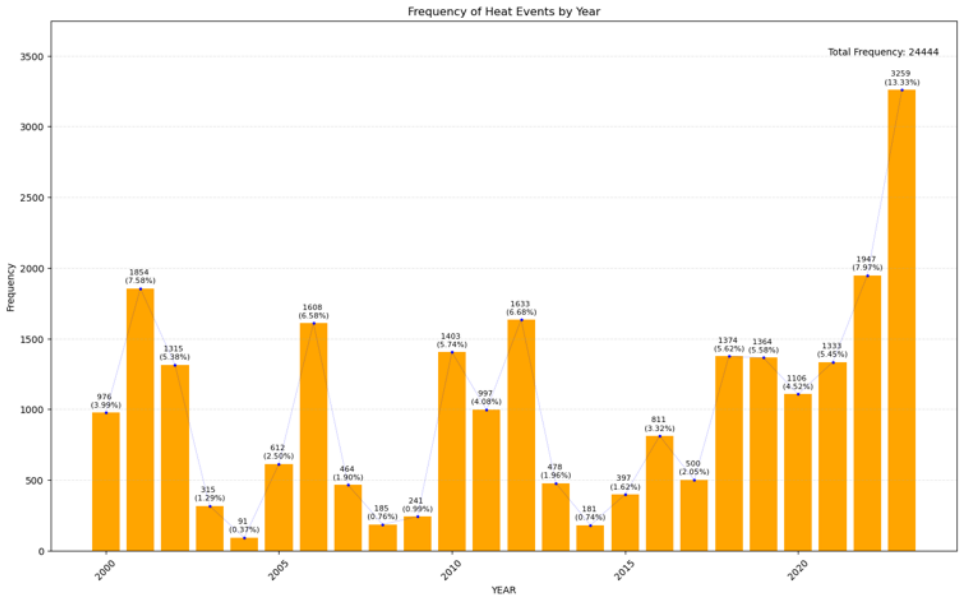

Assigning the NCEI Heat Events to the U.S. Rail Network

The goal of this section is assigning Heat events to the U.S. rail network, using the NWS forecast zone. For NCEI heat events, there is one specific point for each event. There are no latitude and longitude coordinates for the heat events, and in order to assign the frequency events to NWS forecast zones, the events must have first been assigned to the county FIPS. To accomplish this goal, the storm data was matched with the corresponding FIPS codes. The state and county FIPS codes were standardized, and each heat event was linked to its respective county using these codes. The latitude, longitude, and full FIPS code were then assigned to the heat event records. The updated storm data, with each event associated with the correct county, was saved to a new CSV file. With this assumption, we assigned the specific heat events a particular NWS forecast zone to the specific length of the rail network.

Figure 71 represents the NWS forecast zones throughout the United States, focusing on regions impacted by heat events. This figure categorizes the zones into two groups: "No Heat Events" and "At Least One Heat Event."

Figures from 72 to 75 illustrate the rail network to which NCEI Heat occurrences have been assigned. In Figure 72, the rail network is illustrated with 23,357 different recorded heat events (out of 24,444 recorded heat events) that have coordinates from the NCEI dataset, highlighting the specific locations affected by heat. In this figure, the labels show the number of distinctive heat events within the NWS Forecast Zones. Figure 73 presents a binary categorization of the assigned heat, classifying the data into two distinct groups: "No Heat Event" and "At Least One Heat Event."

Figure 71. Geographic Distribution of Heat Events (NCEI Dataset) Across NWS Forecast Zones

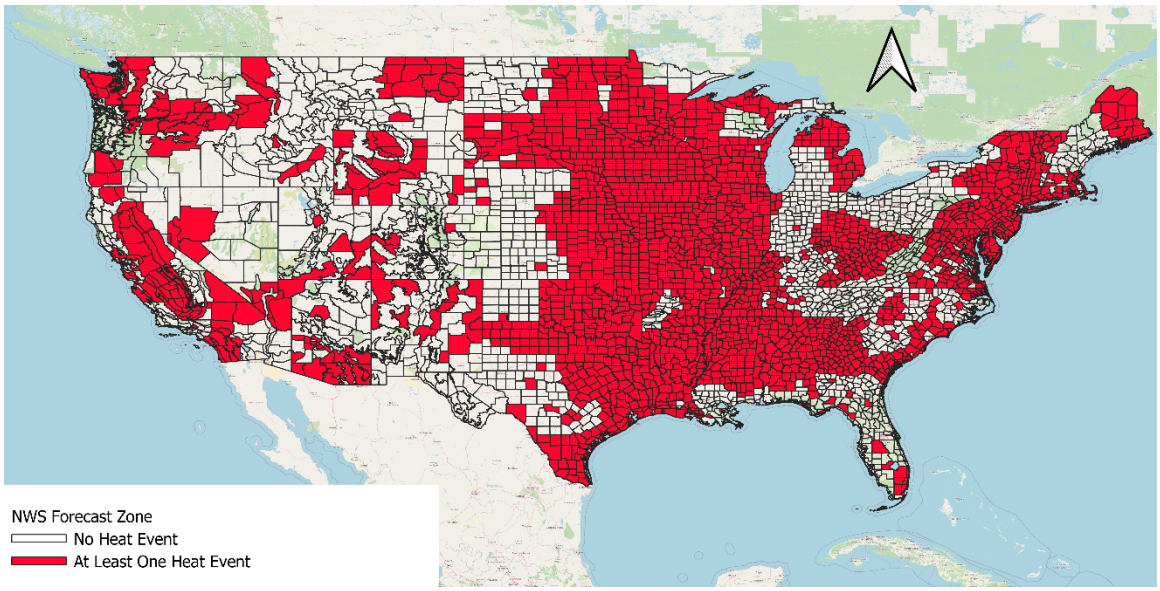

Figure 72. Distribution of Heat Events (NCEI Dataset) Across the Rail Network

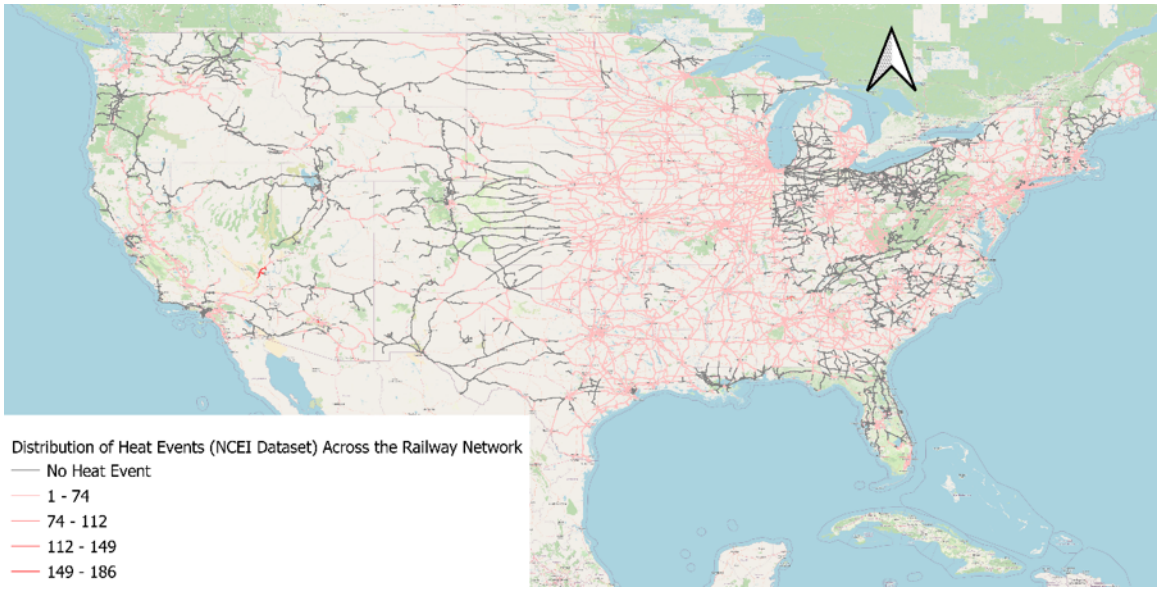

Figure 73. Rail Network Segments with No Heat and Recorded Heat Events (NCEI Dataset)

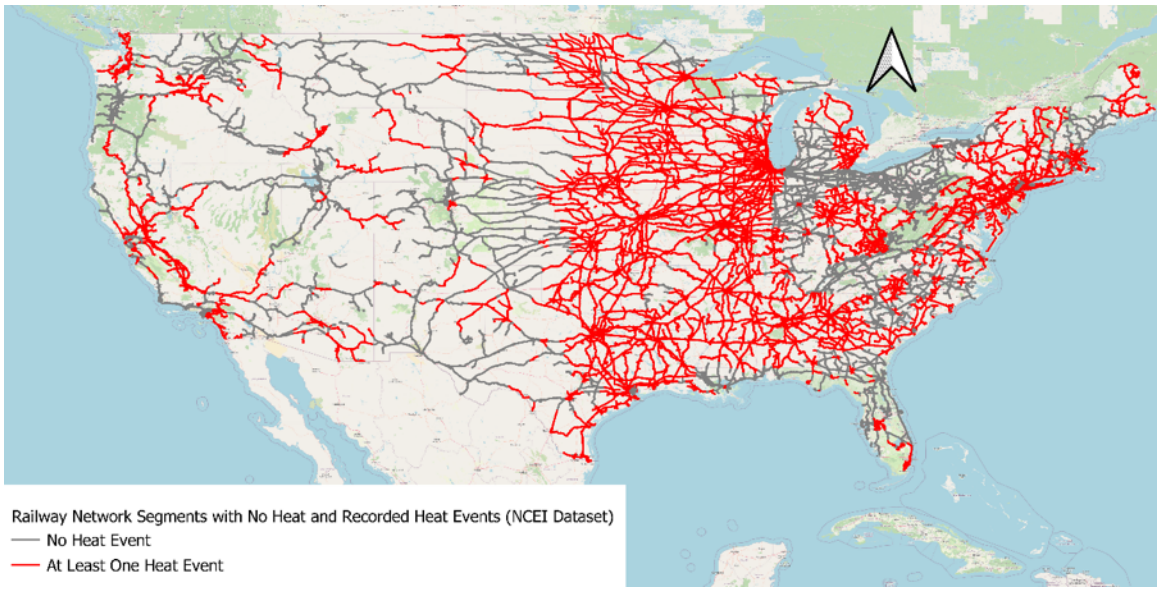

Figure 74. Rail Network Segments with Recorded at Least One Heat Event (NCEI Dataset)

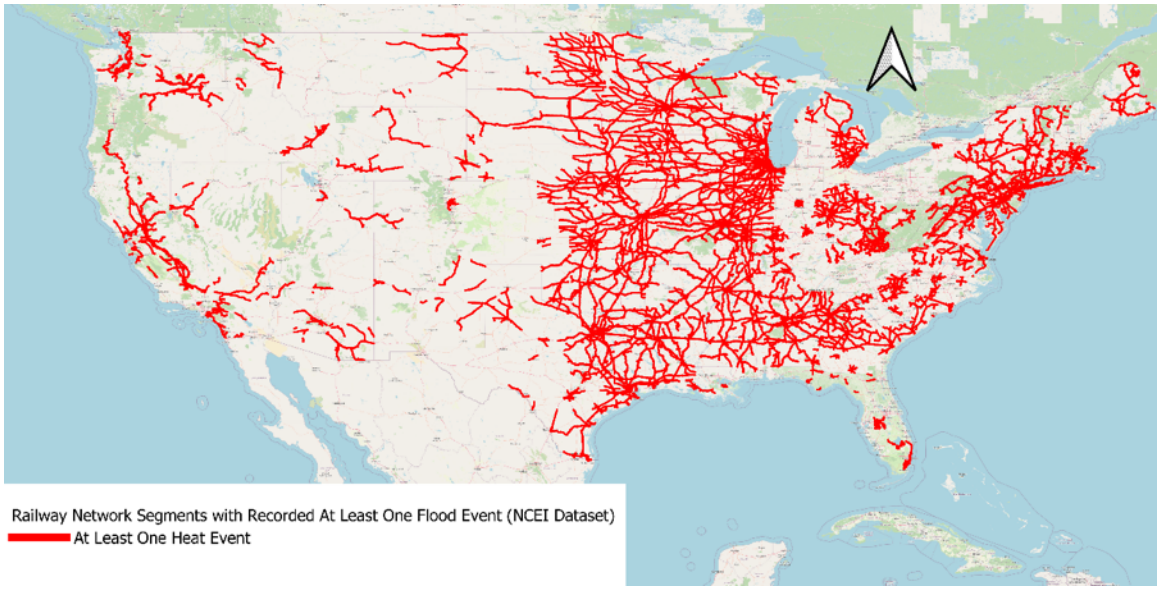

Figure 75. Rail Network Segments with No Heat Event (NCEI Dataset)

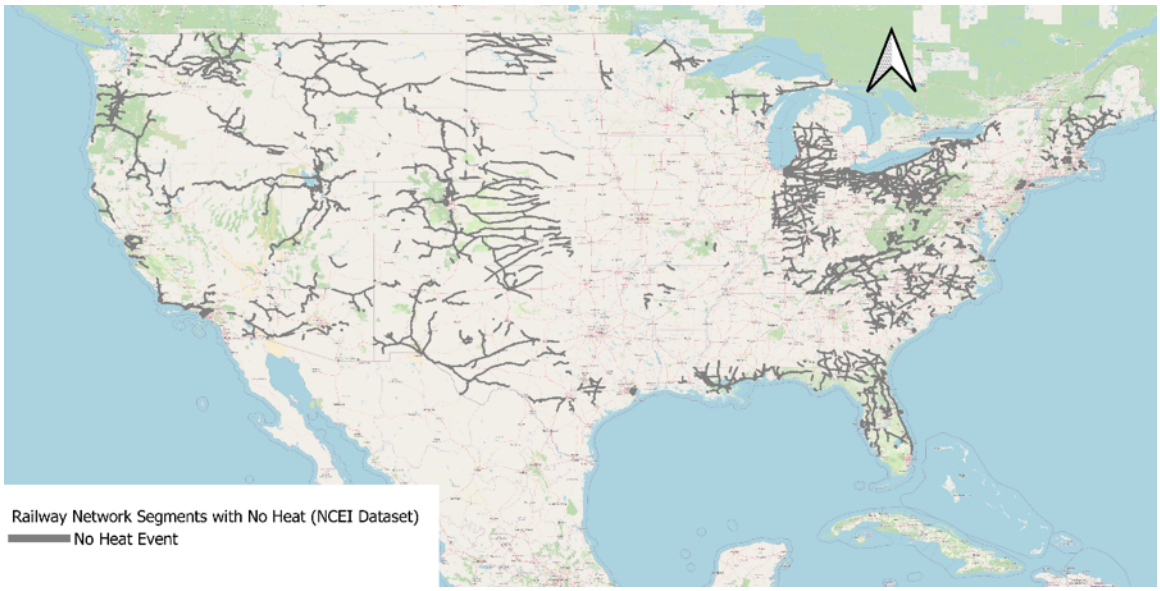

Figure 76 illustrates the distribution of rail segments affected by heat events based on the NCEI dataset. It categorizes the network into two groups: segments with "No Heat" events, comprising 36 % of the total and shown in blue, and segments with "At Least One Heat Event," comprising 64% of the total and shown in red.

Figure 76. Distribution of Rail Lines by NCEI Heat Events Frequency (2000–2024)

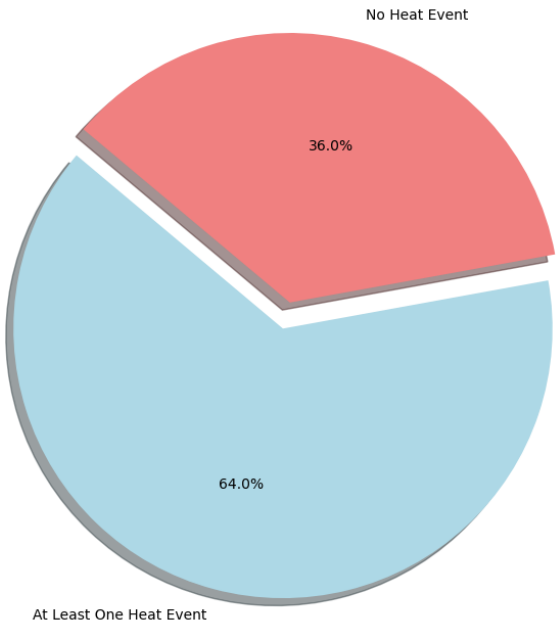

Finally, Figures 77 and 78 depict the classification of rail length by heat frequency events, where the majority of rail segments had less than 10 events, with a single event being the most common. While many segments have a singular event tracked, this may have been the most problematic as a single instance presents a rarity or anomaly to which an unexpected rise in temperature may drastically increase the risk of a sun kink presenting itself.

Figure 77. Sum of Rail Length by Heat Frequency Events (NCEI)

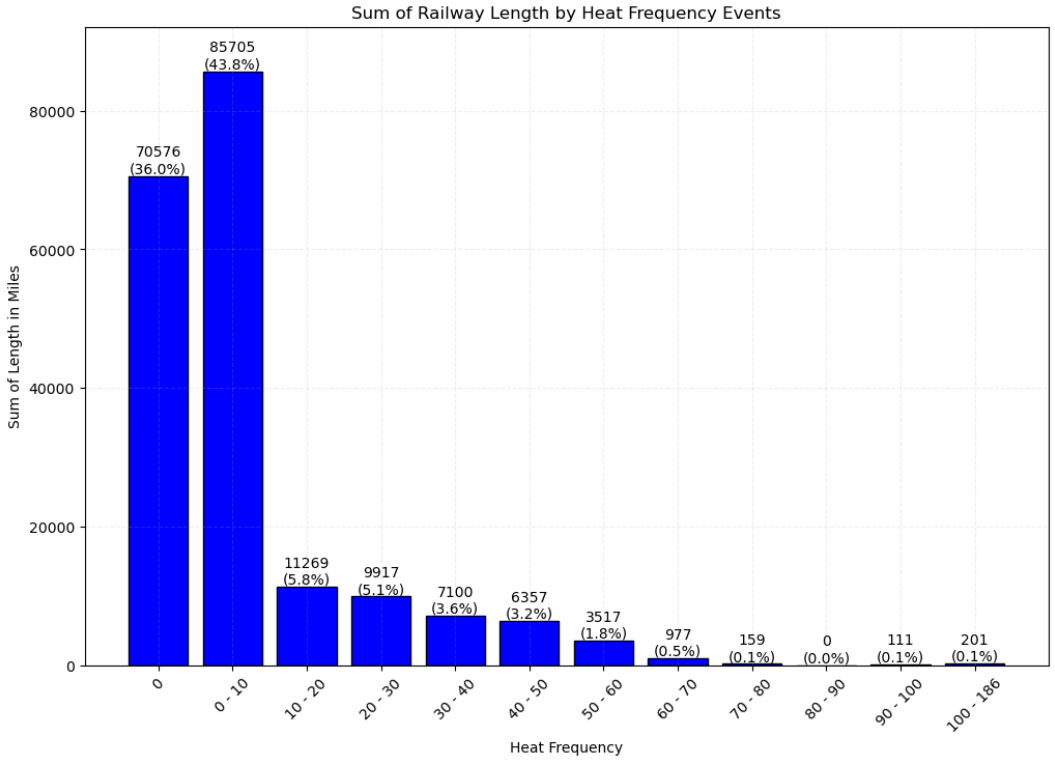

Figure 78. Sum of Rail Length by Heat Frequency Between 1-10 (NCEI)

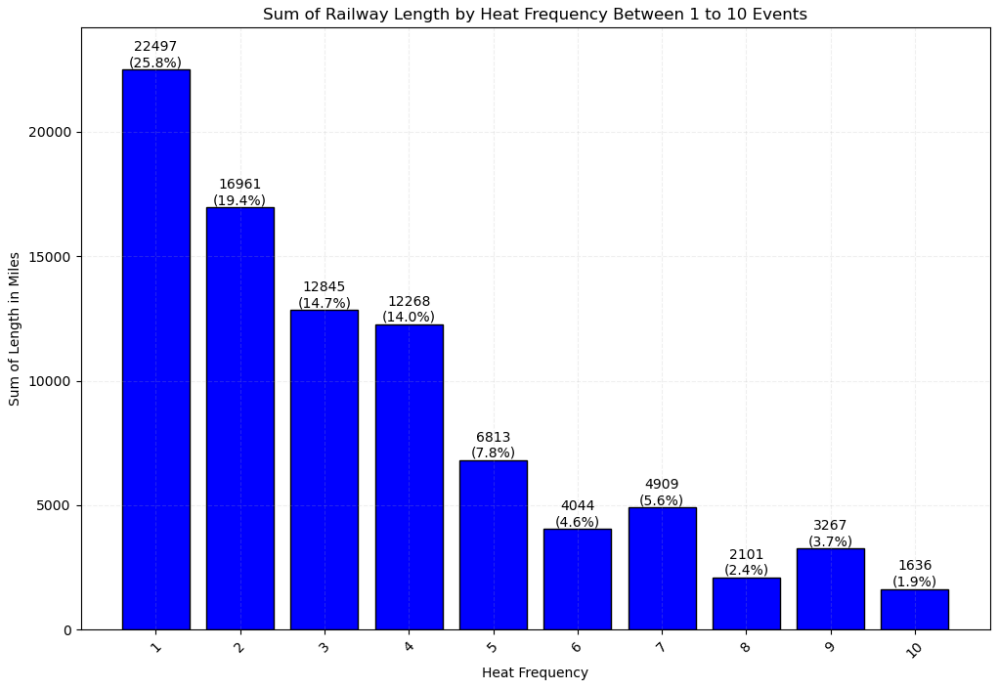

Excessive Heat Events Analysis in the United States (NCEI)

This section of the report analyzes the frequency of excessive heat events across various states in the United States. The specific differences between excessive heat and heat events within the NCEI are predominantly driven by a combination of excessive heat index ranges, which are a function of air temperature and humidity—and the persistence of these extreme conditions over consecutive days. As a result, excessive heat events are often considered more severe than the general heat events discussed in the previous section. Both datasets were included because each dataset captures different aspects of heat-related conditions, and together they provide a more comprehensive representation of heat-based events across the U.S.

Figure 79 illustrates the distribution of these events: Texas, Arizona, and Oklahoma exhibit the highest frequencies, with Texas leading at 1532 events. These states are marked in the darkest blue. Other states such as California, Missouri, and Arkansas also show high frequencies, marked in medium blue shades. States in the northern and northeastern regions, including Maine, Vermont, and North Dakota, have significantly lower frequencies, shown in light blue and white. This map highlights the geographic disparities in excessive heat events, emphasizing the prevalence of these events in the southern and midwestern regions while the northern states experience fewer occurrences.

Figure 79. Excessive Heat Event Frequency Analysis in the United States (NCEI)

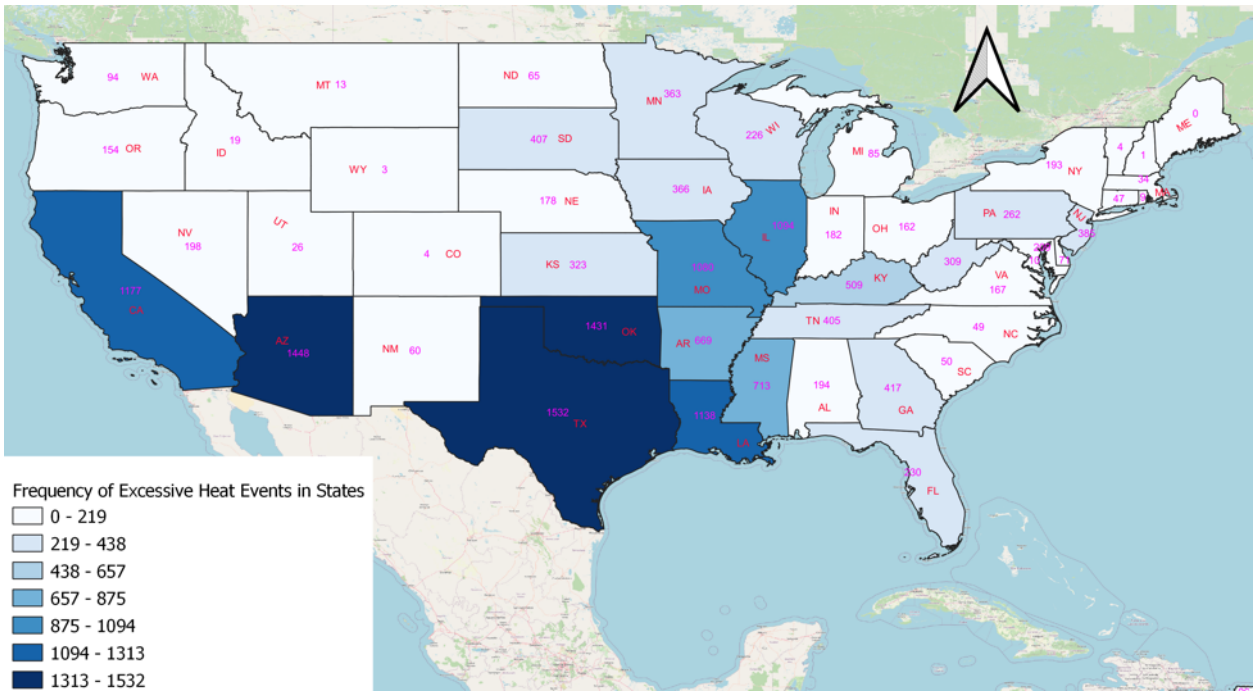

Figure 80 displays the frequency of excessive heat event reports from various sources. The highest frequencies come from official NWS observations (22.56%) and the Automated Surface Observing Systems (ASOS) (22.50%), both contributing significantly to the total reports. Mesonet (17.79%) and the Automated Weather Observing System (AWOS) (12.22%) also provide a substantial number of reports. County officials and cooperative observers account for 8.55% and 5.88%, respectively. Other notable sources include trained spotters, newspapers, and NWS employees, although their contributions are relatively smaller. The total frequency of reports across all sources is 16,794, indicating a wide range of data collection points. Referring specifically to ASOS, AWOS, and Mesonet, these are atmospheric-based agencies that would be considered additional official reports.

Figure 80. Frequency of Excessive Heat Events by Source 2000–2024 (NCEI)

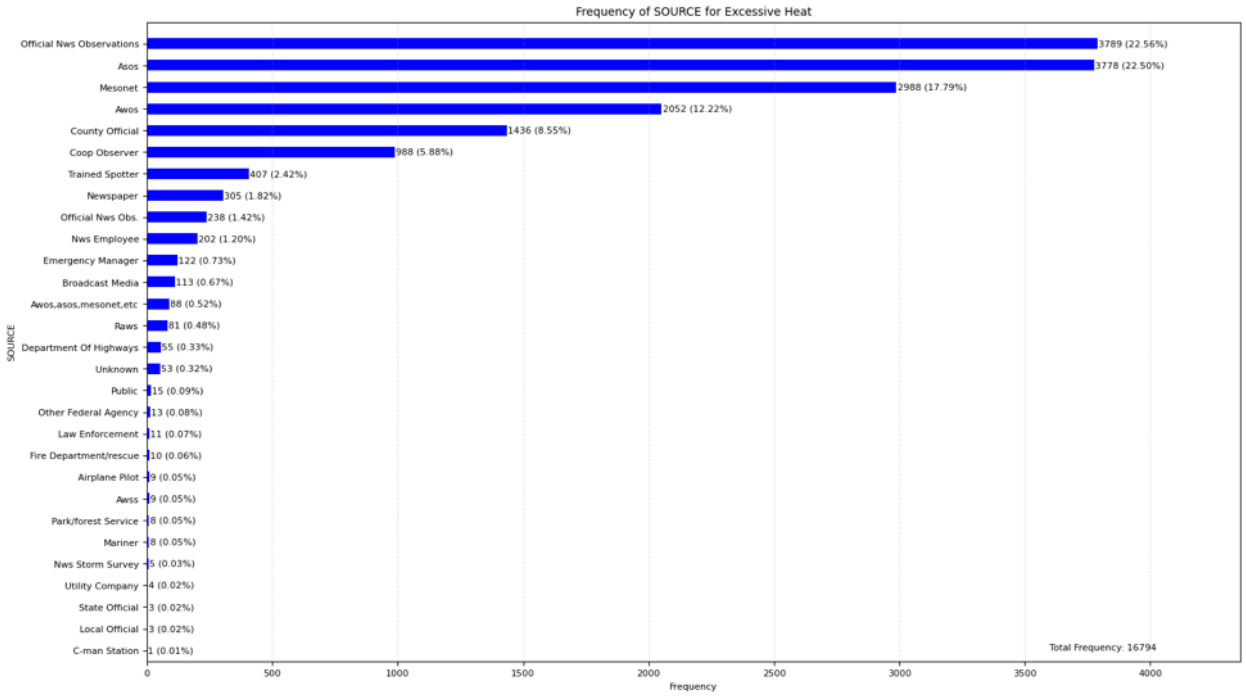

These recorded high-temperature events can be particularly useful in identifying significant locations for track buckling in rail infrastructure. By correlating the frequency and intensity of excessive heat events with occurrences of track buckling, the relationship between extreme heat and infrastructure failure can be better understood and mitigated—an analysis that will be further explored in future sections of the report.

Figure 81 presents the frequency of excessive heat events by year, spanning from 2000 to 2023. The data indicates a significant increase in the frequency of these events over time. Notably, the year 2023 shows the highest number of excessive heat events, with 4,738 occurrences, accounting for 28.21% of the total frequency. This is a substantial rise compared to previous years. Other years with high frequencies include 2011, with 1,698 events (10.11%), and 2010, with 1240 events (7.38%). This trend underscores the growing prevalence of extreme heat events, which may be attributed to increasing global temperatures, and additional agencies across the U.S. measuring such events.

Figure 81. Frequency of Excessive Heat Events by Year 2000–2024 (NCEI)

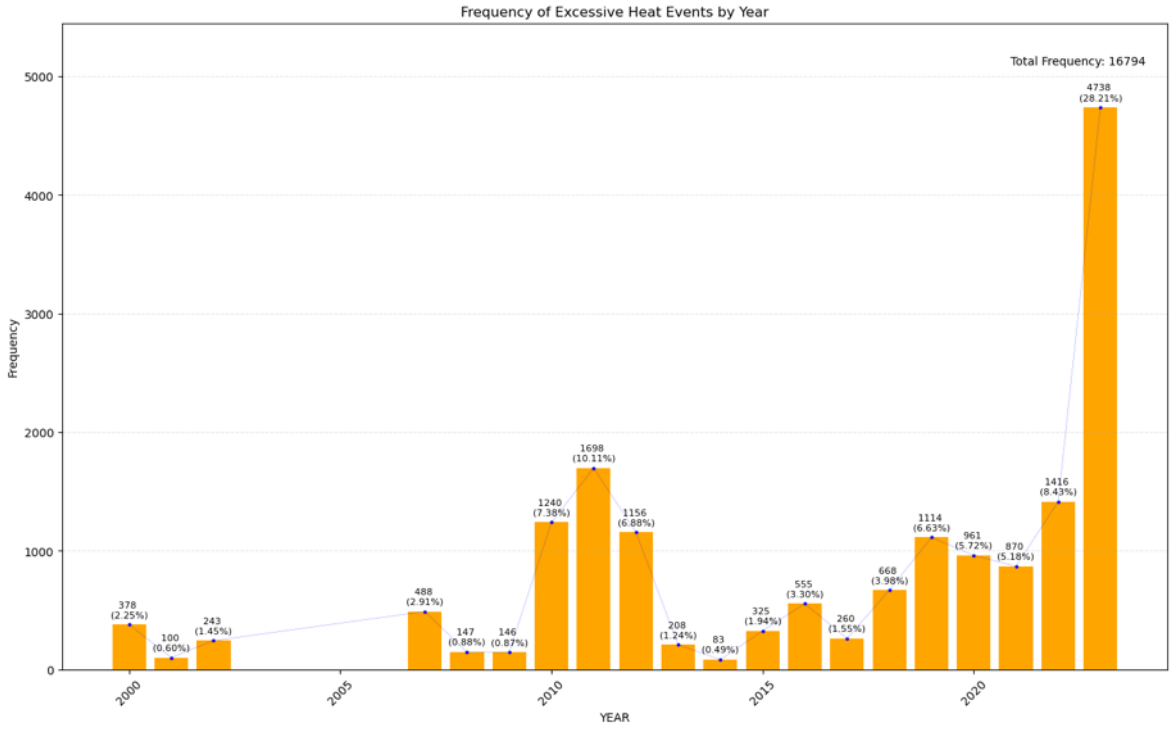

Assigning the NCEI Excessive Heat Events to the U.S. Rail Network

The goal of this section is assigning Excessive Heat events to the U.S. rail network, using the NWS forecast zone. Figure 82 represents the NWS forecast zones throughout the United States, focusing on regions impacted by excessive heat events. The figure categorizes the zones into two groups: "No Excessive Heat Events" and "At Least One Excessive Heat Event."

Figures 83 to 86 illustrate the rail network to which NCEI Excessive Heat occurrences have been assigned. As Figure 83 demonstrates, the rail network has 16,309 different recorded excessive heat events (out of 16,794 recorded excessive heat events) that have coordinates from the NCEI dataset, highlighting the specific locations affected by excessive heat. In this figure, the labels show the number of distinctive excessive heat events within the NWS Forecast Zones.

Figure 84 presents a binary categorization of the assigned excessive heat, classifying the data into two distinct groups: "No Excessive Heat Event" and "At Least One Excessive Heat Event." Figures 85 and 86 provide further clarification by separately illustrating the rail network for "At Least One Excessive Heat Event" and "No Excessive Heat Events," respectively.

Figure 82. Geographic Distribution of Excessive Heat Events (NCEI Dataset) Across NWS Forecast Zones

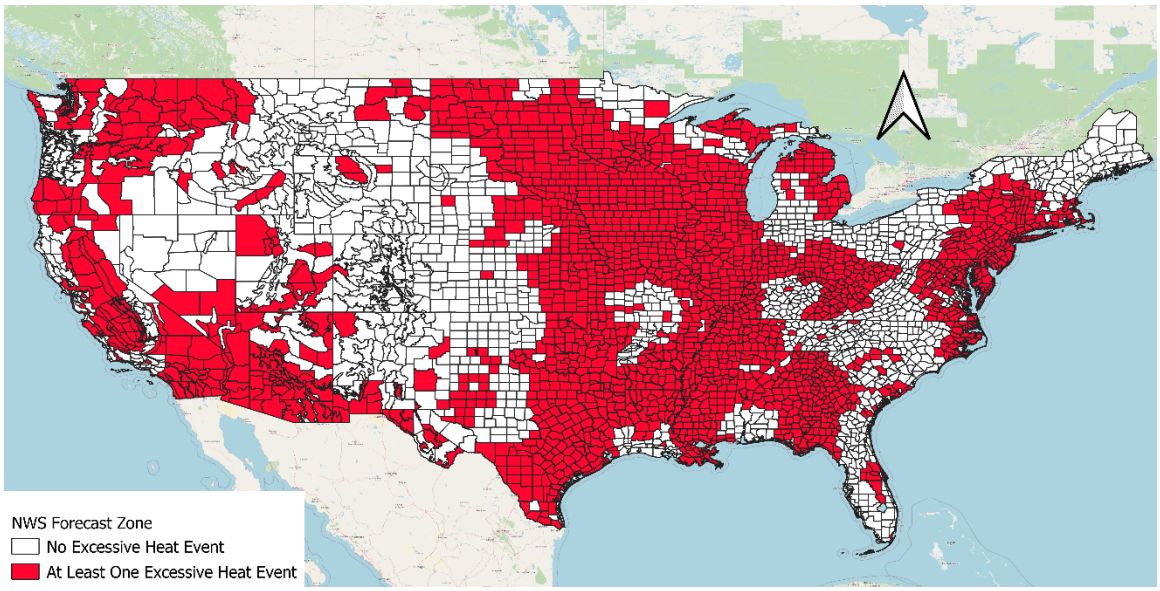

Figure 83. Distribution of Excessive Heat Events (NCEI Dataset) Across the Rail Network

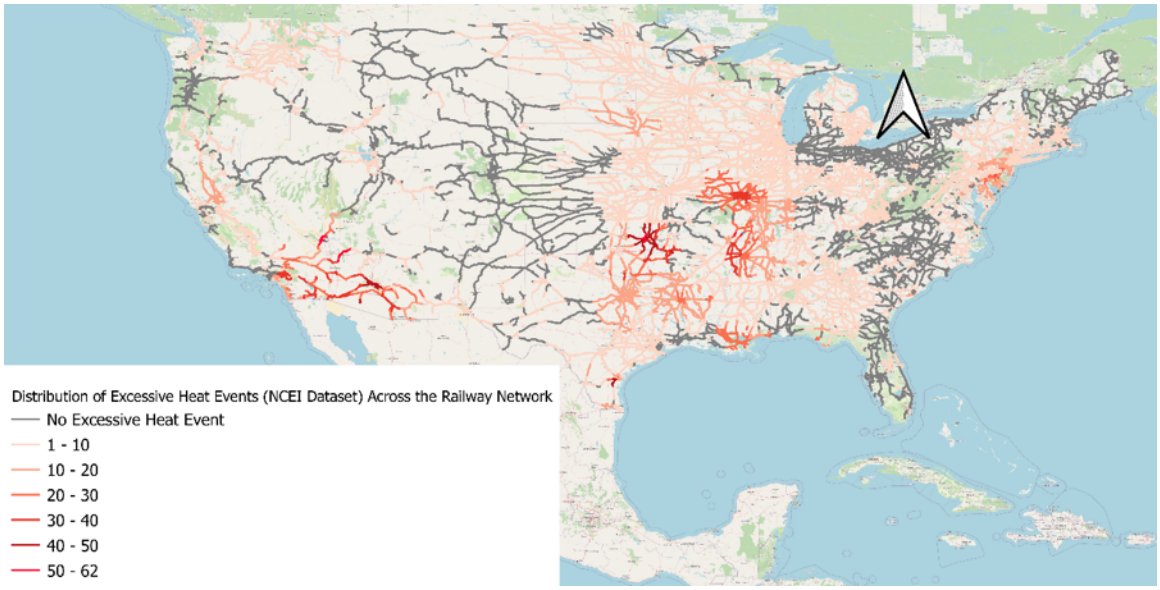

Figure 84. Rail Network Segments with No Excessive Heat and Recorded Excessive Heat Events (NCEI Dataset)

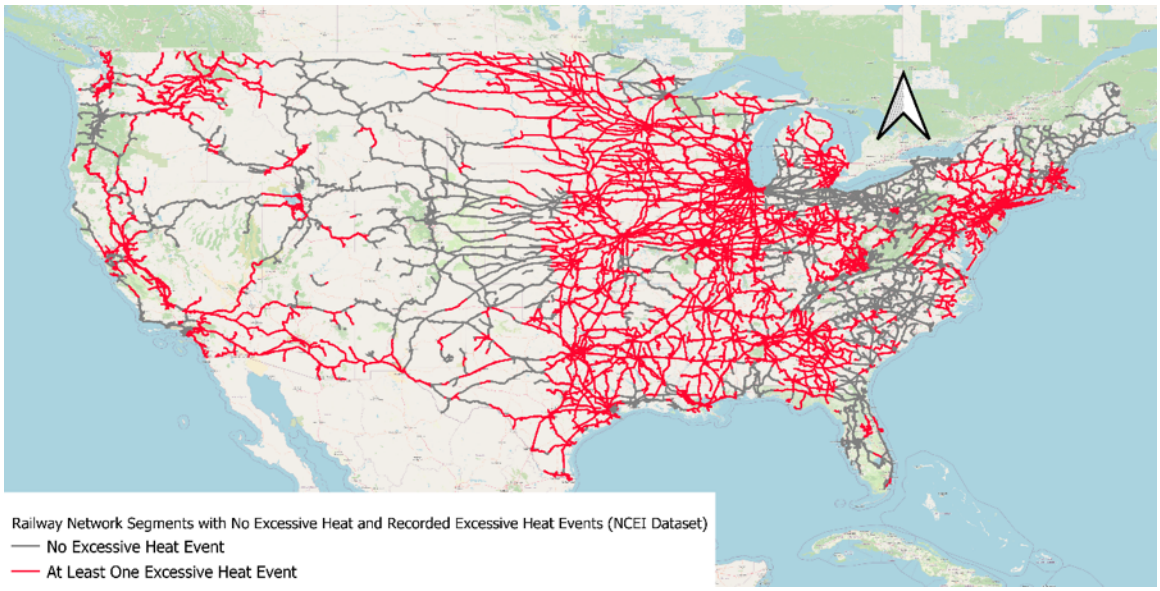

Figure 85. Rail Network Segments with Recorded at Least One Excessive Heat Event (NCEI Dataset)

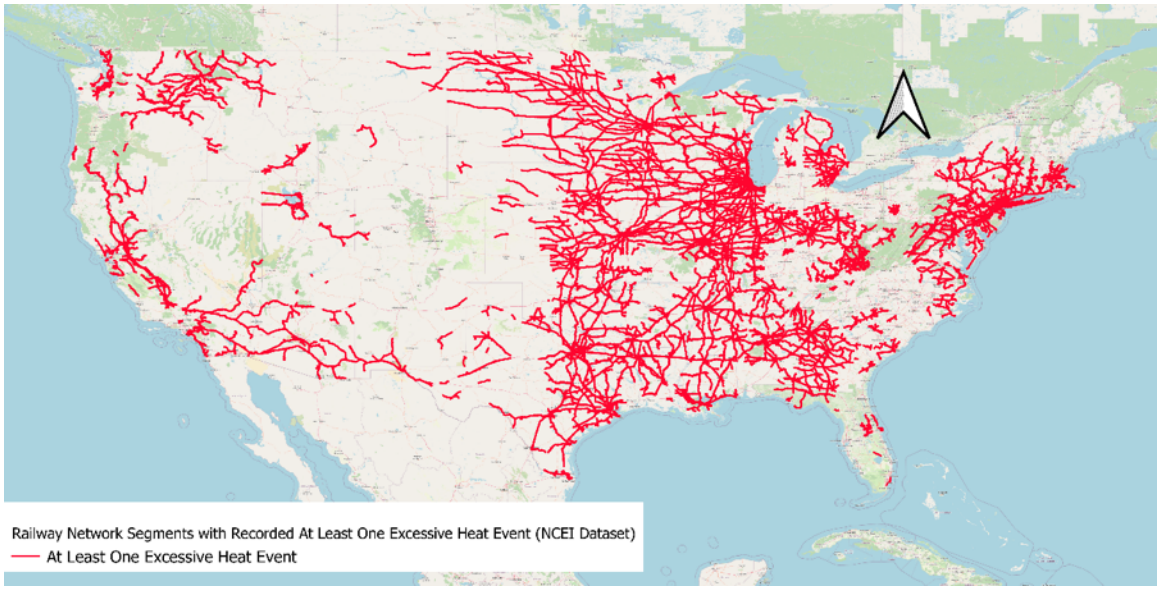

Figure 86. Rail Network Segments with No Excessive Heat Event (NCEI Dataset)

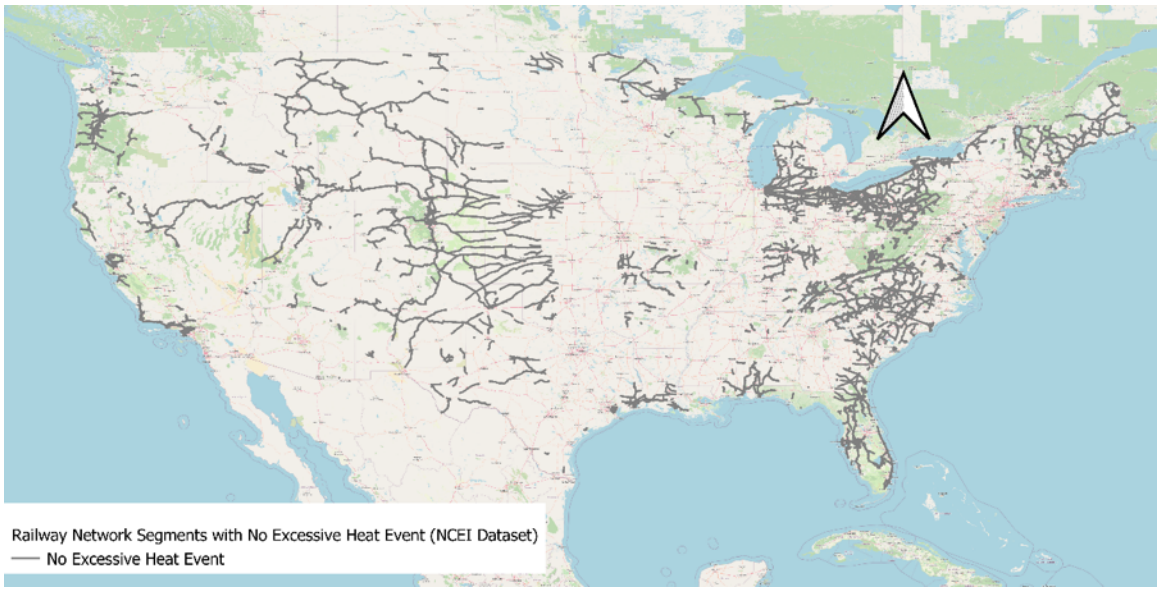

Figure 87 portrays the distribution of rail segments affected by excessive heat events based on the NCEI dataset. It categorizes the network into two groups: segments with "No Excessive Heat" events, comprising 34.6% of the total and shown in blue, and segments with "At Least One Excessive Heat event", comprising 65.4% of the total and shown in red.

Figure 87. Distribution of Rail Lines by NCEI Excessive Heat Events Frequency (2000–2024)

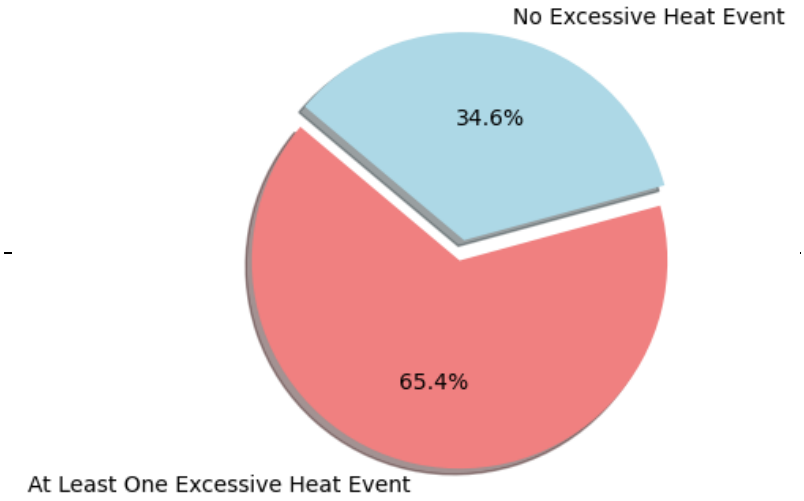

While a large section of the U.S. rail network has no excessive heat events assigned because the NWS forecast zones containing those events did not spatially overlap with any rail segments, Figures 88 and 89 show that there is still a substantial portion of the network where 1 to 10 events were recorded. This likely reflects events that are rare in occurrence, but may also indicate improved monitoring technologies and reporting practices.

Figure 88. Sum of Rail Length by Excessive Heat Frequency Events (NCEI)

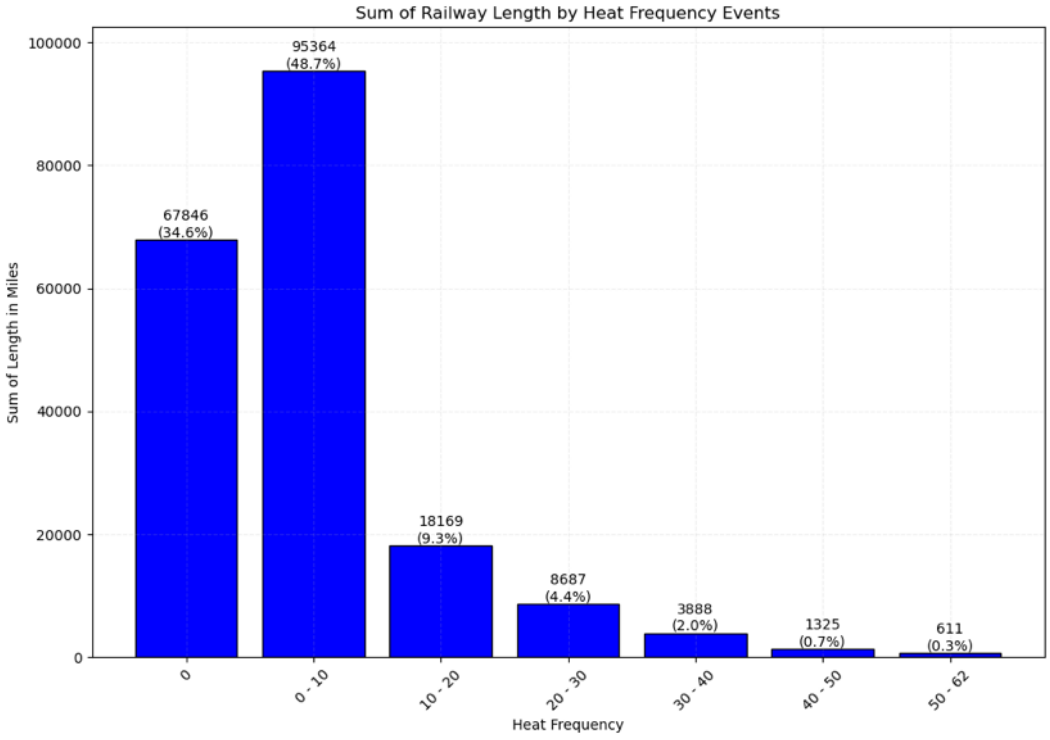

Figure 89. Sum of Rail Length by Excessive Heat Frequency Between 1-10 (NCEI)

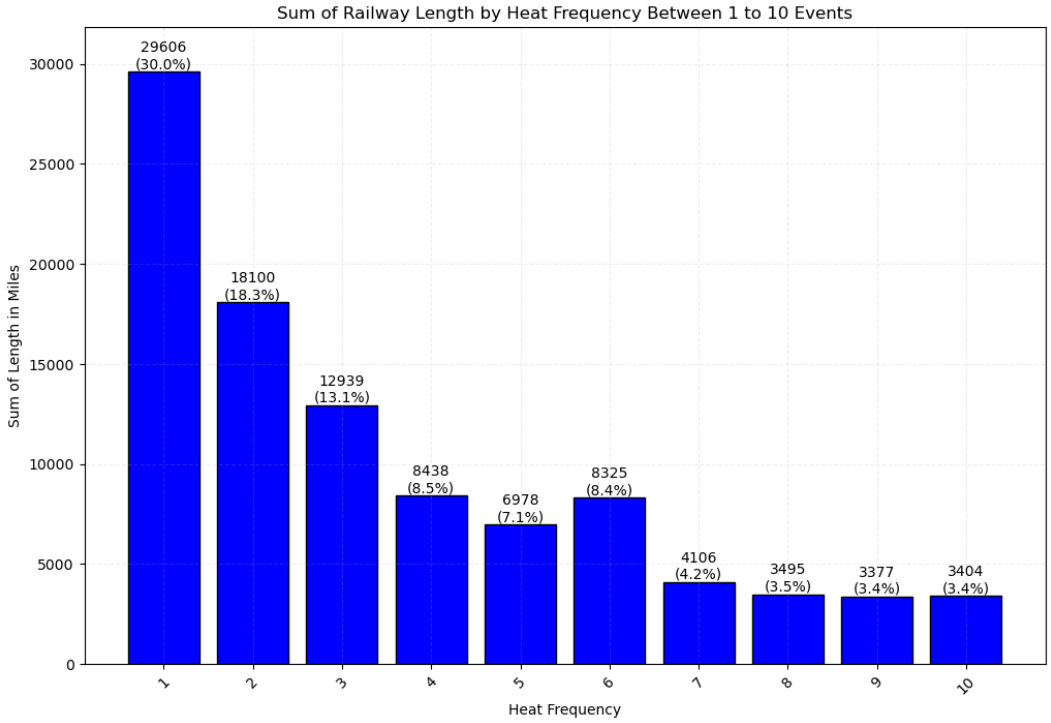

4. Landslides

Landslides frequently occur during or after severe rainfall events, causing fatalities and damage to the natural and/or manmade environment (Dai & Lee, 2002). Landslides are common geological disasters in mountainous or steep slope areas and pose unavoidable challenges leading to significant economic and human losses. Various classifications exist for landslides, but the system developed by the late D.J. Varnes has gained widespread acceptance as the most commonly used (Varnes, 1954, 1978; Cruden & Varnes, 1996). The kinematics of a landslide is a crucial criterion for identifying landslides. As shown in Figure 90, the kinematic movement of landslides can be classified into five types: fall, topple, slide, spread, and flow (Cruden & Varnes, 1996).

Figure 90. Types of Landslides: (1) A Fall; (2) A Topple; (3) A Slide; (4) A Spread; (5) A Flow. (Image Source: (Cooper, 2007))

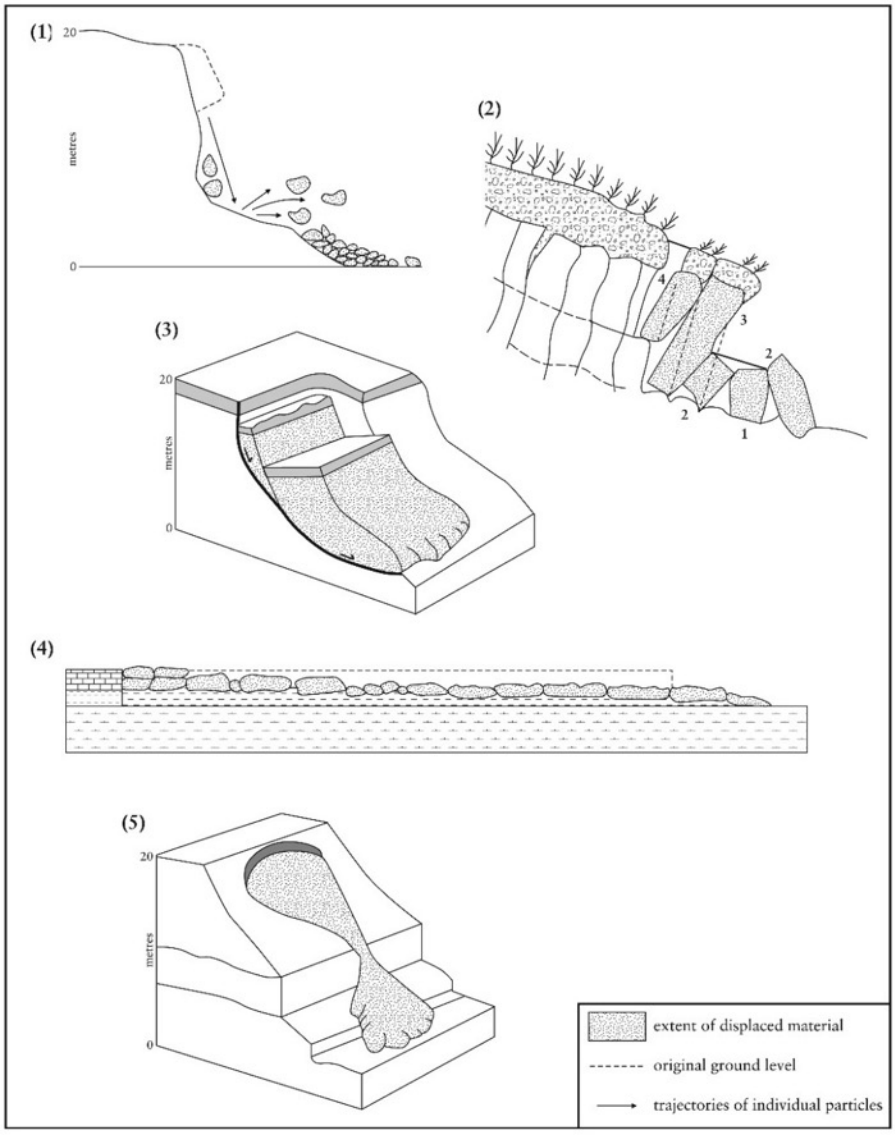

Varnes's 1978 classification categorizes slope movement primarily based on the type of movement and secondarily based on the type of material. Types of movements are classified into five primary groups. The sixth group, complicated slope movement, comprises a combination of the preceding five forms of movement. Material is classified into two basic categories: bedrock and engineering soil. Soil is further classified into debris and earth. Varnes 1978 classification for slide grouping, as given in Hungr et al., 2014, is summarized as follows (Table 14):

Table 14. An Overview of Varnes 1978 Classification Approach
(Table Source: (Hungr et al., 2014))

Type of Movement	Type of Materials		
	Bedrock	Debris	Earth
Fall	1. Rock fall	2. Debris fall	3. Earth fall
Topple	4. Rock topple	5. Debris topple	6. Earth topple
Rotational sliding (few units)	7. Rock slump	8. Debris slump	9. Earth slump
Translational sliding (many units)	10. Roc slide/Block slide	11. Debris slide	12. Earth slide
Lateral spreading	13. Rock spread	—	14. Earth spread
Flow	15. Rock creep	16. Talus flow	21. Dry sand flow
		17. Debris flow	22. Wet sand flow
		18. Debris avalanche	23. Quick clay flow
		19. Solifluction	24. Earth flow
		20. Soil creep	25. Rapid earth flow
			26. Loess flow
Complex	27. Rockslide-debris avalanche	28. Cambering, valley bulging	29. Earth slump-earth flow

Landslides have varying levels of velocity and are classified by the WP/WLI (1995) and Cruden & Varnes (1996). Table 15 depicts the landslide velocity.

Table 15. Landslide Velocity Scale (WP/WLI 1995 and Cruden and Varnes 1996)
(Table Source: (Hungr et al., 2014))

Velocity class	Description	Velocity (mm/s)	Typical velocity	Response[a]
7	Extremely rapid	5×10^3	5 m/s	No response
6	Very rapid	5×10^1	3 m/min	No response
5	Rapid	5×10^−1	1.8 m/h	Evacuation
4	Moderate	5×10^−3	13 m/month	Evacuation
3	Slow	5×10^−5	1.6 m/year	Maintenance
2	Very slow	5×10^−7	16 mm/year	Maintenance
1	Extremely Slow	—	—	No response

Table 16. An Overview of the Updated Version of the Varnes Classification System. The Words in Italics Are Placeholders (Use Only One) (Table Source: (Hungr et al., 2014))

Movement	Rock	Soil
Fall	1. *Rock/ice* fall[a]	2. Boulder/debris/silt fall[a]
Topple	3. Rock block topple[a]	5. Gravel/sand/silt topple[a]
	4. Rock flexural topple	
Slide	6. Rock rotational slide	11. *Clay/silt* rotational slide
	7. Rock planar slide[a]	12. *Clay/silt* planar slide
	8. Rock wedge slide[a]	13. Gravel/sand/debris slide[a]
	9. Rock compound slide	14. *Clay/silt* compound slide
	10. Rock irregular slide[a]	
Spread	15. Rock slope spread	16. *Sand/silt* liquefaction spread[a]
		17. Sensitive clay spread[a]
Flow	18. *Rock/ice* avalanche[a]	19. Sand/silt/debris dry flow
		20. Sand/silt/debris flowsilde[a]
		21. Sensitive clay flowsilde[a]
		22. Debris flow[a]
		23. Mud flow[a]
		24. Debris flood
		25. Debris avalanche[a]
		26. Earthflow
		27. Peat flow
Slope deformation	28. Mountain slope deformation	30. Soil slope deformation
	29. Rock slope deformation	31. Soil creep
		32. Solifluction

[a] Movement types that usually reach extremely rapid velocities as defined by Cruden & Varnes (1996). The other landslide types are most often (but not always) extremely slow to very rapid.

Each category of landslide can be associated with different impacts on rail infrastructure and operations, ranging from minor track disruptions to extensive service interruptions. An in-depth understanding of these effects is deemed crucial for the establishment of effective approaches to mitigate the negative consequences and ensure the long-term resilience of rail networks in locations prone to landslides. In this report, the primary focus is on the impact of landslides on rail infrastructure. As mentioned previously, due to the increase in the frequency of landslide occurrences, operational impacts (such as service disruption, safety risks, etc.) and infrastructure impacts (such as washouts, settlements, etc.) can be observed.

Figure 91 has been developed for the landslide events dataset. The process begins with some sources, including the Rail Equipment Accident/Incident Data (READ), the USGS dataset, and the U.S. Rail Network Shapefile (USRN). First, the financial impact and frequency of rail

accidents caused by landslides were investigated. Then, landslide events (USGS) were filtered and detected in proximity to rail tracks (within a specific distance). The following sections will elaborate on each of these steps in detail.

Figure 91. Process Flowchart for Assigning Landslide Events to Rail Infrastructure

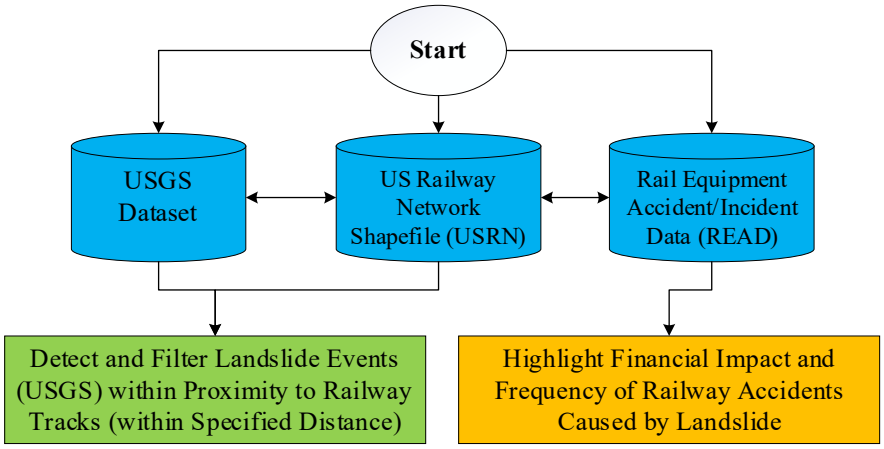

This process flowchart will be updated in upcoming reports or tasks to reflect any new methodologies, data sources, or analysis techniques as they are developed.

4.1 Train Accident Cause Codes

The train accident cause codes contain data on accident causes from 1975 until the present. To focus on recent data that assists in analyzing current trends and patterns, data from 2000 to 2023 has been assessed. To identify all accidents related to landslides, the “Narrative” column of the train accident dataset was filtered using the keyword "slide." Out of 181 entries filtered with the "slide" keyword, a careful investigation further filtered the data for the codes M101, M103, M199, M402, M404, T001, T002, and T002, reducing the data frequency to 114.

Figure 92 illustrates the frequency of landslides in the train accident data codes in different states from 2000 to 2023.

Figure 92. Frequency of Landslides Accidents from 2000 to 2023

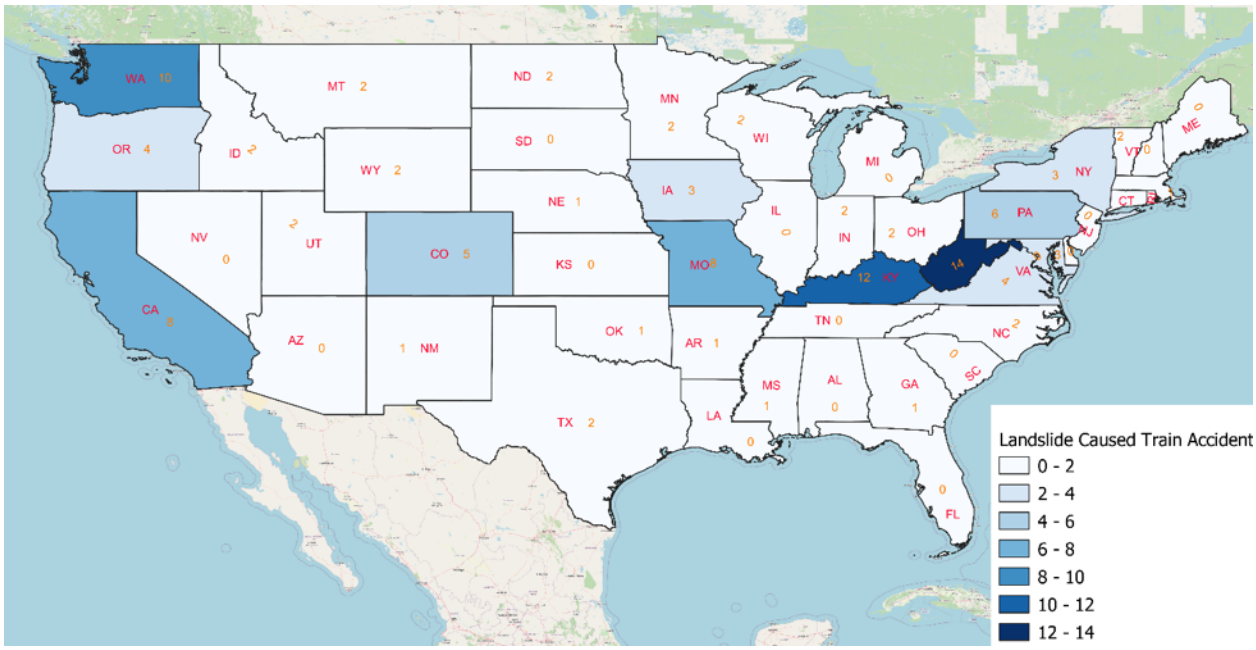

There are 114 different accidents related to landslides (with the keyword "slide") in the whole dataset. West Virginia (WV), Kentucky (KY), Washington (WA), California (CA), Missouri (MO), and Pennsylvania (PA) have the highest frequency among states, while some of the states do not have any recorded data for landslides. This suggests that various factors such as geographical, environmental, or infrastructure differences among the states play roles in landslide occurrences. From 114 landslide incidents, there are coordinates for 62 of them. The remaining data do not have any coordinates. The causes of the landslides have been displayed on the following map (Figure 93), with the six states with the highest frequency of accidents highlighted.

Figure 93. Landslide Train Accident Points Across the U.S. from 2000 to 2023

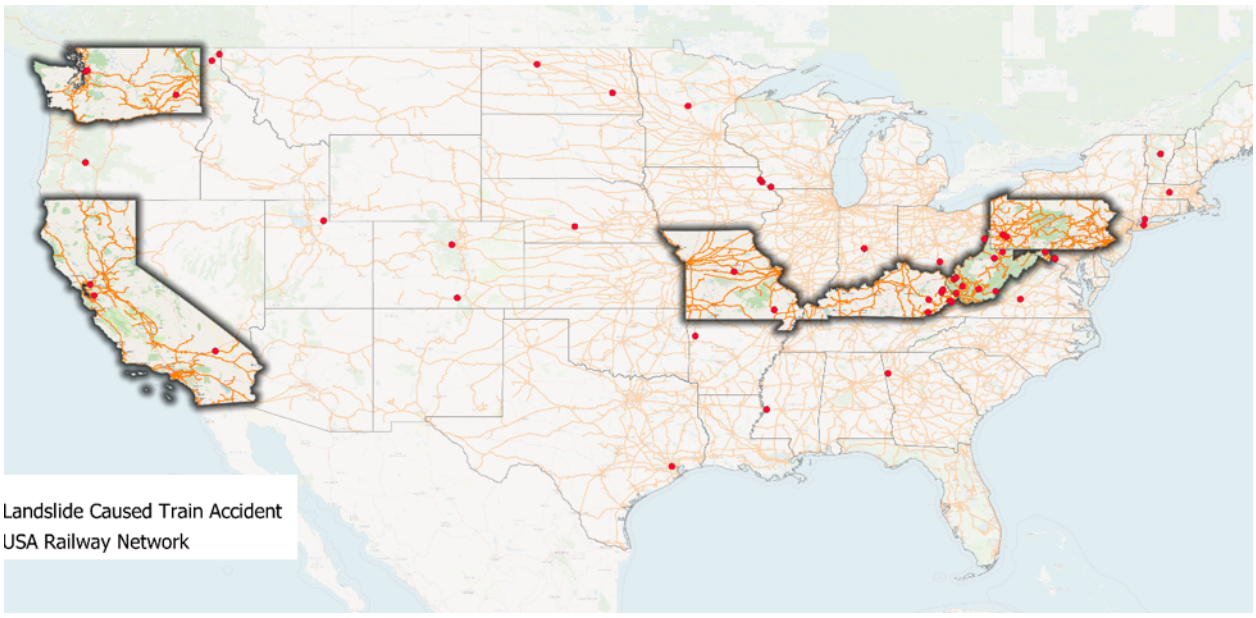

Data representation suggests that landslide occurrences are not evenly distributed across the states, and certain states may require more attention and mitigation efforts to reduce the frequency of such events. Figure 94 illustrates the frequency of landslides over the period spanning from 2000 to 2023.

Figure 94. Distribution of Landslide Train Accident in the U.S. from 2000 to 2023

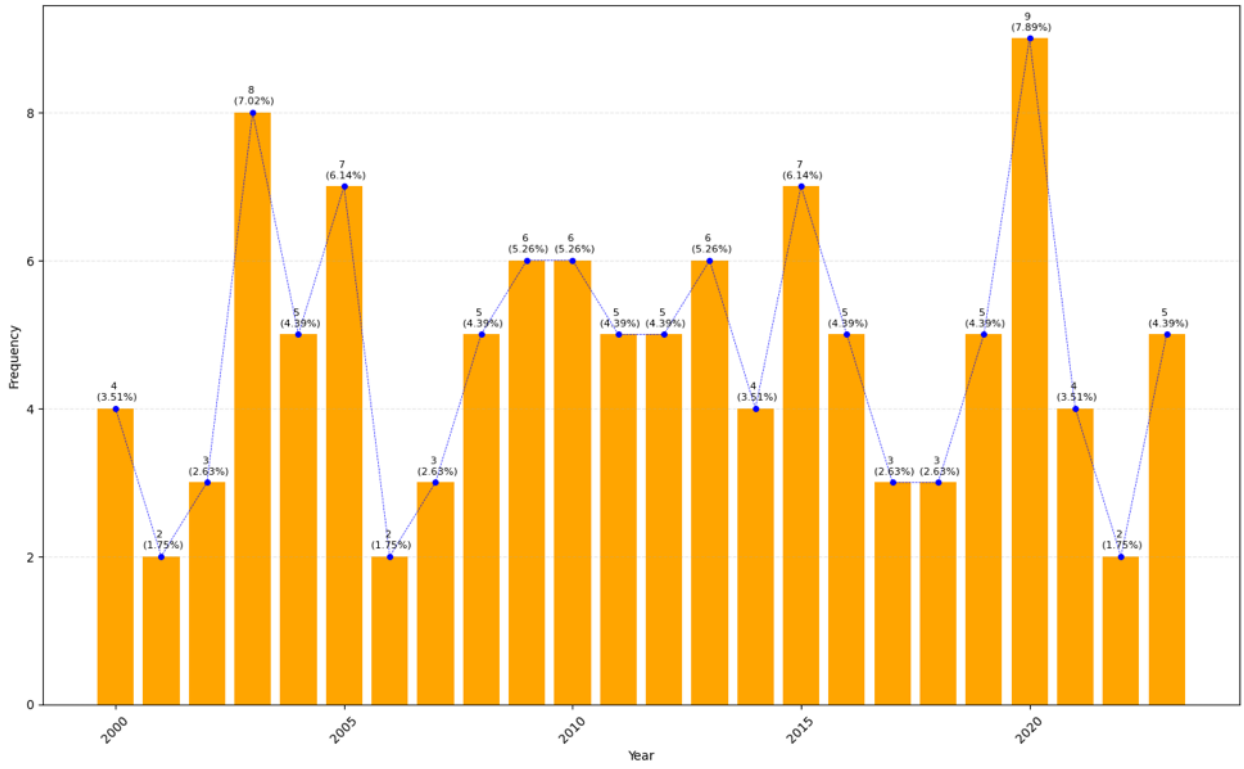

In the accident dataset, there are two types of damage costs for each accident: equipment damage and track damage. There are some accident rows in the dataset where the Total Damage Cost (based on the dataset) exceeds the sum of the two types of accidents (sum of equipment and track). It is not explained in the dataset what the source of this difference is, and here it has been considered as other costs. The following is a summary of the 114 damage costs (Table 17 and Figure 95):

Table 17. Damage Costs of Train Accidents Caused by the Different Types of Landslides

Accident Type	Equipment Damage Cost	Track Damage Cost	Other Costs	Total Damage Cost
Derailment	$24,708,355	$5,631,037	$4,963,857	$35,303,249
Non-Derailment (Other Accidents)	$3,082,520	$779,128	$123,741	$3,985,389
Total	$27,790,875	$6,410,165	$5,087,598	$39,288,638

The breakdown of train accident damage costs reveals significant disparities between derailments and non-derailments. Derailments account for a notably higher proportion of equipment damage costs ($24,708,355) compared to non-derailments ($3,082,520). Similarly, track damage costs are higher for derailments ($5,631,037) than for non-derailments ($779,128). The total damage costs for derailments are nearly nine times that of non-derailments ($35,303,249 vs. $3,985,389).

Figure 95. (a) Proportion of Damage Costs Due to Landslides That Caused Derailments, (b) Proportion of Damage Costs Due to Landslides That Caused Accidents Other Than Derailments, (c) Proportion of Damage Costs Due to Landslides for All Accidents

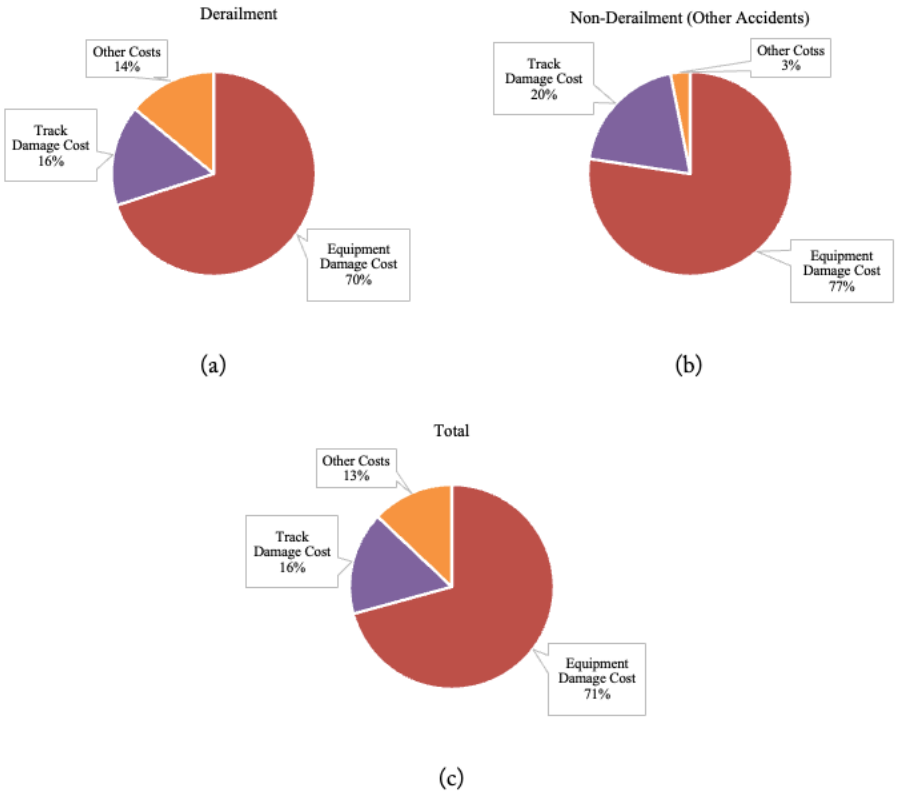

Figure 95 provides further insights into the distribution of damage costs. Chart (a) depicts the proportion of damage costs due to landslides that caused derailments, with equipment damage costs as the largest portion at 70%, followed by track damage costs at 16% and other costs at 14%. Similarly, for non-derailment, equipment damage costs were the largest portion at 77%, followed by track damage costs at 20% and other costs at 3%. Chart (c) offers a comprehensive view by illustrating the proportion of damage costs due to landslides for all accidents combined. Equipment damage costs continue to dominate at 71%, followed by track damage costs at 16% and other costs at 13%. The aggregate damage cost for 114 accidents is around $40 million, with an average of $344 thousand per accident. This observation emphasizes the importance of implementing preventive and mitigation strategies to address the heavy financial burden associated with equipment damage in landslide-related train accidents.

4.2 U.S. Landslide Inventory - USGS Data Set

The interactive map from the United States Geological Survey (USGS) demonstrates a uniform dataset of landslide occurrences in the United States spanning approximately from 1925 to 2019. The map allows users to access the original digital inventory files for detailed information. The U.S. Landslide Inventory, now in its second iteration, is a critical database for understanding landslide occurrences across the United States. The inventory consolidates digital data from various agencies and institutions. The initial release of the inventory was in March 2019. The latest version, which is the second update, was released in March 2022, indicating ongoing efforts to refine and enhance the data.

Data points in the map are classified based on confidence levels, ranging from high confidence in the occurrence and nature of landslides to lower confidence levels indicating probable or possible landslides. The confidence level has been categorized as follows:

- Level 8 (High confidence in the extent or nature of the landslide): This represents the highest degree of certainty about the landslide event's occurrence and its characteristics. Data points with this level are considered highly reliable.

- Level 5 (Confident consequential landslide at this location): This level suggests that there is good confidence that a consequential landslide, one that has a significant impact or size, has occurred at this specific location.

- Level 3 (Likely landslide at or near this location): Here, the data suggests that a landslide event is likely to have happened in or near the reported location, but there might be less certainty about its precise boundary or nature.

- Level 2 (Probable landslide in the area): At this level, there is some indication of a landslide, but the evidence may not be as strong or definitive. The event is probable, but not confirmed with high certainty.

- Level 1 (Possible landslide in the area): This is the lowest confidence level, indicating that a landslide is possible in the area, but there is little concrete evidence to confirm its occurrence or characteristics.

This classification is available for individual points (US_Landslide_point_v2) and polygonal areas (US_Landslide_poly_v2). The map displayed on the slide shows the distribution of landslides across the U.S., with a concentration of high-confidence landslides on the West Coast. The Inventory is accessible via an interactive map, allowing users to explore landslide data in detail. This map represents the Inventory's role in providing geospatial data critical for risk assessment, research, and mitigation planning related to landslides. In this report, an attempt has been made

to leverage these datasets to assess the impact of landslides on rail infrastructure. Figure 96 visually represents the dataset.

Figure 96. Geographical Distribution and Confidence Assessment of Landslide Occurrences Across the United States, Highlighted in the U.S. Landslide Inventory Interactive Map (Version 2, March 2022)

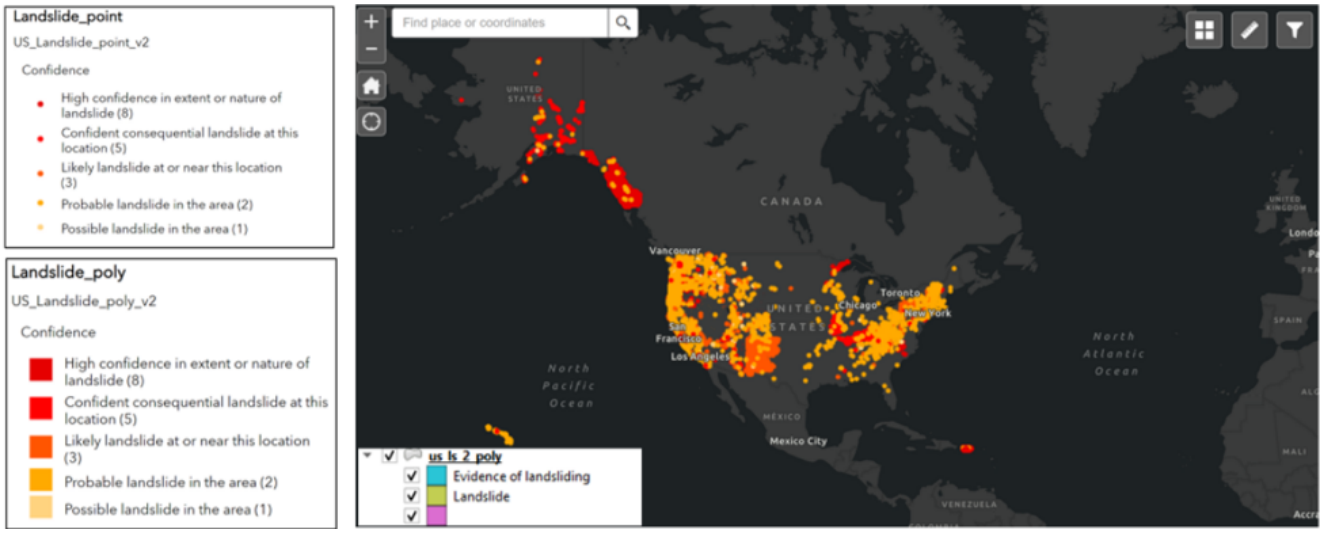

The inventory encompasses a staggering number of data points and polygons, indicating a vast collection of geospatial information on landslide occurrences. Specifically, the data comprises:

- 64,443 points detailing individual landslide events.
- 245,909 polygons that demarcate the affected areas.

The attribute table of the U.S. Landslide Inventory has key attributes including:

- Date: Recording the occurrence of landslide events, with the provided example spanning from September 1 to 9, 2013.
- Fatalities: Enumerating the human cost, which stands at zero for the events shown.
- Confidence: A coded measure of the data's reliability, with “5” signifying a specific level of confidence.
- Inventory: Citing USGS as the source for the data in the examples provided, ensuring traceability.
- Notes: Offering essential descriptors for the type of landslide, enhancing the utility of the data for targeted research and intervention measures.

Figures 97 and 98 present two bar graphs depicting the frequency of inventory data for landslides in the U.S., categorized by points and polygons. Figure 97 illustrates the frequency of data points across different inventories as follows:

- California GS shows the highest frequency with 29,611 points (46.0%).
- OR Slido follows with 13,048 points (20.3%).
- USGS Conterminous and other inventories contribute to the remainder, with notably fewer points.

Figure 98 details the frequency of polygons.

- California GS leads with 68,872 polygons (28.0%).
- OR Slido is next with 51,153 (20.8%).
- USGS Conterminous and other sources provide the rest, with varying numbers.

Figure 97. Frequency of Inventory Data for Landslides in the U.S., Categorized by Points

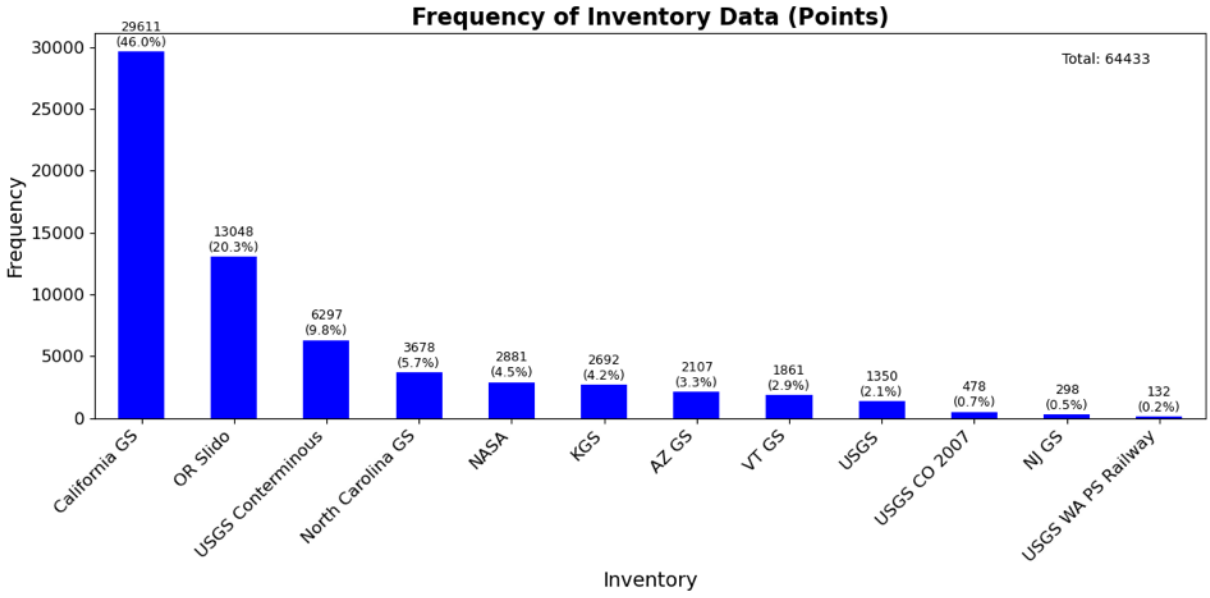

Figure 98. Frequency of Inventory Data for Landslides in the U.S., Categorized by Polygons

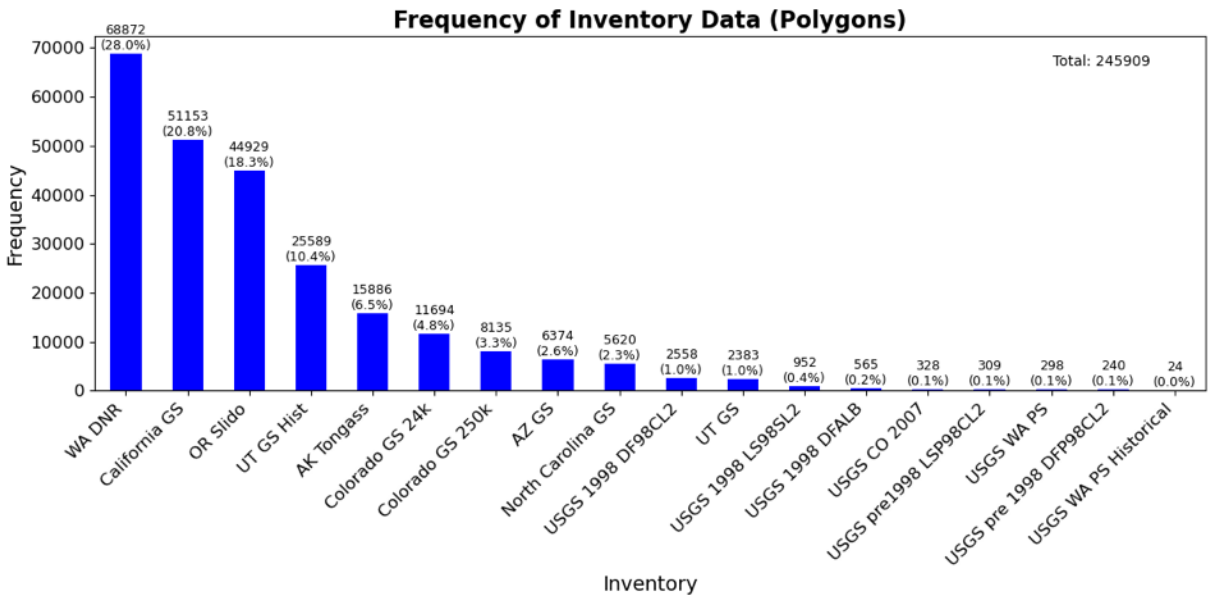

From the point inventories, it can be observed that there are approximately 132 points specifically focusing on landslides along the rail lines in Washington State. This data is related to USGS WA PS Rail and is characterized by the same attribute table as the rest of the inventories. It is associated with the data along the Burlington Northern Santa Fe Rail in Washington State. The inventory includes landslide records represented as both points and polygons, categorized in Tables 18 and 19.

Table 18. Geological Survey Inventory List in the Points Dataset

Inventory Abbreviation	Inventory Full Name
AZ GS	Arizona Geological Survey
California GS	California Geological Survey
KGS	Kentucky Geological Survey
NASA	National Aeronautics and Space Administration
NJ GS	New Jersey Geological Survey
North Carolina GS	North Carolina Geological Survey
OR Slido	Oregon State Inventory Dataset for Landslide
USGS	United States Geological Survey
USGS CO 2007	USGS data related to Colorado in 2007
USGS Conterminous	Dataset covering the contiguous United States (excluding Alaska and Hawaii) from USGS
USGS WA PS Railway	USGS data related to rail in Washington state and the Pacific Northwest region
VT GS	Vermont Geological Survey

Table 19. Geological Survey Inventory List in the Polygons Dataset

Inventory Abbreviation	Inventory Full Name
AK Tongass	Tongass National Forest in Alaska
AZ GS	Arizona Geological Survey
California GS	California Geological Survey
Colorado GS 24k	Colorado Geological Survey 24k
Colorado GS 250k	Colorado Geological Survey 250k
North Carolina GS	North Carolina Geological Survey
OR Slido	Oregon State Landslide Inventory Dataset
USGS 1998 DF98CL2	United States Geological Survey 1998 DF98CL2
USGS 1998 DFALB	United States Geological Survey 1998 DFALB
USGS 1998 LS98SL2	United States Geological Survey 1998 LS98SL2
USGS CO 2007	United States Geological Survey Colorado 2007
USGS WA PS	United States Geological Survey Washington Puget Sound
USGS WA PS Historical	United States Geological Survey Washington Puget Sound Historical
USGS pre 1998 DFP98CL2	United States Geological Survey pre 1998 DFP98CL2
USGS pre1998 LSP98CL2	United States Geological Survey pre1998 LSP98CL2
UT GS	Utah Geological Survey
UT GS Hist	Utah Geological Survey Historical
WA DNR	Washington Department of Natural Resources

Figures 99 and 100 provide a visual representation of the confidence levels count for data points and polygons within the U.S. Landslide Inventory.

Figure 99. Frequency Distribution of Confidence Levels for Point Data in the U.S. Landslide Inventory

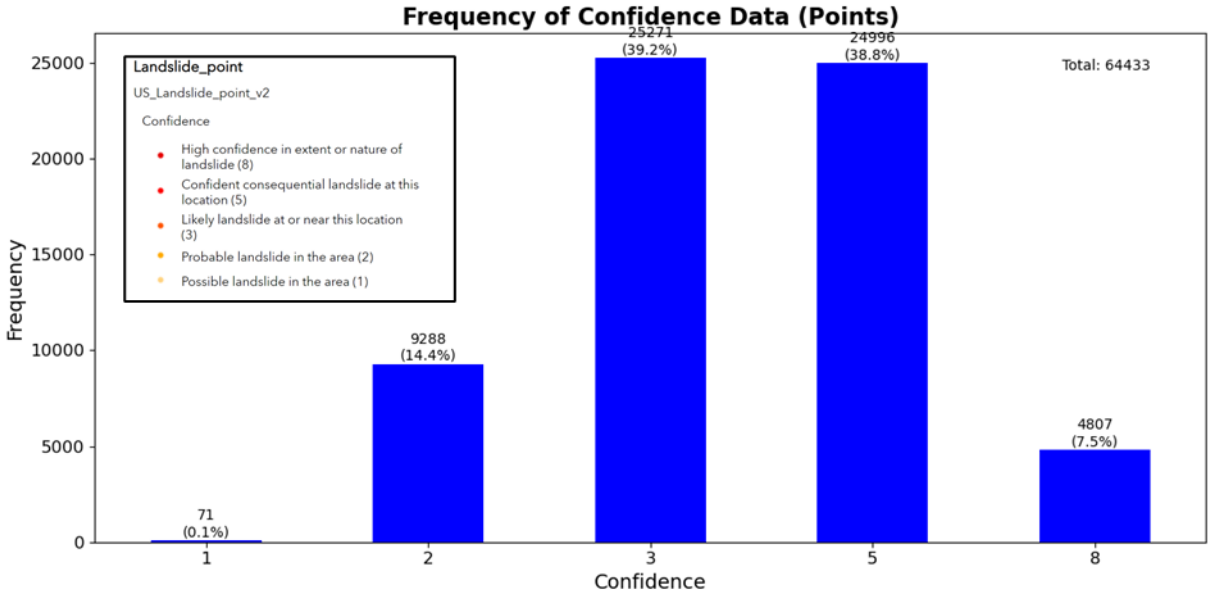

Figure 100. Frequency Distribution of Confidence Levels for Polygons Data in the U.S. Landslide Inventory

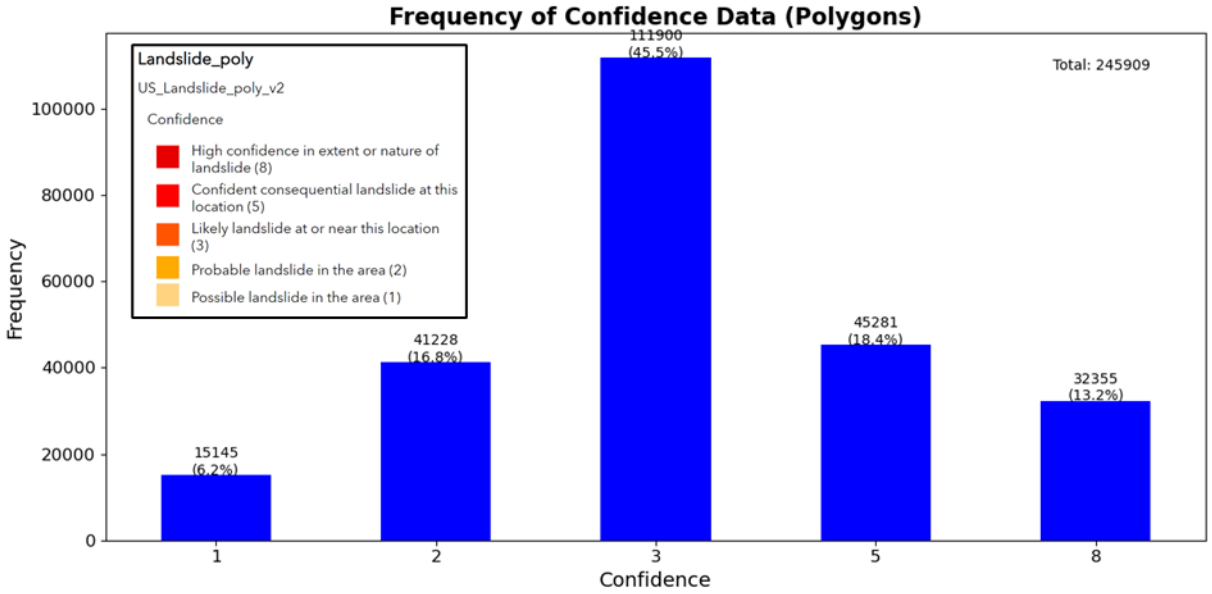

The two bar graphs illustrate the frequency of confidence ratings assigned to individual data points and polygons within the inventory, where the specific methodologies from the USGS dictate high probability that landslides occurred at the point location or within the polygons.

A visual analysis of the confidence levels attached to data within the U.S. Landslide Inventory shows that its dataset is substantial and varied. It's easy to understand why 3 and 5 (used for moderate and very moderate certainty, respectively) are the most common confidence levels assigned: when added up, the majority of the dataset falls into one of these two categories, implying that corresponding proportions of the data are correct and represent actual landslides and that there is indeed enough "firm evidence" to support such claims. Confidence level 8, on the other hand (indicating firm evidence with a high degree of certainty), is much less frequently assigned, indicating that data falling into this category must fulfill an even more extensive set of criteria. The same trend is observed for the polygons, which correspond to much larger areas.

Analyzing the Point Data in the Vicinity of the Rail Tracks

Figures 101 to 103 show the maps from the U.S. Landslide Inventory, delineating landslide events around rail systems with incrementally increasing buffer zones. This approach provides a strategic method for understanding the extent of landslide impacts on rail safety by progressively capturing events that fall within varying distances from the rail network.

15-Meter Buffer Zone (132 Data Points):

- The initial map with a 15-meter buffer zone identifies 132 data points, offering a conservative estimate of landslide occurrences that could directly affect rail operations.

50-Meter Buffer Zone (564 Data Points):

- By expanding the analysis to a 50-meter buffer, the map reveals a broader range of potential landslide impacts with 564 data points, suggesting that the risk area extends beyond the immediate proximity of the rail.

100-Meter Buffer Zone (1,018 Data Points):

- The largest buffer of 100 meters encompasses 1,018 data points, indicating an even more extensive area of potential landslide activity. This expanded analysis considers the indeterminate lengths and widths of landslides, ensuring a comprehensive capture of data to inform rail risk assessments and mitigation strategies.

Incrementally increasing the buffer zones serves a dual purpose: it compensates for the unknown dimensions of landslide events, and it methodically widens the safety margin within which rail systems might be affected. While more refined processes may exist on a per-event basis, the general

approach to assign these past events towards proximity to the rail track provide a basis for future work to be conducted.

Figure 101. Map Showcasing Landslide Events within a 15-Meter Buffer Zone of Rails, Capturing 132 Data Points

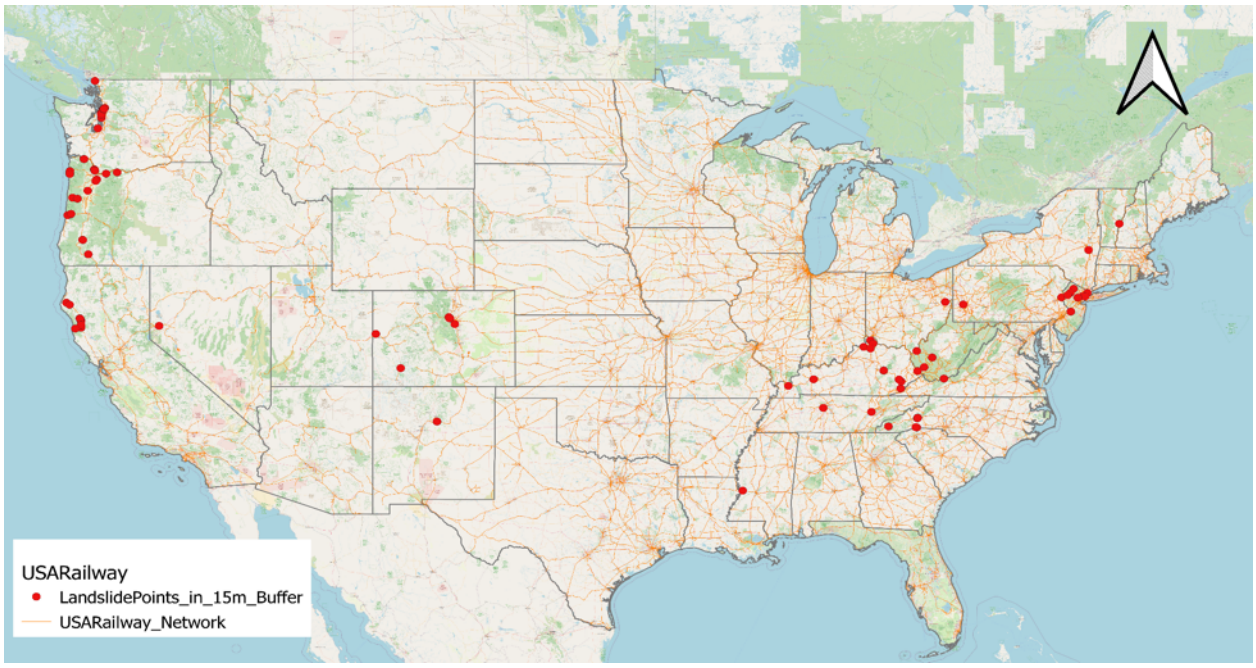

Figure 102. Map Showcasing Landslide Events within a 50-Meter Buffer Zone of Rails, Capturing 564 Data Points

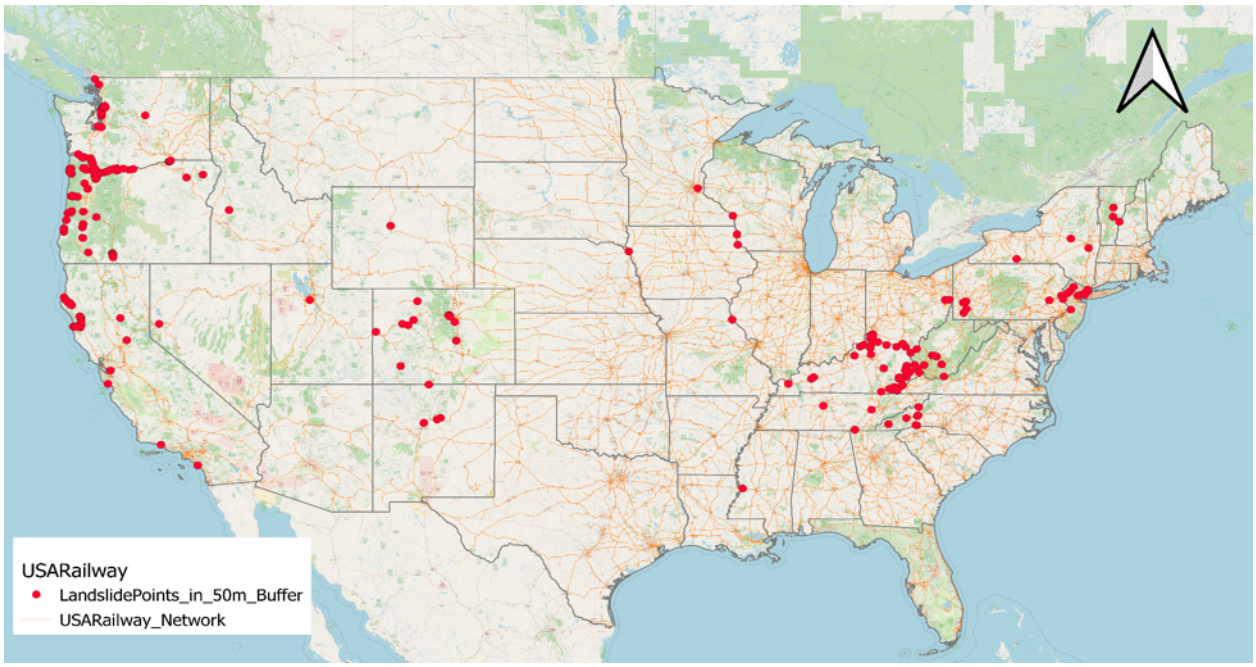

Figure 103. Map Showcasing Landslide Events within a 100-Meter Buffer Zone of Rails, Capturing 1018 Data Points

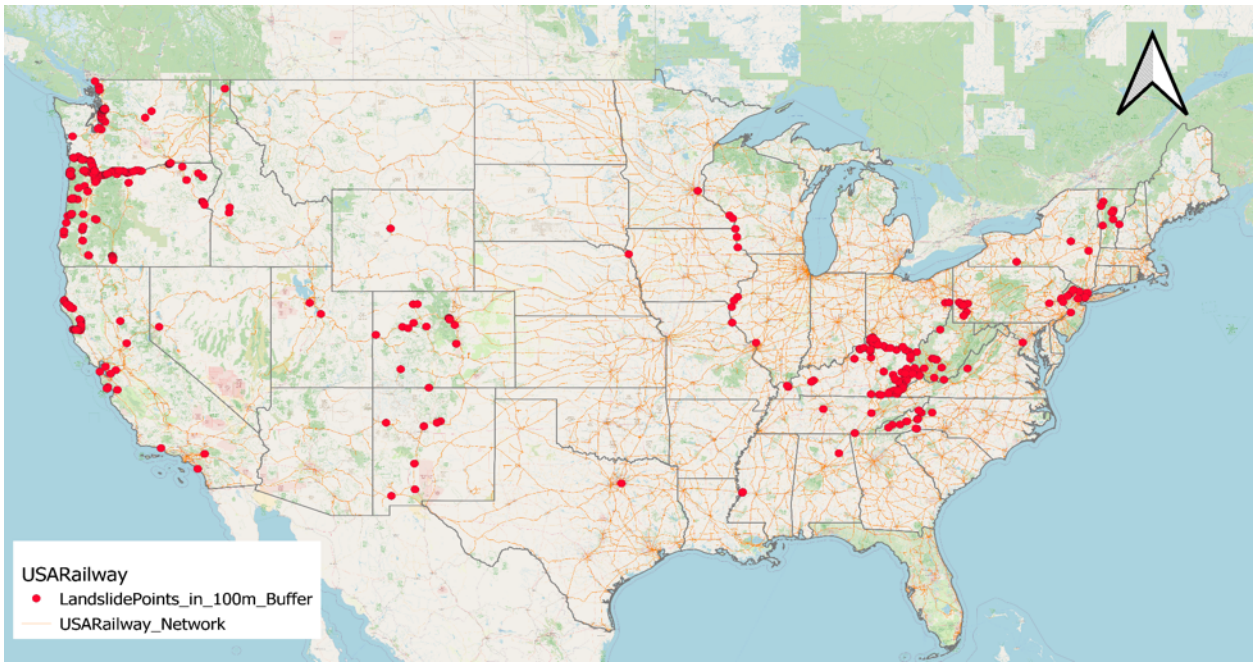

Future Research Directions

As this study lays the foundation for a comprehensive geospatial database of natural hazard impacts on U.S. railroad infrastructure, several avenues for further research have emerged. These opportunities can enhance the accuracy, applicability, and predictive power of the database while addressing key gaps identified throughout the analysis:

- Investigate links between flood activity and climate oscillations such as El Niño and La Niña, to better understand interannual variability in extreme weather events.
- Incorporate river and coastal monitoring systems (e.g., stream gauges, C-MAN stations) to improve the assignment of annual exceedance probabilities and hazard severity metrics.
- Expand the database to include additional natural hazards, such as wildfires, snowstorms, or severe wind events, which also pose risks to rail infrastructure.
- Assess infrastructure vulnerability and exposure, by integrating rail asset condition, age, and criticality into the hazard impact model.
- Analyze regional differences in hazard impact, considering variations in topography, drainage infrastructure, and climate conditions.

- Leverage machine learning or predictive modeling to forecast hazard-triggered rail disruptions using historical patterns and environmental data.
- Explore the use of high-resolution spatial and temporal datasets to refine event-to-infrastructure matching techniques.

Bibliography

Bednarik, M., Magulová, B., Matys, M., & Marschalko, M. (2010). Landslide susceptibility assessment of the Kraľovany–Liptovský Mikuláš railway case study. *Physics and Chemistry of the Earth, Parts A/B/C*, *35*(3–5), 162–171. https://doi.org/10.1016/j.pce.2009.12.002

Cooper, R. G. (2007). Mass Movements in Great Britain, Geological Conservation Review. 348.

Cruden, D., M., & Varnes, D. J. (1996). *Landslide Types and Process*.

Dai, F. C., & Lee, C. F. (2002). 2-Landslide characteristics and slope instability modeling using GIS, Lantau Island, Hong Kong. *Geomorphology*, *42*(3–4), 213–228. https://doi.org/10.1016/S0169-555X(01)00087-3

Eyring, V., Bony, S., Meehl, G. A., Senior, C. A., Stevens, B., Stouffer, R. J., and Taylor, K. E.: Overview of the Coupled Model Intercomparison Project Phase 6 (CMIP6) experimental design and organization, Geosci. Model Dev., 9, 1937–1958, https://doi.org/10.5194/gmd-9-1937-2016, 2016.

Federal Railroad Administration. Office of Safety Analysis: On the fly download. Rail Equipment Accident/Incident Data (Form 54). U.S. Department of Transportation. https://safetydata.fra.dot.gov/OfficeofSafety/publicsite/on_the_fly_download.aspx.

Hungr, O., Leroueil, S., & Picarelli, L. (2014). 1-The Varnes classification of landslide types, an update. *Landslides*, *11*(2), 167–194. https://doi.org/10.1007/s10346-013-0436-y

Hydrologic Unit Maps—USGS. (2024, January 9). *Water Resources of the United States*. https://water.usgs.gov/GIS/huc.html

NGC. (n.d.). https://education.nationalgeographic.org/resource/flood/

NOAA. (n.d.a). https://www.nssl.noaa.gov/education/svrwx101/floods/

NOAA. (n.d.b). https://forecast.weather.gov/glossary.php?word=Flood

NOAA. (n.d.c). https://www.ngdc.noaa.gov/ngdcinfo/

NOAA. (n.d.d). https://www.ncei.noaa.gov/

NOAA. (n.d.e). *NOAA's National Weather Service - Glossary*. https://forecast.weather.gov/glossary.php?word=Flood

NWS Public Forecast Zones (n.d.). https://www.weather.gov/gis/PublicZones

Palin, E.J., Oslakovic, I.S., Gavin, K., and A., Quinn. Implicaitons of climate change for railway infrastructure. *WIREs Clim Change*. 2021; 12:e728. https://doi.org/10.1002/wcc.728

Rossetti, M.A. Potential impacts of climate change on railroads. Federal Railroad Administration. 2003.

Taylor, K. E., R. J. Stouffer, and G. A. Meehl. An overview of CMIP5 and the experiment design. *Bull. Amer. Meteor. Soc.*, **93**, 485–498, https://doi.org/10.1175/BAMS-D-11-00094.1. 2012.

U.S. Geological Survey and U.S. Department of Agriculture–Natural Resources Conservation Service. (2013). Federal standards and procedures for the national Watershed Boundary Dataset (WBD), 4th edn. U.S. Geological Survey. https://pubs.usgs.gov/tm/11/a3/pdf/tm11-a3.pdf

USGS (n.d.). https://stn.wim.usgs.gov/STNDataPortal/#

Varnes, D. (1978). Slope movement types and processes.

WP/WLI. (1995). *Society's UNESCO Working Party on World Landslide Inventory (WP/WLI)*.

About the Authors

Haizhong Wang, PhD

Dr. Haizhong Wang, Professor, School of Civil and Construction Engineering, Oregon State University, is an expert in theoretical and experimental methods for (1) interdisciplinary community and infrastructure resilience and (2) critical resilient interdependent lifeline infrastructure systems analysis.

Brian M. Staes, PhD

Dr. Staes, a Postdoctoral Scholar at the School of Civil and Construction Engineering, Oregon State University, is an expert in traffic flow theory, hazard and risk modeling, and climate change–induced extreme events related to infrastructure resilience.

Benyamin Ghoreishi, MSc

Benyamin, a PhD student at the School of Civil and Construction Engineering, Oregon State University, is an expert in hazard and risk modeling, climate change-induced extreme events affecting transportation infrastructure, and the optimization of roadway and railway alignments.

MTI FOUNDER

Hon. Norman Y. Mineta

MTI BOARD OF TRUSTEES

Directors